Effects of Channel Characteristics on Time Parameters for Small Watershed Runoff Hydrographs

By

Pinhas Golany
Research Fellow, Department of Agricultural Engineering, University of Minnesota

and

Curtis L. Larson
Professor, Department of Agricultural Engineering, University of Minnesota

The work upon which this publication is based was supported in part by funds provided by the United States Department of the Interior as authorized under the Water Resources Research Act of 1964, Public Law 88-379

May 1971

Minneapolis, Minnesota

WATER RESOURCES RESEARCH CENTER
UNIVERSITY OF MINNESOTA
GRADUATE SCHOOL

FOREWORD

This Bulletin is published in furtherance of the purposes of the Water Resources Research Act of 1964. The purpose of the Act is to stimulate, sponsor, provide for, and supplement present programs for the conduct of research, investigations, experiments, and the training of scientists in the field of water and resources which affect water. The Act is promoting a more adequate national program of water resources research by furnishing financial assistance to non-federal research.

The Act provides for establishment of Water Resources Research Institutes or Centers at Universities throughout the Nation. On September 1, 1964, a Water Resources Research Center was established in the Graduate School as an interdisciplinary component of the University of Minnesota. The Center has the responsibility for unifying and stimulating University water resources research through the administration of funds covered in the Act and made available by other sources; coordinating University research with water resources programs of local, State and Federal agencies and private organizations throughout the State; and assisting in training additional scientists for work in the field of water resources through research.

This report is number thirty-one in a series of publications designed to present information bearing on water resources research in Minnesota and the results of some of the research sponsored by the Center. In this study, a mathematical model of a watershed was developed to determine the effects of watershed characteristics length, slope and roughness of the main channel and watershed area on peak streamflow discharges. The physical characteristics of small watersheds in southeastern Minnesota were used in developing the model. The results of the study advance the general understanding of the time parameters involved in the runoff process. The mathematical model can be considered as a satisfactory tool for investigating theories of runoff from small watershed.

This Bulletin serves as the Research Project Technical Completion Report for OWRR Project No.: B-007-Minn., Matching Grant Agreement No.: 14-01-0001-890. The title of the project is "Study of Factors Affecting the Channel Phase of Runoff from Small Watersheds by Mathematical Modeling." The principal investigator of the project is C.L. Larson, Department of Agricultural Engineering, University of Minnesota. The project began January 1, 1966 and it was completed on June 30, 1969.

TABLE OF CONTENTS

LIST OF TABLES

TABLE		PAGE

LIST OF FIGURES

FIGURE		PAGE

FIGURE PAGE

FIGURE PAGE

CHAPTER I

INTRODUCTION

A. General

Hydrology is that part of physical geography which is concerned with the origin, movement, distribution, and properties of the water of the world. Engineering hydrology is that part of the broad field which pertains to the design and operation of engineering projects for the control and use of water.

Adequate hydrologic information is essential for design of hydraulic projects. This information is based on an analysis of data for natural events. The data gain value and significance by the length of their continuance. Short periods of data, nonexistence of data, changes in the watershed regimen, etc., gave rise to the need for basic hydrologic theories and the application of the theories to supply the engineer with fundamental design criteria. The data sought include information on climatic and rainfall events, runoff events, geology, topography, soil types, soil cover, soil infiltration and moisture conditions, the natural channel system characteristics, etc. Statistical analyses are usually used to determine the effects and significance of the interrelated factors that control hydrological events.

Rainfall and climatic records are usually more complete and recorded for longer periods than other hydrologic data. Information from rain gage networks is collected and analyzed continuously and rainfall intensity-duration probabilities are developed for a given location. Information of this type is now available in many parts of the world and the U.S. Weather Bureau Atlas (42) is a very good example.

B. Availability of Runoff Records

Data on runoff events lag far behind the actual needs. Unlike records of meteorological events that can be interpolated between known stations for an ungaged location, runoff data are specific and unique for any individual watershed and relate to the gaged location only. The assumption that data collected on a given watershed can be applied to an adjacent watershed of similar physical characteristics has many inherent faults since no two watersheds are alike in all the natural factors affecting runoff. Nevertheless, because of scarcity of runoff data, techniques based on this assumption are frequently used.

Systematic data collecting from regular hydrologic stations, using current meters, started in the U.S. by the Geological Survey in 1889. Since then it has gradually developed into the present nation-wide program. Only a few reliable records of river flow exceed 70 years and these are available primarily for major rivers. The number of stations and the period of recording decreases with the watershed size while the total number of watersheds increases sharply with decrease of drainage area size. Larson (22) suggested a schematic relation between the number of ungaged watersheds to watershed size and stated:

"It is evident that a very high percentage of the total number of watersheds of any given size up to 100 square miles or more are ungaged. Furthermore, even if the number of gaging stations on small watersheds were increased, we can never hope to obtain even partial records on all of them, because of the tremendous number of 'small' watersheds. It follows that methods of estimating runoff from completely ungaged watersheds will always be needed."

Larson (22) arbitrarily defined small watersheds as those under 100 square miles in size. This definition will be followed in this bulletin.

Data on overland flow, interflow, soil moisture and infiltration, etc., are even more scarce. This information is available primarily from experiment stations and is related only to specific locations. Information on geology and topography for various locations can readily be obtained from available maps.

C. Peak Flow Prediction

One of the most common tasks in engineering hydrology is the prediction of the peak flow for a given frequency of occurrence. Estimates of the peak flows are required for the hydraulic design of channels, culverts, spillways and flood control structures. Availability of data and length of records often determine which method can be used. Frequency analyses of the recorded peak flows are commonly used. The reliability of the prediction depends on the length of the recorded period. When the length is greater than the return period for which the peak flow is desired, these methods are relatively direct and reliable. One major limitation of these techniques is that future changes in the watershed regime cannot be accounted for, since these methods are based on the assumption that historical events can be directly projected to the future. Whenever future changes are anticipated, or the data are not sufficient, which is the case for most small watersheds, the prediction of future peak flows must be based on other methods.

Many techniques have been suggested for computing peak discharge of design floods for ungaged watersheds. Some of them, although known to be inadequate for engineering design, are still in use because of their simplicity. The current available methods can be classified in two general categories, 1) statistical analyses of available flood records, and 2), estimating runoff from the rainfall intensity-frequency data and watershed characteristics. These two approaches are sometimes referred to as stochastic and parametric hydrology, respectively.

The stochastic or statistical approach begins with frequency analysis of flood records for individual streams. It also includes procedures for transferring the information from one watershed to another by developing regional index curves for use in watersheds with similar physiographic conditions. The series of design discharge curves for Minnesota presented by the Minnesota Highway Department (30) is an example of a method in this category. The discharge is given by

$$Q_p = K A^n \tag{1}$$

where Q_p is peak discharge for a given recurrence interval, A is the watershed area in square miles, n is an exponent varying from 0.53 to 0.65, and K is a coefficient depending on watershed characteristics and location. Equations of this type are reliable if based on extensive flow records, including small watersheds.

Methods of the second category rely on climatic data rather than stream flow data. They also rely on the use of watershed characteristics and on understanding of the runoff process. The advantages in using this approach are 1) climatic data are more complete and of longer recorded periods than stream flow, 2) climatic events are more "continuous" in space and can be subjected to interpolation procedures while hydrologic events are more "discrete" and affected by the physiographic characteristics.

The rational formula is an example of methods of the second category. It is given by Linsley (27) as

$$Q_p = C\ i\ a \tag{2}$$

where Q_p is the peak discharge in acre-inches per hour or, with an error of one percent, in cubic feet per second. The factor C is a coefficient (with values less than unity,) depending on watershed characteristics, i is the mean rainfall intensity in inches/hour for the design storm and A is the watershed area in acres. The duration of the design storm is chosen equal to the "time of concentration" of the watershed, T_c, when all parts of the watershed first contribute to the flow at the outlet. This assumption and the assumption that runoff is a percentage of rainfall are oversimplified and this has long been recognized by hydrologists. Nevertheless, the rational method is still used frequently for estimation of peak runoff for watersheds up to five square miles, mainly in urban areas, because of its simplicity and the lack of more reliable methods.

Other methods of this category start with precipitation volume and reduce it to runoff volume by considering various factors of the watershed that cause losses. The runoff volume is then "routed" to the watershed outlet by one of a variety of methods to obtain the peak flow. The basic assumption that the precipitation is the only probabilistic factor that affects the hydrological process is retained.

D. Time Parameters

Most, if not all, parametric methods for predicting peak runoff require some type of time parameter as part of the routing. The time of concentration, used in the rational method, is a familiar example. In general, for a given watershed, time parameters indicate the speed of response of a given watershed and are inversely related to the peak flow, although the exact nature of the relationship has not been established.

The time parameters most commonly used in hydrology are:

1) Time of concentration, defined as the time required for the surface runoff from the remotest part of the watershed to reach the outlet station.

2) Time to equilibrium, defined as the time required for the rate of runoff at the outlet to become equal to the supply rate.

3) Time to peak, defined as the time required for the outflow hydrograph to reach its peak.

4) Lag time, most frequently defined as the time from centroid of rainfall to the hydrograph peak.

Various investigations have shown the time parameters to vary inversely with the supply rates. Pilgrim (35) in his study used radioactive tracers to measure the flow time in a channel of a 100 acre watershed, as an index of the time of concentration. He found the flow time decreases with increasing discharges. Larson (22) used an analytical approach and found the time to virtual equilibrium (97% of supply rate) to relate inversely to the 1/5 power of the supply rate. Machmeier (29) used a mathematical model of a watershed to route various uniform supply rates for various durations. He found that the time to virtual equilibrium varied inversely as the 0.23 power of the supply rates for a watershed of 21.35 square miles. He also found time to peak and lag time to vary with duration, and vary inversely with the supply rate.

In order to be useful in prediction of peak flow, the time parameter should be capable of determination (from the factors that control it) both for gaged and ungaged watersheds. As part of the routing process, time parameters are affected by the physiographic characteristics of the watershed. Studies of the effect of watershed characteristics on the time parameters have been based mainly on analyses of records of natural events and correlation analyses with one or more of the watershed's measurable characteristics.

Although the time of concentration and the time to virtual equilibrium represent a definite physical property, they cannot be obtained from recorded hydrographs. The time to virtual equilibrium is rarely achieved since it requires by definition long durations with constant supply rate, a condition that is unrealistic for natural events, especially for large watersheds.

Relating any time parameter to watershed characteristics by use of actual runoff data is very difficult since the factors involved are interrelated and cannot be varied independently. With a watershed model, however, the input as well as the watershed characteristics can be controlled independently.

E. Objective of this Study

The major purpose of this study is to investigate the effect of watershed characteristics such as length, slope and roughness of the main channel and watershed area on the time parameter, time to virtual equilibrium. In order to do this a mathematical model of the watershed will be developed. The model will be based on the best routing methods available, and will be representative of realistic natural conditions. The geometric and physical characteristics of the model watershed will be capable of independent variation. A computer program will be used for solving the dynamic equations of continuity and momentum to route the nonsteady flow through the channel system.

A uniform supply rate will be applied to the model watershed sufficiently long for the system to reach equilibrium. Each factor investigated will be varied independently within its normal range and its effect on the time to virtual equilibrium will be studied from the data obtained. A theoretical equation of time to virtual equilibrium, based on an analytical approach will be presented and compared with the empirical equation based on the data obtained.

CHAPTER II

PREVIOUS WORK

A. Peak Flow Equations

As mentioned before, parametric-type methods of estimating peak flows for a given frequency are composed of two parts: 1) determination of runoff volume from the probable rainfall; and 2) routing this volume through the channel system. It is assumed that the probabilities of runoff events are the same as those of rainfall events. This study is concerned primarily with the routing or channel phase of the runoff process.

The Rational formula is given, as mentioned before, by

$$Q = C\ i\ a \qquad (2)$$

This equation is based on the "rational" assumption that for uniform intensity the peak flow will occur when all parts of the watershed are contributing to the flow at the outlet. At this time, outflow rates are equal to runoff supply rates, which are the rainfall rates less some percentage of losses due primarily to infiltration. This time is defined as time of concentration, T_c, and is equal to time to peak and to time to equilibrium. Under these assumptions, the mean intensity for a duration equal to T_c for a given frequency is assumed to produce the maximum peak flow. Various investigators (6), (22), (27), however, showed that a lesser duration, referred to as critical time or characteristic duration, will produce the peak flow for a given frequency.

The U.S. Soil Conservation Service (41) uses a peak flow equation

$$Q_p = \frac{484\ A\ R}{T_p} \qquad (3)$$

where Q_p is peak discharge in c.f.s., A is watershed area in square miles and R is storm runoff in inches for a given return period. T_p is the time to peak in hours given by

$$T_p = \frac{D}{2} + L \qquad (4)$$

where D is storm duration and L is drainage area lag, both in hours.

The storm runoff Q is found from rainfall-frequency data and converted to runoff amounts by use of SCS technique of curve number (42).

The routing equation is based on the following assumptions: that (1) outflow hydrographs of small watersheds can be represented by one dimensionless hydrograph; (2) this hydrograph can be simplified into a

triangular shape with fixed geometrical relations; (3) the outflow hydrograph of a large watershed can be composed by unit hydrograph techniques from hydrographs of the smaller watersheds.

In this case, a triangular dimensionless hydrograph is assumed for which the time to peak is fixed as 3/8 of the hydrograph base, T_s. The routing coefficient is a constant and equals 0.75. The watershed lag time L is the time parameter that has to be evaluated from watershed characteristics.

Chow (6) proposed a method of runoff prediction for culvert and waterway design in Illinois. Rainfall for a given return period for various durations is estimated from rainfall-frequency data and adjusted to a specific location by means of a climatic factor. The rainfall amounts are then converted to runoff amounts by using the Soil Conservation Service technique of curve numbers (40). The discharge is given by

$$Q = P\ R \qquad (5)$$

where Q is peak discharge in c.f.s., P is the unit hydrograph peak in c.f.s./in., and R is the runoff amount in inches.

The unit hydrograph peak is given by

$$P = 1.008\ \frac{A\ Z}{D} \qquad (6)$$

where A is watershed area in acres, D is rainfall duration in hours and Z is a peak reduction or routing coefficient.

Chow's routing method is based on the principle of linearity, or the principle of superposition of the unit hydrograph technique. Under this principle, the ordinates of the runoff hydrographs of a given watershed for the same durations are assumed directly proportional to the total volume of the direct runoff, and the time to peak and base time of the hydrograph are assumed constant. Various investigators (1), (9), (30), have criticized this assumption and have shown a definite non-linear response of the watershed with respect to storm variations.

The routing coefficient in this method is considered a variable given as a function of the ratio of rainfall duration to the lag time, L, the time parameter to be evaluated from watershed characteristics. Chow's method also recognizes that for a given return period there is one specific duration that will produce the maximum peak discharge.

Larson (22) suggested a two phase approach to prediction of peak flow rates. The routing is part of the channel phase in which the flow is dependent on the channel hydraulic characteristics, channel length and watershed area. The channel phase is assumed independent of the location and does not involve probability if channel losses (or gains) are neglected.

The routing equation as presented by Larson and Machmeier is

$$Q_p = 646\ C_p\ A\ \frac{R}{D} \qquad (7)$$

where Q_p is peak discharge in c.f.s., A is watershed area in square miles, R is runoff in inches, D is rainfall duration in hours and C_p is the routing coefficient.

No assumption of linearity is introduced in Larson's equation. The routing coefficient C_p is defined as the ratio of peak discharge to uniform supply rate. It was found to be a general function of the ratio of duration to the time to virtual equilibrium, T_{ve}. Defined this way, C_p specifies the magnitude of the peak flow but not its position. Machmeier (29) (30) presented the relation as shown in Figure 1 for a watershed of 21.35 square miles. The time to virtual equilibrium has to be evaluated from watershed characteristics.

The characteristic duration is defined by Larson (22) as the duration of runoff which will cause the maximum peak flow for a given recurrence interval.

Bell (3) suggested the "rational-loss rate" method for estimation of design runoff rates. The volume of runoff is taken as the residual rather than a percentage of the rainfall.

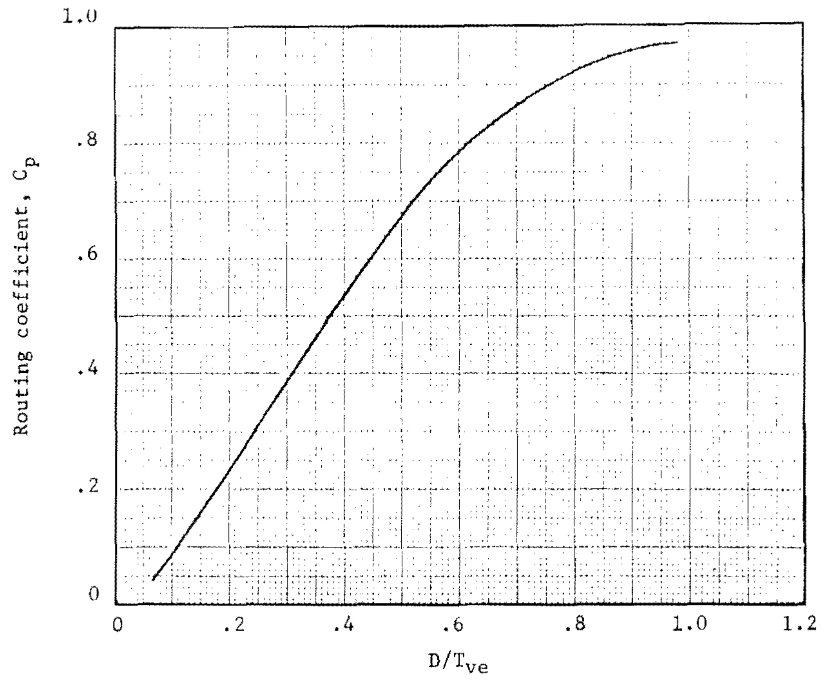

Figure 1. Relation of routing coefficient (C_p) to the time parameter D/T_{ve}) for 21.35 sq. mi. watershed according to Machmeier.

$$R = P - W \tag{8}$$

where R is volume of runoff, P is volume of rainfall and W is volume of total losses. The routing equation is given by

$$Q = \frac{0.9}{L_r} R \tag{9}$$

where Q is peak discharge and L_r is the representative lag, defined as the average lag for extreme floods for a given watershed. The time parameter L_r is used to represent the effective duration of rainfall as well as the characteristic duration. The routing coefficient for the design floods is assumed constant with a value of 0.9, based on a dimensionless relation between the ratio of peak flow rates to constant supply rates, q/i, and the ratio of duration to representative lag, D/L_r. The representative lag is the time parameter to be evaluated from watershed characteristics.

B. Time Parameters

As shown in the previous sections, estimation of peak flow rates involves the routing of the runoff supply. Unless the routing is performed by successive time increments, some type of time parameter is needed. The time parameters indicate the speed of response of the given watershed. Various studies (24), (30) (35) have shown the time parameters for a given watershed and duration to be inversely related to the flood magnitudes, tending towards a constant minimum value. Some of the time parameters are also functions of duration.

1. Time of Concentration

The time of concentration T_c is defined as the time required for the surface runoff from the remotest part of the watershed to reach the point being considered, the watershed outlet. This time will vary, depending on the hydraulic characteristics of the channel. For a large and complex watershed it will be the summation of the respective travel times over the reaches along the path from the most remote point to the outlet. According to the above definition the input rainfall can be of various intensities. For a large complex watershed, for some time distribution of the rainfall intensities, the runoff of the most remote part of the watershed may arrive at the outlet too late to contribute to peak flow. Therefore, the time of concentration can be greater than the time to peak. For small watersheds where the time of concentration is short and the intensity can be assumed uniform it may be very close to the time to peak. For uniform rainfall intensities it will be equal to the time to equilibrium.

The time of concentration is not defined on recorded hydrographs and therefore is not readily obtained. The SCS (42) considers it as the point on the falling limb of the hydrograph where the recession curve begins.

Various methods for determination of time of concentration have been suggested. Ramser (36) determined the time of concentration for small agricultural watersheds by the time difference between low flow stage and the maximum flow stage on outflow records. Kirpich (21) suggested an empirical formula for small watersheds based on observations by Ramser's method for time of concentration in hours as

$$T_c = 0.00013 \left(\frac{L}{\sqrt{S}}\right)^{.77} \qquad (10)$$

where L is the length of the watershed in feet measured along the main channel from outlet to the most remote point of the watershed, S is the mean slope of the main flow path from the watershed divide to the outlet. The Soil Conservation Service (42) suggested various methods for estimating the time of concentration depending on the available data. All of these methods involve some empirical parts. They recognized the difficulties involved in this time parameter by the definition of the "remotest point" especially for storms of partial cover over the watershed.

The above empirical methods assume the time of concentration to be a function of some physical characteristics of the watershed but constant for a given watershed.

2. Time to Equilibrium

The time to equilibrium is defined as the time required for the rate of runoff at the outlet of the watershed to become equal to the supply rate. This implies the following: 1) the rainfall supply rate is uniform in time and space; 2) the rainfall duration is long enough to reach equilibrium. Thus, under these conditions the time to equilibrium will be equal to the time of concentration. Although the two time parameters are equal they vary by the definition. The time to equilibrium which is often used by hydrologists, is rarely, if ever, achieved in nature on a watershed of appreciable size. The rainfall intensity is seldom uniform for long duration and rarely covers the whole watershed uniformly. Thus, although smaller parts of a large watershed may reach equilibrium for a given rainfall intensity and duration the total watershed likely will not.

Izzard (20), in his study of overland runoff defined time to equilibrium as the time for the outflow to reach 97 percent of the supply rate and states:

> "The geometric significance of this point is that the volume of water in detention (overland flow) is substantially equal to the volume of water which has been discharged in the time required to reach this point."

Larson (22) defined time to virtual equilibrium T_{ve} for a watershed as the time for the outflow to reach virtual (97%) equilibrium with a constant inflow of long duration. Although Izzard's reasoning for choosing 97% of equilibrium does not hold for the channel phase, Larson chose the point of 0.97 Q_e by noting that, since the flow approaches equilibrium

very slowly, the time of 97% of equilibrium flow is clearly defined on the rising limb of the hydrograph, while 100% is not.

The time to virtual equilibrium is given by Larson as

$$T_{ve} = K \frac{Lm}{qA}^{1/5} \sum_{i=1}^{m} \frac{l_i}{L_i^{3/10}\ S_i^{1/5}} \qquad (11)$$

where i is a subscript denoting the reach, m = the number of reaches, L = accumulative length, l = length of the reach, q = supply rate, A = watershed area, S = channel slope and K is a coefficient representing the combined effects of channel geometry, area shape and channel roughness.

According to Eq. 11, the time to virtual equilibrium varies inversely as the 0.2 power of the supply rate. Machmeier (29) (30) found the time to equilibrium to vary inversely as the 0.23 power of the supply rate.

3. Time to Peak

The time to peak, t_p, is defined as the time from beginning of rainfall until peak flow occurs. Usually it is the most readily defined on recorded hydrographs. For storms of duration less than the time to equilibrium and with uniform intensity, the peak of the hydrograph will be clearly defined. For longer and more complex storms the runoff hydrograph may have multiple peaks not well defined.

4. Lag Time

There are a number of definitions of the lag time, sometimes called "basin lag". Horner and Flynt (17) defined the lag time T_{lc}, as the time difference between the centroid of rainfall and the centroid of the runoff hydrograph.

Snyder (32) in his study of synthetic hydrographs defined lag time as the time from centroid of rainfall to peak of the resulting runoff hydrograph, T_{lp}. This definition, while less rigorous than the first, is much simpler to apply. He found that for the Appalachian mountain region the lag time could be expressed as

$$T_{lp} = C_t \ (L\ L_c)^{0.3} \qquad (12)$$

where L is the length of the main channel from outlet to the divide in miles. L_c is the distance from the outlet to a point on the main stream nearest to the centroid of the watershed and C_t is a watershed coefficient. The product L L_c serves as a measure of the size and shape of the watershed. The coefficient C_t has the value of 1.8 to 2.2 for the Appalachian region with indication of lower values for watersheds with steeper slopes.

Taylor and Schwarz (41) in their study of 20 watersheds in the North and Middle Atlantic States found

$$C_t = 0.6/\sqrt{S} \qquad (13)$$

where S is the main channel slope.

Linsley, Kohler and Paulhus (27) expressed lag time in a form similar to the expression for time of concentration by Kirpich.

$$T_{lp} = C_t \left(\frac{L\ L_c}{\sqrt{S}} \right)^{0.38} \qquad (14)$$

Values of C_t vary with watershed characteristics.

Still another definition of the lag time is as the time difference between the centroid of the rainfall and the mid (50%) of the runoff volume. While this definition requires information on the total volume of runoff, it is simpler to evaluate the point of 50% volume than the centroid of the hydrograph.

The Soil Conservation Service (42) in its handbook considers lag a weighted time of concentration. It suggests that it is usually sufficient to estimate the lag from the empirical equation:

$$T_l = 0.6\ T_c \qquad (15)$$

In a more recent publication, the SCS (43) suggested the following equation for estimation of lag time:

$$T_l = \frac{L^{0.8}\ (S+1)^{1.67}}{9000\ \ Y^{0.5}} \qquad (16)$$

where T_l = lag time in hours, L = length of mainstream to farthest divide in feet, Y = average slope of watershed in percent, S = (1000/CN) - 10 and CN is the curve number representing the watershed's hydrologic soil cover characteristics.

In this equation the lag time is considered a function of channel length, average slope and the overland flow retardance as represented by the curve number.

Hickock, Keppel and Rafferty (15) in their study of hydrograph synthesis for small watersheds in arid areas suggested two equations for estimation of lag time. The first is

$$T_l = K_1 \left(\frac{A^{0.3}}{S\sqrt{DD}} \right)^{0.61} \qquad (17)$$

where A is watershed area, S is average slope of watershed, and DD is drainage density. For watersheds which differ widely in physiographic characteristics in some major portion of the area from the rest of the watershed the equation was given as

$$T_l = K_2 \left(\frac{L + W}{S\sqrt{DD}} \right)^{0.65} \qquad (18)$$

where L is the length from the outlet to the center of gravity of the source area and W is the width of source area. The source area is the part of the watershed with appreciably larger average slopes that may control the time to peak.

Bell (3) defines the "representative lag" as the average lag for extreme floods. The representative lag is given as a function of the watershed area and a coefficient related to vegetation cover of the watershed

$$L_r = M\ A^{0.33} \qquad (19)$$

where L_r is representative lag in hours, A is watershed area in square miles and M is a coefficient with values from 0.5 to 3.0. Machmeier and Larson (30) found lag time to vary inversely with supply rates and also to be a function of rainfall duration.

CHAPTER III

TIME TO VIRTUAL EQUILIBRIUM - THEORETICAL APPROACH

In natural occurrences uniform supply rates are very rare even for short durations. For long durations they can be assumed as nonexistent. Thus, the time parameters, time to equilibrium or time to virtual equilibrium are not measurable from hydrographs of natural events although they have definite physical meaning.

For gaged watersheds, it may be possible to derive the time to virtual equilibrium by the S-hydrograph of the unit hydrograph method. But in doing so linearity is introduced into the system. It has been found in practice that the end of the S-curve often does not approach equilibrium smoothly making it rather difficult to evaluate the time to virtual equilibrium accurately. Also, the separation of the base flow at the end of the recorded hydrograph is not clearly defined, causing large variations in the time to virtual equilibrium.

To be useful, the time to virtual equilibrium must be capable of being determined for both gaged and ungaged watersheds from the factors that control it, i.e., from the physical characteristics of the watershed. The objective of this study is to investigate the effect of watershed characteristics on the time to virtual equilibrium.

The time to virtual equilibrium was defined as time required for the flow at the outlet of the watershed to reach virtual (97%) equilibrium with a constant supply rate of long duration. Consider now a generalized watershed with a defined channel system (Fig. 2).

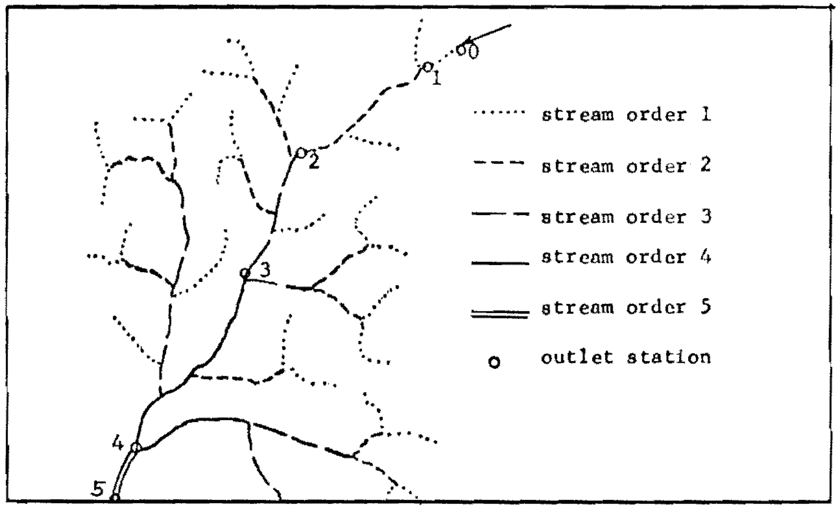

Figure 2. Schematic watershed showing the various stream orders.

The arrow at the upper right corner represents the overland flow plane. Station 0 represents the point where the overland flow plane joins the elementary channel and stations 1 to 4 represent the outlets of stream orders 1 to 4, respectively along the main channel. By its definition, the time to virtual equilibrium is the point on the outflow hydrograph of each station, 0 to 4 when the flow reaches 97% of the supply rate (Fig. 3). By the time that station 0 reaches T_{ve} the rest of the stations are still on the rising phase of the flow. The time to virtual equilibrium of any stations along the main channel includes the time that other stations above it have taken to reach T_{ve}. The time difference between T_{ve} of any station i, where $i > 1$, the T_{ve} of station one will be referred to as the channel rise time for station i, deducted by T_{chi} and defined by

$$T_{chi} = T_{vei} - T_{ve1}$$

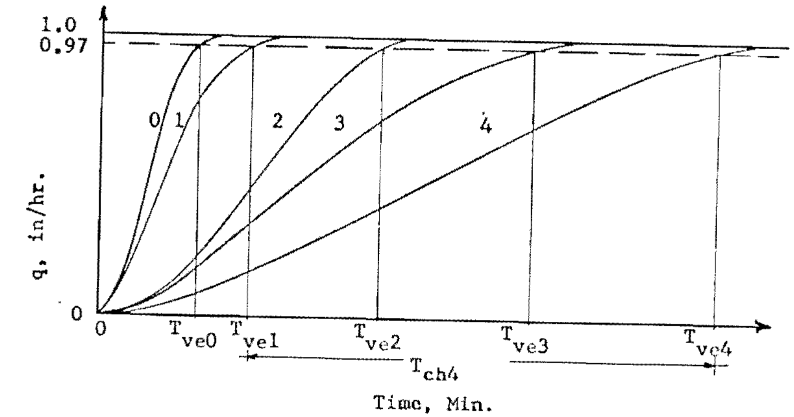

Figure 3. Schematic hydrographs for various stream orders.

Note that by definition the T_{ve} of station one is always subtracted from the T_{ve} of any station in the downstream direction to yield the T_{ch}. Station one is always the outlet station of the elementary watershed in which the lateral inflow dominates the flow in the channel.

If the rise of the tributary of stream order 3 that enters the main channel below station 3, Fig. 2, is faster than the rise in the main channel, a backwater wave will occur and it will move in the upstream direction at the same time that the flood wave is moving downstream. Thus, the effect of both waves is included in the time to virtual equilibrium of station 4.

Assume that no lateral flow exists along the reaches and that any additional discharge enters the main channel at junction points, at the end stations of each reach. The time to virtual equilibrium can be taken

$$\bar{d} = K_2 Q^{0.4} \tag{29}$$

$$\bar{v} = K_3 Q^{0.1} \tag{30}$$

where W, $\bar{d}$ and $\bar{v}$ are top width, mean depth and velocity respectively, Q is the discharge at any point for a given frequency. By continuity

$$Q = W \bar{d} \bar{v} \tag{31}$$

and therefore

$$K_1 K_2 K_3 = 1.0 \tag{32}$$

The relationships of Eqs. 28-30 are of course generalized. Individual streams can and do vary greatly. The width seems to be the least sensitive to local changes in slope and this relationship will be assumed generally applicable.

For wide streams the top width can represent the wetted perimeter. Assuming that W is less than but proportional to P

$$W_i = K_4 P_i \tag{33}$$

Substituting Eq. 33 and 28 into Eq. 24 the travel time is given by

$$T_i = \frac{l_i n_i^{3/5} (K_1/K_4)^{2/5}}{Q_i^{1/5} S_i^{3/10} 1.49^{3/5}} \tag{34}$$

and following the previous derivation, T_{ve} is obtained as

$$T_{ve} = 0.317 \left(\frac{K_1}{K_4}\right)^{2/5} q^{-1/5} \sum_{i=1}^{m} \frac{l_i n_i^{3/5}}{S_i^{3/10} A_i^{1/5}} \tag{35}$$

By combining the unknown coefficients and the constant Eq. 35 can be given in an empirical form as

$$T_{ve} = K q^{-1/5} \sum_{i=1}^{m} \frac{l_i n_i^{3/5}}{S_i^{3/10} A_i^{1/5}} \tag{36}$$

where the value of K has to be evaluated empirically.

Although Eqs. 35 and 36 have the advantage of having independent variables only in the expression for T_{ve}, neither equation provides a suitable basis for this study. The reasons are: 1) the wetted perimeter was related to the discharge only while all other factors were included in a coefficient; 2) the assumption that the top width can represent the wetted perimeter holds for low flows when the cross section is wide and shallow. For flood flows this assumption is doubtful; 3) the assumption that the linear coefficient K_4 is constant for all reaches of the watershed is questionable; and 4) the coefficients will have to be evaluated for each watershed.

It was decided instead to utilize Eq. 27 as the basis for analysis. The coefficient in Eq. 27 is of known value and the problem is to express P_i as a function of the independent measurable factors.

An analytical expression of the wetted perimeter of a given reach as a function of the discharge can be derived from Manning's equation for a triangular cross section as

$$P_i = K_5 Q_i^{3/8} \tag{37}$$

in which K_5 is a coefficient, constant for the reach, given by

$$K_5 = \left\{ \frac{n}{1.49 S^{1/2}} \left[\frac{4(z+1)}{z} \right]^{5/3} \right\}^{3/8} \tag{38}$$

where z is the side slope ratio.

For a trapezoidal cross section an analytical expression of this type cannot be derived, since the relationship of P and Q depends on the bottom width also. For given S, n and cross section geometry of a reach, the wetted perimeter and the discharge can be calculated for normal flow at various depths by Manning's equation. Fig. 4 presents a schematic diagram of log P vs. log Q for a given reach.

It can be seen that the line is flat for low discharges and becomes steeper for higher discharges. The line approaches asymptotically the slope of a triangular cross section. This can be expected since the relative effect of the flat channel bottom diminishes as Q and P increase. A change in the bottom width will shift the line at low discharges but the line will still approach the line for triangular shape at high discharges. A change in the side slope ratio will shift the line for the triangular cross section and the lines of trapezoidal shape will change accordingly. Based on this relationship of P and Q, an expression for the wetted perimeter as a function of the independent factors of the watershed will be derived in Chapter VII following the presentation of the watershed model.

The derivation of an equation for the time to virtual equilibrium is based on many assumptions and generalizations that will be carefully studied later in this study. The assumption that the unsteady flow close

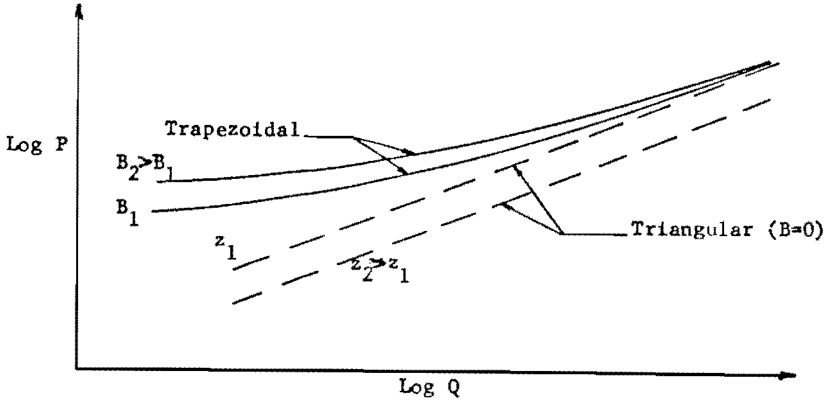

Figure 4. Schematic diagram of relationship of the wetter perimeter vs. discharge for a given reach.

to equilibrium condition can be approximated by uniform flow at equilibrium is the most doubtful. With backwater effect the flow at equilibrium is unsteady and nonuniform. Thus, the validity of this assumption is questionable and will have to be tested subject to the results of backwater effect on the time to virtual equilibrium. Eq. 27 will have to be modified accordingly, or another approach considered.

An assumption was made that at the time the flow at the outlet reaches 97% of the supply rate most of the channel system above a certain point close to the outlet flows at equilibrium conditions. The calculation should proceed to this point, which is rather difficult to evaluate. Similarly it can be argued that, at the time to virtual equilibrium, the lower 97% of the watershed is contributing to the flow at the outlet. At this time the flow in most of the channel system is at equilibrium and the lower part is above 97% of equilibrium flow. Thus, the channel system to consider in the calculation can be the lower 97% of the watershed area.

It was also assumed that no lateral flow exists and all flow enters the upper end of each reach. Lateral flow tends to become insignificant compared with the total flow in the reach at the downstream reaches but at the upper reaches, and especially at the elementary channel, it is most significant and the flow here cannot be considered uniform. For small watersheds the travel time of overland flow and of the elementary channel are the major part of the T_{ve} while in very large watersheds it becomes insignificant. Further analysis of T_{ve} is presented in a later chapter.

CHAPTER IV

THE MODEL WATERSHED

The time to virtual equilibrium cannot be measured or evaluated from recorded hydrographs of natural events since, by definition, it requires a constant supply rate over a very long duration. If an analysis of the effect of each physical watershed characteristic on the time parameter is sought, each factor should be varied independently and this again is not possible in natural watersheds. However, such an analysis can be done with a mathematical model.

Except for very small watersheds, most of the time delay will occur in the channel system. The time to virtual equilibrium starts from the beginning of rainfall excess, at which the elementary channel starts to flow. Therefore, the channel system should be represented by the model.

The mathematical watershed model should, as nearly as possible, satisfy the following requirements:

1) the input to the system should be the runoff supply,

2) the flood flow should be simulated through the system by use of the differential equations describing the process of unsteady flow in open channels,

3) no assumption of linearity or steady flow approximation should be introduced into the model,

4) effect of translation as well as effect of storage should be incorporated,

5) all factors represented in Eq. 27 should be included in the model as constants which can be varied independently, and

6) the output of the model should be the watershed outflow hydrograph at a selected downstream station.

To develop a channel system under the above criteria a model watershed was synthesized following in general the model watershed used by Machmeier (29). However, several basic changes and other improvements were made, making it necessary to construct the model from the beginning.

A. Size and Shape

The model watershed was to be about 10 square miles in area and to agree as close as practical to natural conditions. Gray (11) in his study of measurable physical characteristics and their relation to hydrographs of small watersheds found that

$$L = 1.40\ A^{0.568} \tag{39}$$

where L is the length of the main channel in miles and A is the watershed area in square miles.

This equation is based on analysis of 64 watersheds ranging in size from about one half of a square mile to over a thousand square miles with 95 percent confidence limits. Stall and Fok (39) in their study of stream geometry suggested the following relation

$$\text{Ln } A = -0.25 + 1.19 \; U \tag{40}$$

where A is the area in square miles and U is the proportional stream order as defined by Stall and Fok. The stream order depends on the scale of the map used to define it and the coefficient 0.25 depends on the size of the watershed designated as stream order one. By Eq. 40 the area for stream order one is 2.56 square miles. In order to reduce the size down to the elementary channel that is fed by the overland flow this coefficient will have to change to -5.010. From the plot given by Stall and Fok the area of a given stream order can be given by

$$A_u = 3 \; A_{u-1} + A_{u-2}$$

where the subscript denotes the stream order. This indicates that a watershed of a given stream order is composed of three watersheds of the smaller order. Machmeier (29) in his model used seven branches of smaller stream order to compose the watershed of a given stream order. It was decided to use five branches and to follow Gray's relation as closely as possible.

The shape factor is commonly defined as

$$F_s = L^2/A \tag{41}$$

where F_s is the shape factor, L is length of main channel in miles and A is watershed area in square miles. Substituting Gray's relationship for L in Eq. 41,

$$F_s = 1.96 \; A^{0.136}$$

which indicates that the shape factor is not constant, but changes as the 0.136 power of the watershed area. Thus, Eq. 39 indicates that complete geometric similarity does not exist between watersheds of different size.

Using Gray's relationship (Eq. 39), a trial and error procedure was used to develop the total watershed from a series of unit watersheds with five branches of the smaller stream order composing the next stream order.

The unit watershed was chosen like Machmeier's (39) as 32 acres or 0.05 square miles in area. The length and width of the unit watershed was varied for various trials so that the watershed closely approximates Eq. 39. The length of 1750 feet and a width of 800 feet was found to give best fit, making the overland flow length 400 feet.

The angle between the main channel and the tributary was assumed to be 45 degrees. In the trial and error process other angular values were tested as well as a scheme where the angle varies with the stream order, but were found less agreeable with Eq. 39.

The main channel was assumed to be a straight line with identical tributaries on both sides of the main channel. Fig. 5 shows the general arrangement of the watershed units. Table 1 gives the watershed area, length and shape factor of the model watershed for each stream order. As shown by the calculated value in the last column, Gray's general relationship (Eq. 39) is closely approximated.

Stream order	Watershed area sq. mi.	Main channel length mi.	Shape factor	Calculated length (Eq. 39) mi.
1	0.05	0.33	2.18	0.26
2	0.25	0.65	1.68	0.64
3	1.45	1.98	2.69	1.73
4	8.28	4.59	2.54	4.65

Table 1. Model watershed length-area relationship.

B. Overland Flow

The runoff supply is the input to the channel phase of flow. It is defined as the overland flow as it enters the channel system. No available data was found to be used as input to the model. Thus overland flow had to be routed for use in the model. Machmeier (29) used constant excess rainfall routed by the dimensionless hydrograph proposed by Morgali (30) for the rising part, and by the linear depletion equation $q_1 = q_0 \; k_r$ for the recession part. Woolhiser and Liggett (47) in their study of unsteady flow over a plane conclude that "in general there is no single dimensionless rising hydrograph for overland flow. However, most field cases approach kinematic wave solution."

The kinematic wave solution of overland flow does not involve any linear assumption either in the rising part or in the recession part. Although this study considers flows to equilibrium only, the model was developed for testing of most general cases including receding flows. Therefore, the kinematic wave solution was used to route the overland flow.

Since the study considered the channel phase with no probability aspect involved, excess rainfall was used as input to the land phase of the flow thus eliminating all factors that are effected by climatic conditions. A detailed description of the overland flow model is given in a later chapter.

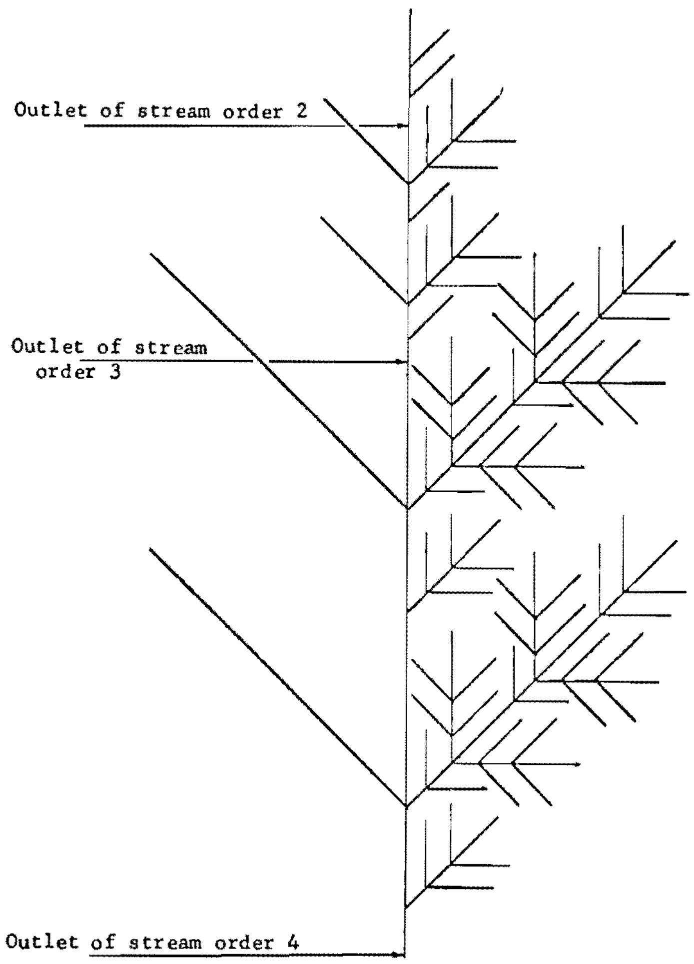

Figure 5. Schematic diagram of the model watershed. (Most of the tributaries omitted on left hand side)

C. Elementary Channel

An assumption was made in the model that no lateral inflow takes place and that all additional discharges are added to the channel system at junction points. While the assumption is reasonable for downstream reaches where lateral inflow, if it exists, will be a relatively small portion of the total flow in the channel, it is definitely wrong for the elementary

channel. Machmeier (29) assumed the outflow of the elementary channel to follow the overland dimensionless hydrograph. The kinematic wave solution, however, can be used to route the flow through a channel with lateral inflow. Therefore, this method of routing the flow was utilized for the elementary channel routing.

A separate computer program was used to route the excess rainfall for the overland flow. The outflow hydrograph of overland flow was then used as input for routing the elementary channel flow by the same computer program. The routing of the channel system started from the uppper-most junction of elementary (first order) watersheds.

D. Channel Characteristics

The use of routing procedures requires that the channel characteristics of cross section and slope be defined at each net point or station at which the solution of velocity, depth and discharge is to be calculated. Machmeier (29) defined the channel main slope, bottom width and side slopes as a function of watershed area, based on Leopold-Maddock (25) relationships (Eqs.28-30), as close as possible to natural conditions in southeastern Minnesota. In his model the values of these factors were fixed for each station along the channel. In this study the basic relation of the bottom width and the channel slope, as a function of the area was retained. All channel characteristic factors were treated as possible variables in the model.

Values of main channel slope, channel bottom width and channel side slope were set for the so-called "standard condition" by using Machmeier's (29) functions. The "standard condition" was taken as an intermediate value in each case. Table 2 gives the "standard condition" values for the model watershed. The channel characteristics were constant throughout each reach.

E. Channel Roughness

The frictional resistance as expressed by Manning's equation is used in this study. The use of "n" as a measure of roughness was originally established for steady uniform flow, although many investigators have also employed it to unsteady flow problems. Chow (7) recognizes that, while engineers commonly assume a single value of "n" for a given channel, it is a variable and depends on factors such as surface roughness, vegetation, channel alignment and irregularities, silting and scouring, size and shape of channel, stage and discharge. Although it is generally agreed that the value of n varies with stage there is lack of agreement as to the nature and magnitude of the variations. Isaacson, Stoker and Troesch (19) in their study of the Ohio River, found that n increases with stage. However, in their simulated routing, they used constant values for all flow depths since their study showed that the roughness did not change appreciably. Machmeier (29) used a constant value of n=0.04 for the watershed for all runs of various supply rates and durations. This value was used as the "standard condition" in this study. The roughness coefficient n was varied from 0.02 to 0.08 to cover a wide range of natural conditions.

Table 2. Watershed channel system geometry

Reach	Bottom Width Ft.	Side Slope Ratio	Channel Slope ft/ft	Channel Roughness "n"
2	4.0	1.0	.0047	0.04
3	4.5	1.0	.0043	0.04
4	4.5	1.0	.0043	0.04
5	6.0	1.0	.0033	0.04
6	6.5	1.0	.0033	0.04
7	7.5	1.0	.0033	0.04
8	7.5	1.0	.0030	0.04
9	7.5	1.0	.0030	0.04
10	10.5	1.0	.0024	0.04
11	11.5	1.0	.0024	0.04
12	12.5	1.0	.0021	0.04
13	13.0	1.0	.0021	0.04

F. Channel Junctions

Whenever a change occurred in the channel characteristics, or additional flow was considered, the station was set as a junction. At these points station numbers were assigned to the last station of the upper reach and to the first station of the lower reach. The distance between the two stations was considered infinitesimal. The effect of backwater on channel storage and thus on time to virtual equilibrium was recognized and the solution was set to "flow" continuously through the junctions taking into account the backwater.

It was assumed that the mean annual flood controls the longitudinal profile of the stream bed, and that at this flow the water profile is closest to normal flow. Machmeier (29) found that the mean annual flood in southeastern Minnesota for watersheds of sizes similar to his model (21.35 square miles) to be 49 cubic feet per second per square mile (cfsm). At any channel junction, the drainage area increases and the annual flood increases also. Thus, at each junction, the channel cross section was increased according to the Leopold-Maddock relation. Assuming the water surface elevation equal above and below the junction, the bed elevation of the downstream station is given by

$$H_d = H_u + Y_u - Y_d$$

where the subscripts u and d denote the upstream and downstream stations of the junction, respectively, H is the bed elevation and Y is the flow depth. This indicates that a drop, D, given by

$$D = H_d - H_u \qquad (42)$$

exists at each junction where the drainage area increases.

G. The Main Channel Model

The routing is performed along the main channel of the model. The uppermost station, Station 1, is the outlet of the elementary channel. This station is considered as the end station of stream order one. Station 2 is the downstream station of the first junction. At this station the flow from two more elementary watersheds enter the main channel from both sides. No backwater was considered at this junction with no effect in the elementary channels. The combined discharge of the three unit watersheds flows through reach 2 to the upstream station, of the next junction, Station 34. At Station 35 two more elementary channels are discharging into the main channel. Backwater effect is considered in the main channel but not in the tributaries. By this scheme, disregarding backwater effect into the tributaries or "floating" them at the junction, the discharge of all first stream order tributaries are equal for any given watershed time regardless of their location in the watershed model. If backwater effect were considered in the elementary models, its effect would have been a function of time as well as location, making it necessary to route the flow in every tributary separately. By using the "floating" scheme the flow needs to be routed along the main channel only.

Station 51 is the end station of stream order 2. Since the discharge of this station is to be used as the discharge of the tributaries for the next stream order the junction is considered "floating" and no backwater is allowed to pass through this junction.

Four tributaries of stream order 2 enter in two junctions into the main channel. In order to fill the gap in area and to satisfy the length-area relation (Eq. 39), four unit watersheds and two junctions are added. Fig. 5 shows the general arrangement of the model watershed. Table 3 gives the information on distance along the main channel, watershed area, station numbers, and the drop at each junction.

At this time it should be mentioned that a watershed model following Eq. 40 would have required nine "floating" junctions along the main channel. Also, the large number of junctions required would have caused a lack of agreement with Eq. 39.

Table 3. Model watershed stations

Reach	Begin Sta.	End Sta.	Δ x ft.	Reach length Mi.	Area Sq. Mi.	Drop ft.
2	2	34	35.38	0.22	.15	.2424
3	35	51	35.38	0.11	.25	floating
4	52	84	54.65	0.33	.25	.7827
5	85	101	54.65	0.17	.75	.0554
6	102	150	54.65	0.50	.85	.3283
7	151	167	54.65	0.17	1.35	.1622
8	168	184	107.71	0.17	1.45	floating
9	185	217	107.71	0.65	1.45	1.6556
10	218	242	107.71	1.50	4.37	.1597
11	243	283	107.71	0.81	4.87	1.1421
12	284	308	107.71	0.50	7.78	.0868
13	309	317	107.71	0.17	8.29	floating

CHAPTER V

OVERLAND AND ELEMENTARY CHANNEL MODEL ROUTING

The land phase of runoff flow is an extremely complicated physical system with stochastic inputs. However, once the watershed parameters, the initial conditions and the inputs are specified in physical terms, the system becomes deterministic. For surface runoff considerations the system includes an overland flow plane discharging as lateral inflow to the elementary channel. The flow is unsteady and spatially varied. The lateral inflow to the overland plane is excess rainfall that can vary in space and time.

Izzard (20) in his study of experimental data suggested an empirical dimensionless hydrograph in which the effects of the surface roughness, slope and length as well as the excess rainfall rates are considered. His excellent data are still used for comparison. Morgali (32) used the unsteady flow dynamic equations in a mathematical model of overland flow and suggested a dimensionless hydrograph other than Izzard's. Wooding (46) used the kinematic equations for analytical study of watershed runoff. Brakensiek (5) used the kinematic equations to simulate overland and channel flows.

Woolhiser and Liggett (47) compared the various methods of modeling with Izzard's data. They proposed a kinematic parameter K defined as

$$K = \frac{SL}{H_o F_r}$$

where S is the slope, L is the slope length, H_o is normal depth at the downstream end for equilibrium discharge, $F_r = V_o^2/gH_o$ is the Froude number and V_o is the velocity at the downstream end for equilibrium discharge. They showed that for $K > 10$ a model based on the kinematic theory gave approximately the same results as a model based on the full dynamic equation and can represent most field cases. An excellent literature review is also included in their work.

A. Kinematic Wave Solution

Consider an impermeable surface of length L, slope $S = \sin\theta$ and a unit width perpendicular to the plane of Fig. 6, where I is the excess rainfall rate per unit area with the dimensions of inches per unit time. The discharge per unit width q for steady flow is

$$q = a\, y^m \tag{43}$$

The kinematic wave method assumes that the slowly varied flow can be represented by this steady flow equation, providing that the Froude number, F_r, is less than two. Eq. 43 can be used for both laminar and turbulent flows, depending on the values of a and m.

For two dimensional, unsteady flow over a plane surface, the continuity equation has the form

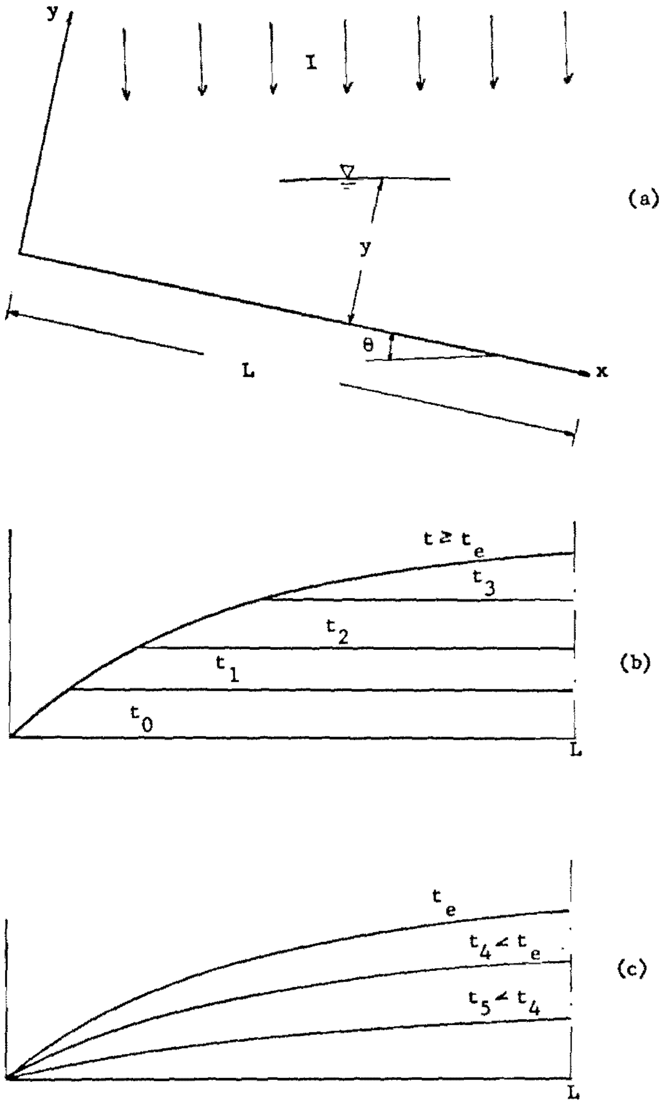

Figure 6. Overland flow plane. (a) definition. (b) rising stage. (c) receding stage.

$$q_x + y_t = I \tag{44}$$

where the subscripts x and t denote partial derivatives with respect to distance and time, respectively. The kinematic wave velocity C is given by

$$C = \frac{dq}{dy} = m\ a\ y^{m-1} \tag{45}$$

Next, let

$$\frac{\partial q}{\partial x} = \frac{\partial q}{\partial y}\frac{\partial y}{\partial x} \tag{46}$$

Since q in Eq. 43 is a function of y only, $\frac{\partial q}{\partial y}$ is a total derivative and

$$\frac{\partial q}{\partial x} = \frac{dq}{dy}\frac{\partial y}{\partial x} = C\frac{\partial y}{\partial x} \tag{47}$$

Eq. 44 therefore becomes

$$\frac{\partial y}{\partial t} + C\frac{\partial y}{\partial x} = I \tag{48}$$

In Eq. 44, y is a function of x and t. Thus

$$\frac{dy}{dt} = \frac{\partial y}{\partial x}\frac{dx}{dt} + \frac{\partial y}{\partial t} \tag{49}$$

and

$$\frac{dx}{dt} = C \tag{50}$$

Therefore,

$$\frac{\partial y}{\partial t} + C\frac{\partial y}{\partial x} = \frac{dy}{dt} = I \tag{51}$$

The initial and boundary conditions are

$$y = 0 \text{ at } t = 0 \text{ for all } x$$

$$y = 0 \text{ at } x = 0 \text{ for all } t.$$

Thus, two simultaneous equations are obtained,

$$\frac{dy}{dt} = I, \tag{52}$$

and

$$\frac{dx}{dt} = may^{m-1} \tag{53}$$

For the general case the excess rainfall intensity is assumed to vary with time and to be spatially uniform. The integral $\int I\,dt$ is bounded for any finite range of integration and y is non-negative for all t's.

If the excess rainfall intensity is assumed constant and non-variable with respect to time an analytic solution can be obtained as shown by Wooding (46). For this case, the time to equilibrium or time to virtual equilibrium can be defined.

By integration Eq. 52 becomes

$$y = I\,t \tag{54}$$

and from the initial conditions and at time to equilibrium,

$$y_e = I\,t_e\,. \tag{55}$$

The discharge at equilibrium is

$$q_e = I\,L = a\,y_e^{\,m},$$

and

$$y_e = \left(\frac{I\,L}{a}\right)^{1/m}. \tag{57}$$

Solving for t_e from Eqs. 55 and 57,

$$t_e = \left(\frac{L}{a\,I^{m-1}}\right)^{1/m}. \tag{58}$$

Eq. 58 shows that the time to equilibrium is definitely a function of the supply rate.

The time to equilibrium is given by

$$t_e = \frac{Ye}{I}\,. \tag{59}$$

Expressing q_e by Manning's formula, it becomes

$$q_e = \frac{1.49}{n}\,S^{\frac{1}{2}}\,Y_c^{\,5/3} = I\,L, \tag{60}$$

and

$$y_e = \frac{q_e^{\,3/5}\,n^{\,3/5}}{1.49^{3/5}\,S^{3/10}} = \frac{I^{3/5}\,L^{3/5}\,n^{3/5}}{1.49^{3/5}\,S^{3/10}}\,. \tag{61}$$

Substituting Eq. 61 into Eq. 59 and changing I to units of inches per hour,

$$t_e = 56.3\,\frac{L^{3/5}\,n^{3/5}}{S^{3/10}\,I^{2/5}}\,. \tag{62}$$

Morgali (30) used the dynamic equations in his studies. He obtained the empirical relationship

$$t_{max} = 59.6\,\frac{L^{0.593}\,n^{0.605}}{S^{0.38}\,I^{0.388}}\,. \tag{63}$$

Note that, except for S, the exponents and the coefficients agree closely.

The solution for the kinematic wave routing can be achieved by two methods: 1) approximating Eq. 44 by a finite difference equation based on a grid of points in the x-t plane, solving for y and substituting y into Eq. 43 and 2) solving the ordinary differential equations, Eqs. 52 and 53, by forward integration from the given initial condition by any of the standard numerical procedures. In this case, Eqs. 52 and 53 are solved simultaneously along the characteristic lines in the x-t plane spaced by t. Values of y and t at which each characteristic line intersects the line x = 1 are found by interpolation and q is given by Eq. 43.

The stability of the solution by the first method depends on the finite difference scheme and the spacing of the net points in the x-t plane, as shown by Brakensiek (5). The rising limb of the hydrograph is a smooth "S" shape curve and approaches the equilibrium state asymptotically.

In the second method the stability is insured by using small time steps. The rising limb of the hydrograph does not show the "S" type curve found in field data but rises steeply and intersects with the line of constant supply rates.

The second method was chosen in this study since the method of characteristics was also used in solving the dynamic equations for the channel routing. The solution can be applied to any general case and the input can be given as constant or variable by array or equation. Eqs. 52 and 53 were solved simultaneously by a simple Runge-Kutta integration routine for fixed time increments for values of y and x at t. Interpolation was used for values of y and t at x = L.

The steady state flow is given by the general form of $q = ay^m$. Laminar or turbulent flow conditions will determine the values of a and m. For laminar flow m = 3 and $a = gS/3\nu$, where S is the slope, g is gravitational acceleration and ν is the kinematic viscosity. For turbulent flow $a = 1.49S^{\frac{1}{2}}/n$ and m = 5/3.

B. Overland Flow Simulation

Various investigators have tried to fit the various flow equations to experimental data. Izzard (20) obtained the relationship

$$q_e = \frac{1}{k^3} y^3 \qquad (64)$$

where y is average depth of flow on the plane, and

$$k = (0.0007 \; I + c)/S^{1/3} \qquad (65)$$

where I is rainfall intensity, S is the plane slope and c is a retardance coefficient with values given for various surfaces. The exponent of y is the same as for laminar flow, therefore

$$a = \frac{1}{k^3} = \frac{g\;S}{3\nu} \qquad (66)$$

which shows that although Izzard used laminar flow, he defined k not only by fluid properties but as a function of surface roughness and the additional retardance as affected by the rainfall intensity.

Schaake (37) in his study of synthesis of overland flow hydrographs in urban paved areas used laminar flow for the overland flow and turbulent flow for the elementary channel. He used the friction coefficient f as defined by Darcy-Weisbach equation. The coefficient f was related experimentally to Reynolds number by

$$f = c/R_e$$

where R_e is the Reynolds number and c is coefficient evaluated from experimental data. Harbaugh and Chow (13) introduced a conceptual measure of roughness N' given by

$$N' = W_c y^{-x} \qquad (67)$$

where x is an exponent assumed by Harbaugh (13) to be a function of slope only and W_c is the coefficient of watershed roughness equal to

$$W_c = C_u + C_i + C_{iv} \; . \qquad (68)$$

C_u is a coefficient accounting for variations of Manning's n with depth, C_i is a coefficient based on added resistance due to rain drop impact at the water surface, and C_{iv} is the coefficient based on the variation of rain drop impact for different depths of flow, y. N' is then used in Manning's formula. W_c is given as a function of the rainfall intensity I in the form

$$W_c = c I^z \qquad (69)$$

where z is an exponent. For constant I the value of W_c is constant. If Eq. 69 with W_c constant is substituted into Manning's formula,

$$q = \frac{1.49}{W_c \; Y^{-x}} S^{\frac{1}{2}} y^{5/3} = \frac{1.49}{W_c} S^{\frac{1}{2}} y^{(5/3 + x)} .$$

In effect, a constant roughness coefficient other than n and a constant exponent for y greater than 5/3 is obtained.

Morgali (32) suggested that the flow is laminar during the early portion of the flow but found that the turbulent flow equation gives a better overall result. All literature reviewed indicates that the coefficient of friction cannot be selected from the usual qualitative description of the soil surface.

An attempt was made to evaluate m and a in Eq. 43 by fitting model results to experimental data by Izzard. Since the flow was shown to vary between laminar to turbulent, it follows that the exponent m will vary accordingly between m = 3 to 5/3 respectively, and as shown by Harbaugh (12), may be any value in between.

Three values of m were tried and compared to experimental data that was available. For turbulent flow, Manning's formula was used with m = 5/3 and the corresponding $a = 1.49\;S^{1/2}/n$. Various values of n were tried in order to obtain the best fit on the rising limb of the hydrograph.

For laminar flow the exponent was m = 3 and the corresponding **a** value was taken as given by Parsons (32)

$$a = \frac{Sg}{3\nu\;K^3}$$

where S, g and are as defined before and K (not the k used by Izzard) is defined by

$$K = \frac{y_a}{y_{th}}$$

where y_a is the actual measured depth and y_{th} is the theoretical depth as calculated by the laminar flow equation. Values of K vary from 1.0 to 10 for surface roughnesses from very smooth to grass surfaces. Values of K were varied to obtain the best fit on the rising part of the hydrograph.

For the case between laminar and turbulent flow, m=2 was taken following the concept of "75 percent turbulent flow" as suggested by Horner and Jens (18). In their study, the discharge is given by $q = ay^2$ and $a = k_h \; S^{1/2}$. Values of k_h are given for two special cases only. An attempt to express a, following Harbaugh, in the form

$$a = \frac{1.49\;S^{\frac{1}{2}}}{(c\;I^z)\;y^{-1/3}}$$

for constant I failed because of insufficient data. Since the effect of the various exponents was of interest at this time, an initial value of k_h was assumed and then varied to obtain best fit on the rising hydrograph.

Table 4 gives the summary of the exponents m, the corresponding forms of a and the values of roughness found to fit the rising part of Izzard's run No. 173 best. Run No. 173 was chosen randomly from the available data.

	Value of Exponent m	Form of Coefficient a	Best fit roughness values Rising	Receiding
Turbulent	5/3	$1.49\ S^{1/2}/n$	n = 0.0145	n = 0.009
75% Turb.	2	$k_h\ S^{1/2}$	k_h = 525	k_h = 700
Laminar	3	$g\ S/3\nu\ k^3$	k = 1.45	k = 1.45

Table 4. Values and forms of $q = ay^m$ fitted to Izzard's run No. 173.

Figure 7 shows the best-fit computed results for the three exponents compared to Izzard's run No. 173. It can be seen that, although all lines agree reasonably well with the experimental data for the rising hydrograph, the laminar model came to equilibrium a little short of the supply rate and shows a convex trend on the second rise. In general, for the larger exponents the computed hydrographs starts flatter but becomes steeper as the flow approaches equilibrium. In view of Morgali's conclusions and considering the fact the Manning's n can be selected for various surfaces while k_h values will have to be fitted to experimental data it was decided to represent Eq. 43 for the rising part by turbulent flow expressed by Manning's formula.

In all cases the computed results of the recession part did not agree with the field data. This can be expected in light of Harbaugh's conceptual watershed roughness, since C_i and C_{iv} vary with rainfall intensity and, after cessation of the rain, should come to a constant minimum value, smaller than Manning's n.

Another set of tests were run for fitting of the recession part of the hydrograph. Eq. 43 expressed by Manning's formula with n = 0.0145 was used for all periods of rainfall. For the recession part the exponents as in the first series were used, and for each exponent the best fitting value of the roughness coefficient was found. These values are given in Table 4 for the recessional part.

Fig. 8 shows the best fitting hydrograph for each exponent in comparison with Izzard's run No. 173. All calculated hydrographs agree well with the field data. In the laminar recession flow, except for the concave shape of the second rising limb, the agreement is very good. Since this concave shape, which is in contrast to the regular shapes of rising hydrograph, could not be explained, turbulent flow expressed by Manning's formula was chosen to represent the recession part, following the same arguments as for the rising part.

Roughness coefficients of n = 0.0145 and n = 0.009 were established for the rising part and the recession part respectively, for Izzard's run No. 173 having a surface made of commercial slate roofing-felt impregnated with asphalt. Simulated results were compared to three more

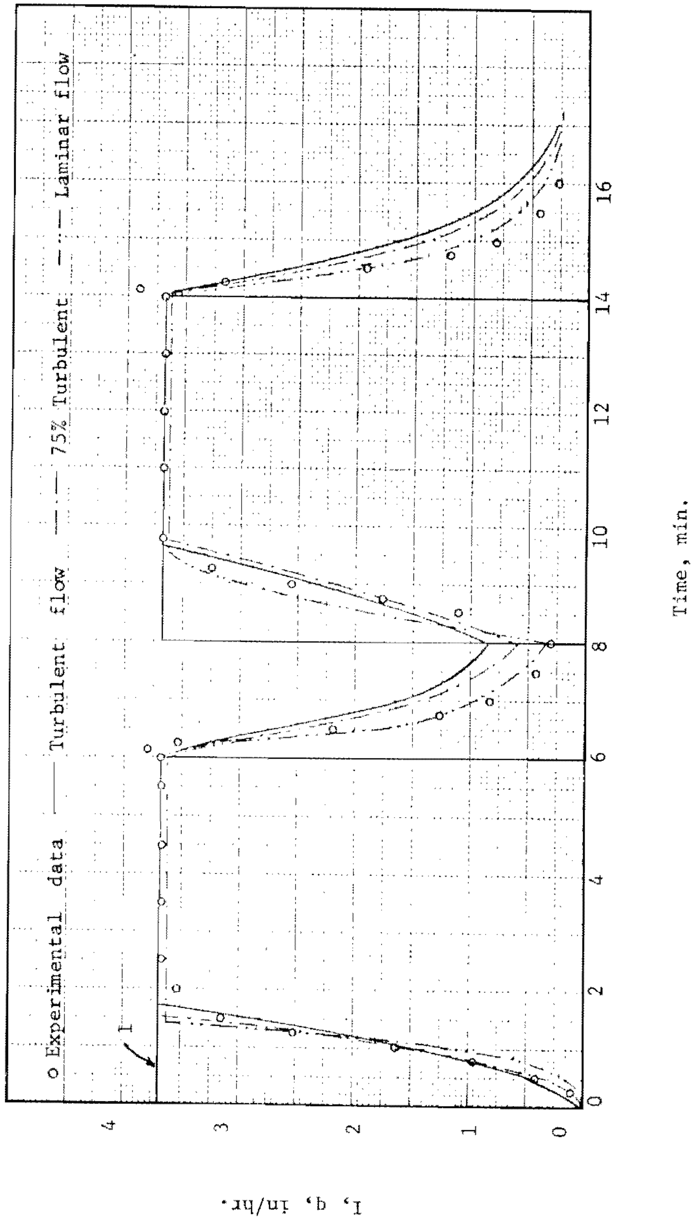

Figure 7. Comparison of simulated results and experimental data, Izzard's run No. 173, rising part.

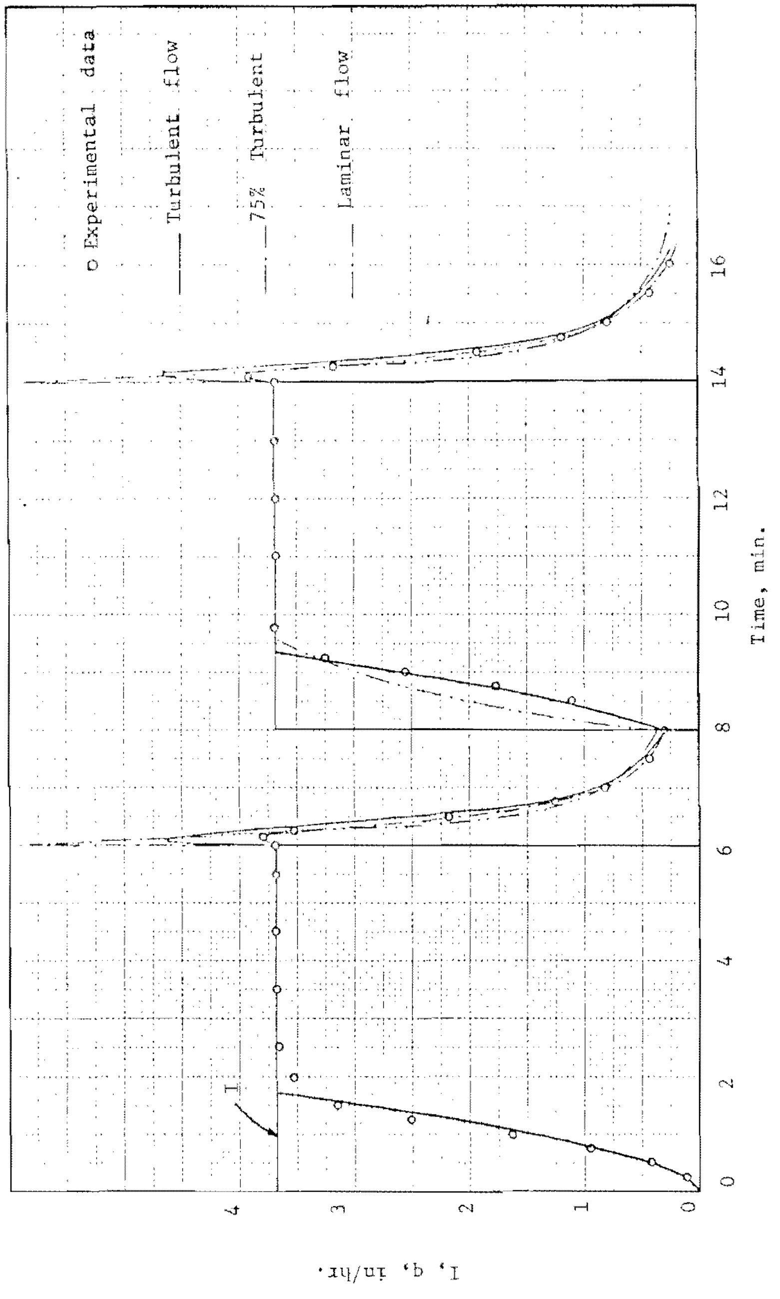

Figure 8. Comparison of simulated results and experimental data, Izzard's run No. 173, recession part.

sets of experimental data which had the same surface. Izzard's runs No. 174, 133, and 134 were used, with the same roughness coefficients. The test factors are given in Table 5.

Table 5. Design factors of overland flow tests simulated by the model.

Izzard's Run No.	Length (ft.)	Slope (ft/ft)	Rainfall Intensity (in/hr)
173	72	0.04	3.68
174	72	0.04	1.90
133	72	0.005	3.67
134	72	0.005	1.87
301	72	0.010	3.56

Figs. 9, 10 and 11 show the comparison of the simulated hydrographs and the experimental data. For the runs of S = 0.04 the overall agreement is very good while the run with S = 0.005 shows that an exponent larger than 5/3 will give better agreement at the beginning of the rising limbs since the experimental data show a "flatter" rise. The instantaneous increase in the discharge at the end of the rainfall appears in all simulated hydrographs although in some cases it is larger than the experimental data.

To further test the simulation model a comparison with Izzard's run No. 301 was tried. The surface was blue grass turf. The test factors are given in table 5. Eq. 43 was expressed as before by Manning's formula and the roughness coefficient was varied for the rising limb and the recession part respectively to obtain the best fit.

Fig. 12 shows the simulated hydrograph compared to the experimental data. A value of n = 0.4 gave best overall agreement on the rising limb but no single value of n gave any satisfactory agreement on the recession part. Foster, Huggins, and Meyer (10), in their study of simulation of overland flow noticed the same phenomenon and suggested that the percentage of soil surface covered by the flow should be considered for infiltration. This explanation does not satisfy the case of Izzard's run since the surface was an impervious one. A variable exponent and roughness coefficient as suggested by Harbaugh (13), appears necessary to obtain good agreement.

Two limitations of the model should be considered. First, in all the simulation runs the purpose was to test the roughness and the laminar or turbulent response. The length of the overland flow plane in the simulation runs was 72 feet. The length of the overland flow plane in the model watershed is 400 feet, considerably longer than that of the experimental data. The model's overland flow length of 400 feet might be too long compared with natural cases. However, if it is assumed that channeling does not occur and interflow is ignored, this length can be accepted theoretically.

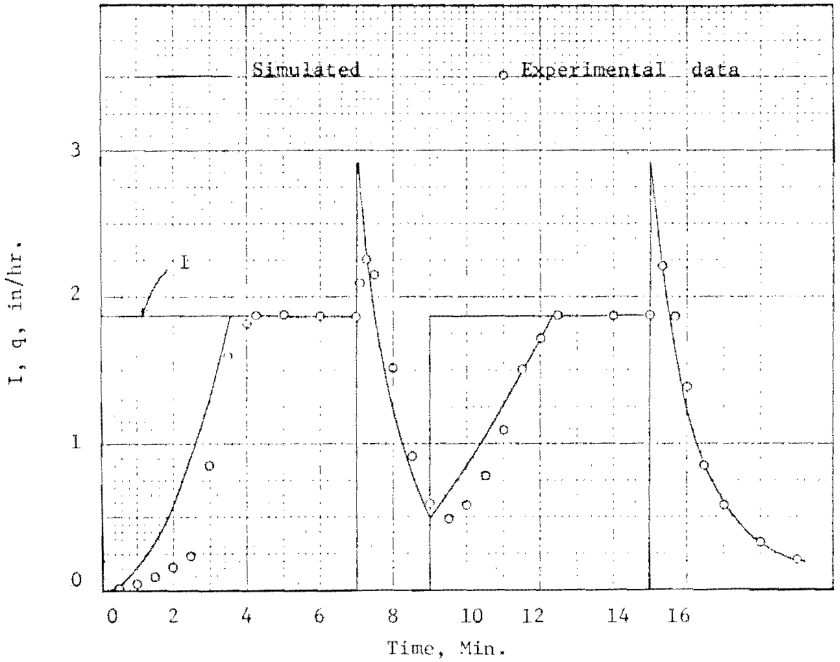

Figure 9. Simulation of Izzard's run No. 174, using turbulent flow and two roughnesses

The second limitation is the definition of excess rainfall. In order to simplify the model and to avoid complications caused by infiltration and interflow the excess rainfall rates were used as input. The excess rainfall rate is defined by

$$I = v - f$$

where I is the excess rainfall rate, v is the rainfall rate, and f is the infiltration rate assumed spatially uniform and positive, i.e., no interflow.

Since v and f are each a different function of time, I is also a function of time different than that of v or f. At the time when the rain stops and $v = 0$ we assume that the excess rainfall $I = 0$. This implies that at this time the infiltration rate is also $f = 0$. This implication is definitely wrong since the infiltration continues to draw from the surface storage. Hence, the definition of excess rainfall is over-simplified and although applicable for the rainfall period is rather unsatisfactory for the recession period except for experimental plots with impervious surfaces.

Since in this study the object was to simulate the channel phase of flow to equilibrium and simulation of the overland phase of flow was necessary to obtain runoff supply, the factors upon which the model

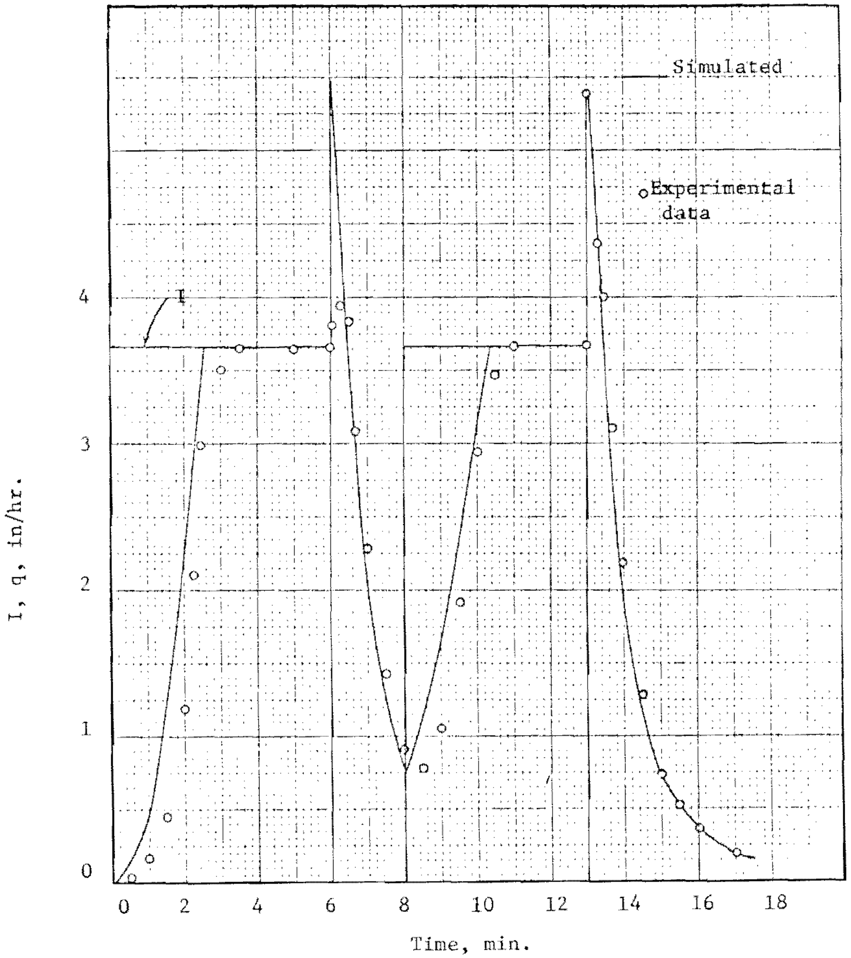

Figure 10. Simulation of Izzard's run No. 133, using turbulent flow and two roughnesses.

was developed as described above were accepted. Eq. 43 was represented by Manning's formula as turbulent flow and the roughness coefficient was taken $n = 0.2$ as accepted by Machmeier following Morgali's recommendation for overland flow. Machmeier also found the average land slope in southwestern Minnesota to be 10.2 percent. This value was used in the overland flow simulation in this study. All factors of the overland flow were kept constant in this study.

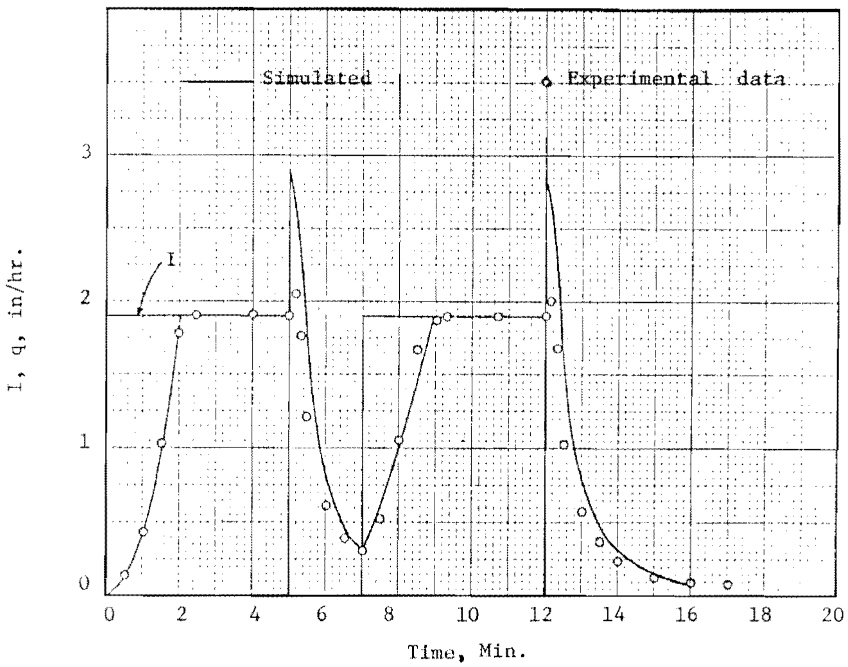

Figure 11. Simulation of Izzard's run No. 134, using turbulent flow and two roughnesses.

C. The Elementary Channel Simulation

The unit watershed area was taken as 800 x 1750 feet as described previously. The unit watershed arrangement is shown in Fig. 13. The elementary channel was assumed to be formed by the intersection of the overland flow planes. This determined the channel shape as a triangular cross section with the side slopes equal to the slope of the overland flow plane, i.e., 10.2 percent, and a length of 1750 feet.

The runoff supply, routed by the overland flow is the input to the channel phase. Since the runoff supply enters the elementary channel laterally the kinematic wave solution was used for simulation of the flow.

For the elementary channel, Eq. 43 becomes

$$Q = a\ Y^{m}$$

where Q is the discharge, Y is the depth of flow in the center of the channel, m is the exponent derived from Manning's formula for triangular channel, m = 8/3 and

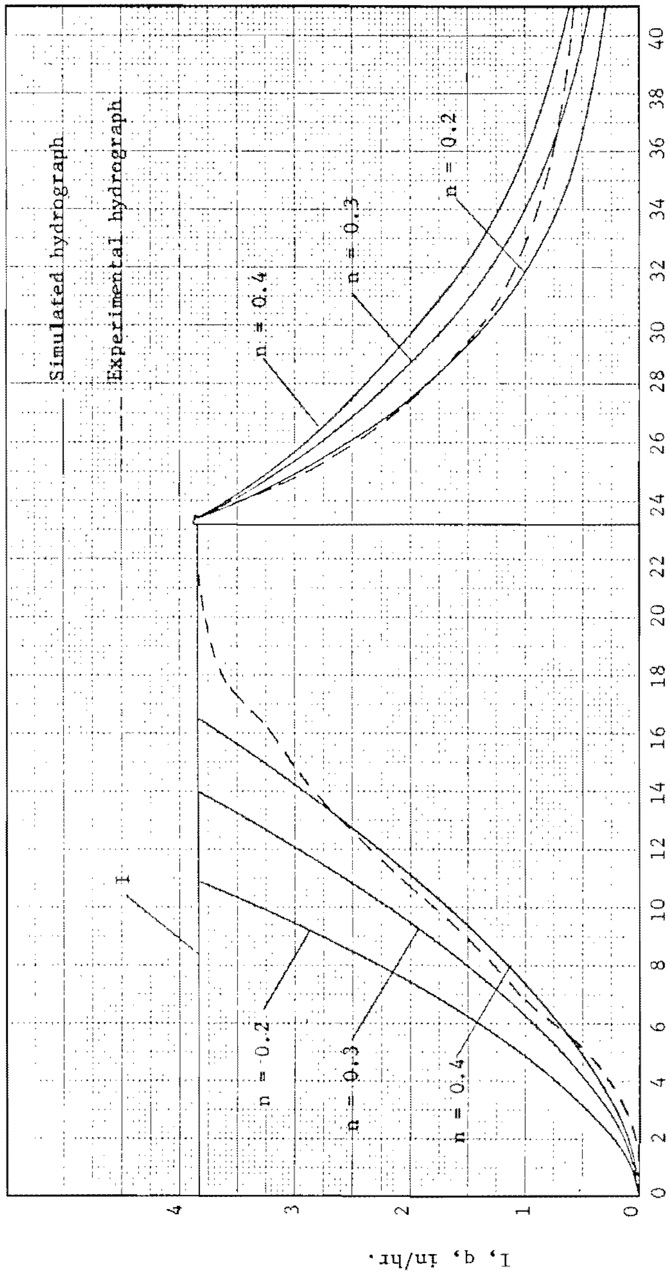

Figure 12. Simulation of Izzard's run No. 301, blue grass turf

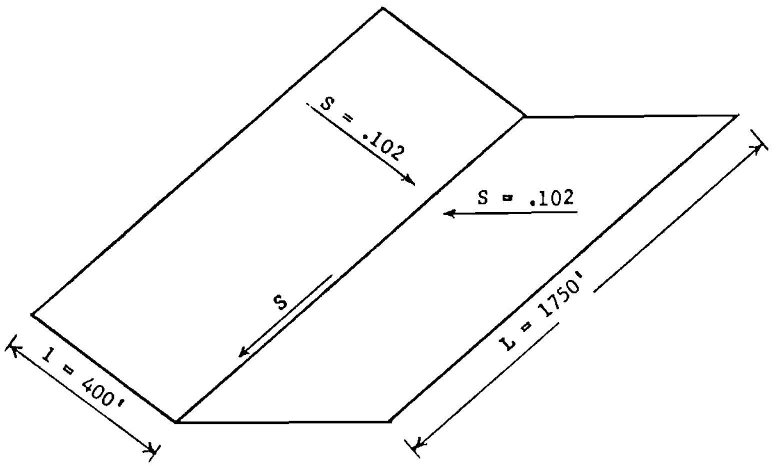

Figure 13. Unit Watershed.

$$a = \frac{1.486}{n} S^{\frac{1}{2}} \frac{z^{5/3}}{4(1 + x^2)^{1/3}} \qquad (71)$$

where n is Manning's roughness coefficient, S is the channel slope, z is the channel side slope ratio. The channel slope, S, and the roughness, n, are part of the channel characteristics and their values were varied as part of the study.

For the elementary channel, Eq. 44 becomes

$$Q_x + Y_t = q \qquad (72)$$

where x is the location along the elementary channel, t is time and q is the lateral inflow from both sides of the channel at the end of the overland flow plane. The initial and boundary conditions are given as

$$Y = 0 \text{ at } t = 0 \text{ for all } X$$

$$Y = 0 \text{ at } X = 0 \text{ for all } t$$

The same computer program that was used for overland flow routing was used again for the elementary channel. Since the integration is performed over equal time increments the overland flow discharges for various times t were further interpolated to give q as an array of equal time increments. Then Eqs. 52 and 53 were solved simultaneously for Y and X by the Runge-Kutta integration routine, and the values of Y and t were

interpolated for the values at X = L. The discharge of the elementary channel was calculated by Eq. 70 for each time t and finally values of Q were interpolated for equal increments of t to give them the elementary channel outflow hydrograph.

CHAPTER VI

CHANNEL ROUTING

A. Routing Equations

Many flow problems in natural channels can be solved accurately enough by using steady flow concepts providing that the rate of change with respect to time is small. In these cases a pseudosteady flow is assumed. However, there are many cases in which this assumption does not hold and the unsteady condition prevails. A flood wave is a very common case of the latter.

The general open channel equations of unsteady, nonuniform flow are based on the physical laws of conservation of mass and conservation of momentum. By considering an infinitesimal length of a channel that is bounded by two vertical cross sections and considering inflow, outflow and accumulation of mass inthe element, the equation of continuity is obtained. Likewise, by applying Newton's law of conservation of momentum to the flow through the element of water, the equation of motion is obt ained. The detailed derivation of these two equations can be found in many testbooks (7), (14) and will not be repeated here. The derivation of the two equations is based on the following assumptions:

1) the fluid in the channel is of homogeneous density;

2) the velocity is uniform over any cross section;

3) the pressure distribution at any cross section is hydrostatic;

4) the flow is turbulent and subcritical;

5) the channel is straight and of simple geometry;

6) the bed slope is uniform for each reach of the channel and mild enough so that $\sin\ \theta \cong \tan\ \theta$; and

7) secondary forces like Coriolis acceleration can be neglected.

Chow (7) gives the equation of continuity as

$$(VA)_x + T\ Y_t - q = 0 \tag{73}$$

where the subscripts x and t denote partial derivatives with respect to distance and time, respectively. A is the cross section area of the channel, V is the mean velocity over the cross section, T is the top width of the cross section, Y is the depth of water in the channel measured from the bottom and q is lateral inflow per unit length of the channel.

Likewise, the equation of motion is given as

$$\frac{V}{g} V_x + Y_x + \frac{1}{g} V_t + q \frac{V}{A} + S_f - S_b = 0 \tag{74}$$

where g is acceleration of gravity, S_b is the slope of the channel bed, Sf is the friction slope. The latter is assumed to be equal to the friction slope for steady flow at the same depth and thus can be approximated by steady flow formulas like Chezy or Manning. In this paper it will be expressed by Manning's equation as

$$S_f = \frac{V\ |V|}{(1.486/n)^2\ R^{4/3}} \tag{75}$$

where R is the hydraulic radius and n is Manning's roughness coefficient.

Expanding $(VA)_x$ and substituting the terms $TY_x = A_x$ and $E = -g\ (S_b - S_f)$ the equations of continuity and motion can be written as

$$AV_x + VTY_x + TY_t - q = 0 \tag{76}$$

and

$$VV_x + gY_x + V_t + E + qg \frac{V}{A} = 0 \tag{77}$$

respectively, for a prismatic channel cross section of any shape. For channels with no lateral inflow, with additional discharge occurring only at the junctions, q is equal to zero.

With the development of the modern high-speed, large storage digital computers, numerical methods of solving the above set of equations become practical. Several numerical techniques have been used to solve the equations. They can be classified as follows:

1) The implicit method. In this method the set of equations is transformed into the corresponding finite difference equation set according to the conventional scheme in the x-t plane. The transformed equations are solved implicitly, that is, by setting up as many equations as there are unknowns and solving them simultaneously.

2) The power series method. In this method the set of equations is expanded by means of a power series, usually the MacLaurin series of f(x), for a given time t at a point, x_1, in terms of depth, Y, and by transforming the expanded equations to a finite difference form, the depth Y_2 is solved for a nearby point x_2, at time t.

3) The method of characteristics. In this method the set of partial differential equations is added linearly and transformed into a

set of four ordinary differential equations known as the characteristic equations. These four equations are subsequently integrated along the characteristic lines at successive time levels on the x-t plane.

The implicit method, although it is generally known to be free of stability problems in the solution, was not considered for this work since it requires known downstream boundary conditions at all times t, in order to match the number of equations with number of unknowns. In this work the downstream boundary condition, or the outflow hydrograph at the watershed outlet is the desired solution.

Many investigators have used the method of characteristics successfully for solution of unsteady flow in a channel system (2), (19), (28), (45). Although stability problems are known to exist in this method and short time steps are needed to insure convergence of the solution, it was thought at the beginning of this work that this method would be more flexible and more efficient in computer time than the power series method. Therefore, the method of characteristics was selected for this study. As will be explained later second order solutions with several iterations at each station proved to be necessary to insure stability and the computer efficiency was drastically reduced.

B. Method of Characteristics

The continuity and motion equations form a set of simultaneous quasi-linear partial differential equations with four variables. Two are independent variables x and t and two are dependent variables, Y and V.

$$L_1 = VTY_x + TY_t + AV_x = 0 \tag{78}$$

$$L_2 = g\,Y_x + V\,V_x + V_t + E = 0 \tag{79}$$

Consider a linear combination of $L = L_1\,\lambda_1 + L_2\,\lambda_2$

$$L = (VT\lambda_1 + g\lambda_2)Y_x + T\,\lambda_1 Y_t + (A\lambda_1 + V\lambda_2)V_x + \lambda_2\,V_t + \lambda_2\,E = 0 \tag{80}$$

If $t = t(x)$ is the equation of a curve, then dt/dx is the slope of the tangent of this curve and if $Y = Y(x,t)$ and $V = V(x,t)$ are solutions for Eqs. 78 and 79, then the total derivatives are

$$dY = Y_x\,dx + Y_t\,dt,$$

and

$$dV = V_x\,dx + V_t\,dt.$$

The differential expression of L can be written as

$$dxL = (VT\lambda_1 + g\lambda_2)\,dY + (A\lambda_1 + V\lambda_2)dV + E\lambda_2 dx = 0 \tag{81}$$

if the constants λ_1 and λ_2 are chosen so that

$$\frac{dx}{dt} = \frac{VT\lambda_1 + g\lambda_2}{T\lambda_1} = \frac{A\lambda_1 + V\lambda_2}{\lambda_2} \tag{82}$$

By letting $\lambda_2 = 1$,

$$\lambda_1^2 = \frac{g}{TA}\ ,$$

and

$$\lambda_1 = \pm\sqrt{\frac{g}{TA}}\ . \tag{83}$$

Substituting Eq. 83 in Eq. 82, then

$$\frac{dx}{dt} = V \pm \frac{g}{T}\,\frac{1}{\sqrt{g/AT}} = V \pm \sqrt{\frac{Ag}{T}} = V \pm C$$

where C is the celerity of a small wave in the channel.

The derivatives of Y and V are combined so that they are in the same direction dt/dx, called the characteristic direction. Then

$$\frac{dt}{dx} = \frac{1}{V \pm C} \tag{84}$$

Eq. 84 implies that any disturbance of a point (x,t) in the x-t plane will propogate in two different directions, one in the direction given by the positive value of Eq. 84 and the second in the direction given by the negative value of Eq. 84. The loci of the propagations in the x-t plane are known as the "characteristic lines".

Let

$$W_f = 1/(V + C) \tag{85}$$

and

$$W_b = 1/(V - C) \tag{86}$$

be the direction of the forward characteristic line C^+ and the direction of the backward characteristic line C^-, respectively. From Eqs. 82, 85 and 86, an expression of λ_1 and λ_2 can be obtained in terms of W_f and W_b as

$$\lambda_1 = \frac{g\,W_f}{T\,(1-W_f)}$$

and

$$\lambda_2 = \frac{gW_b}{T\ (1-W_b)} \tag{87}$$

By substituting Eq. 87 in Eq. 81 two equations are obtained

$$(gT)\ dY + \left((gA - VVT)\ W_f + VT\right) dV + (TE - VTE\ W_f)dx = 0 \tag{88}$$

in the forward direction, and

$$(gT)\ dY + \left((gA - VVT)\ W_b + VT\right) dV + (TE - VTEW_b)\ dx = 0 \tag{89}$$

in the backward direction.

By introducing $C = \sqrt{gA/T}$ in Eqs. 84, 85, 86 and dividing Eqs. 88 and 89 by T the final form of the forward and backward equations respectively are

$$\left.\begin{aligned} dt - W_f\ dx &= 0 \qquad (90) \\ dV + \frac{g}{C}\ dY + E\ dt &= 0 \qquad (91) \end{aligned}\right\}\ \text{along } C^+$$

$$\left.\begin{aligned} dt - W_b\ dx &= 0 \qquad (92) \\ dV - \frac{g}{C}\ dY + E\ dt &= 0 \qquad (93) \end{aligned}\right\}\ \text{along } C^-$$

Eqs. 90, 91, 92 and 93 are of a simple form since each equation contains only total derivatives of all the variables. A solution that satisfies these equations will also satisfy the original equations, Eqs. 78 and 79.

Eqs. 90 and 92 express the propagation of any disturbance in the flow which occurs, at any point x at time t. The disturbance travels at a rate given by the equations and will move downstream along C^+ and upstream along C^- (Fig. 14.). If a disturbance occurs at point (x_1, t_1), its effect will not be felt in the flow at any other point x at time t_1 but will spread downstream and upstream at the time $t > t_1$, along C^+ and C^- respectively. If we follow this disturbance to point (x_2, t_2) along C^+ it will spread downstream along C^+ and upstream along C_1^- and, following the disturbance in the C^- direction, it will spread along C^- and C_2^+. It can be seen that the area between C^+ and C^- will be affected by the orginal disturbance at (x_1, t_1) for all $t > t_1$. This area is called the range of influence. In this range Y and V will be affected.

Consider simultaneous disturbances in the flow at two adjacent points L and R. Their characteristic lines are shown in Fig. 15 and they define four zones in the x-t plane. In Zone I no effect is felt in the character of the flow either from point L or from point R since the most advanced disturbance must follow lines C_L^+ and C_R^- in downstream and

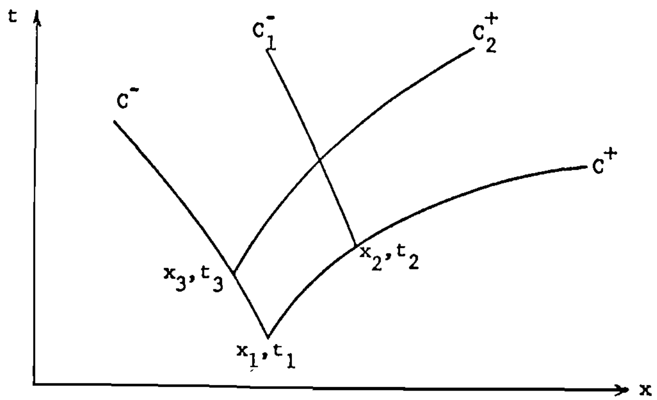

Figure 14. The range of Influence

upstream directions, respectively. It is therefore called the domain of dependence. Zone II is affected by the disturbance at point L only and Zone III is affected only by the disturbance at point R. Zone IV is the area where the range of influence of Point L and R overlap and it is therefore affected by the disturbances of both points. The value of t at P, the point of intersection of C_L^+ and C_R^-, is the time when all channel sections between points L and R respond to the disturbances.

The disturbance in the flow can be considered as an abrupt change in the flow regime and therefore it represents a discontinuity in the flow or specifically in the functions of Y and V. Hence, the characteristic lines C^+ and C^- may be considered as boundaries of continuity of the function of Y and V. For a solution to exist in some region in the x-t plane Eqs. 90 to 93 must be integrable in that region and the functions of Y and V must be continuous within this region. It therefore implies that integration of Eqs. 90, 91, 92 and 93 must be within the domain of dependence. This is an important factor in the solution by the method of characteristics.

The slope of the forward and backward characteristic lines C^+ and C^- is given at any point in the x-t plane by Eqs. 85 and 86. If the flow is a steady uniform flow, the values of V and C are constant and W_f and W_b are constant. In an unsteady flow the values of V and C are not constant and will vary with x and t and the lines C^+ and C^- will be curvilinear. The celerity of propagation of a small wave in the channel, C, is given by $\sqrt{gA/T}$. The ratio of V/C represents the Froude number of the flow and will determine whether the flow is subcritical, critical or supercritical. The effect of the ratio V/C on the slope of the characteristic lines is shown graphically in Fig. 16.

It can be seen that for a solution to the set of Eqs. 90, 91, 92, and 93 to exist, W_b in particular must be defined and in the proper direction. Hence, an important condition is that the flow must be subcritical.

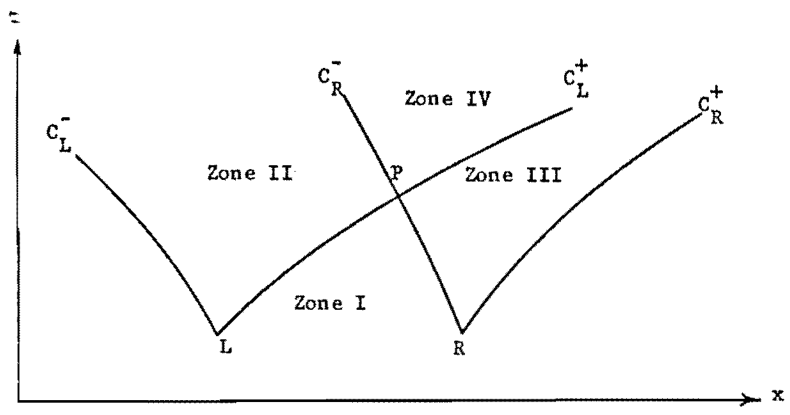

Figure 15. Domain of dependence

C. Numerical Solution

In the following sections, the low case subscripts f and b will denote the forward and backward directions, respectively, and the capital subscripts will denote the grid points at which the variable is evaluated.

The solution to the set of ordinary differential equations, Eqs. 90, 91, 92 and 93, is obtained by integrating along the characteristic lines C^+ and C^-. The integration is approximated by a finite difference scheme expressed by

$$\int_{x_0}^{x_1} f(x)\, dx = f(x_0)\,(x_1 - x_0) \qquad (94)$$

and will be called the first order approximation. The first order approximation is represented graphically by Fig. 17.

Let P be the point of intersection of C^+ characteristic line through point L and C^- the characteristic line through point R, as shown in Fig. 18.

It is assumed that values of x_L, t_L, Y_L, V_L and x_R, t_R, Y_R, V_R are known and that the values of x_p, t_p, Y_p, V_p, are to be found. Using Eq. 94 the set of Eqs. 90, 91, 92 and 93 are approximated as

$$(t_p - t_L) - W_{fL}\,(x_p - x_L) = 0; \qquad (95)$$

$$(V_p - V_L) + \frac{g}{C_L}\,(Y_p - Y_L) + E_L\,(t_p - t_L) = 0; \qquad (96)$$

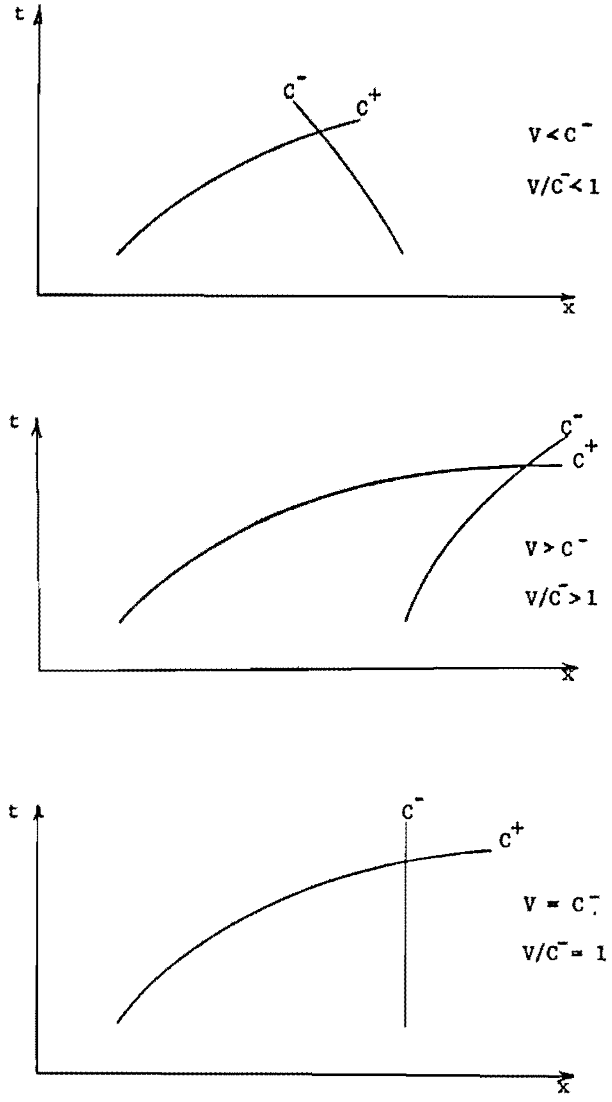

Figure 16. Slope of characteristic lines as affected by V/C.

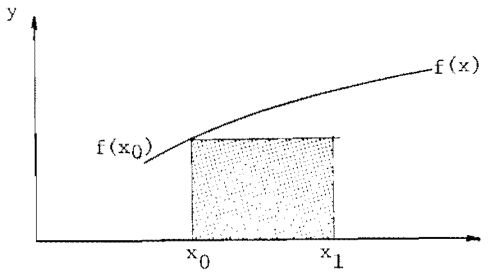

Figure 17. Graphical representation of Eq. 94.

$$(t_P - t_R) - W_{bR}\,(x_P - x_R) = 0; \qquad (97)$$

and

$$(V_P - V_R) - \frac{g}{C_R}\,(Y_P - Y_R) + E_R\,(t_P - t_R) = 0. \qquad (98)$$

Now, W_f, W_b, C and E are functions of x, t, Y and V. For initial conditions they can be evaluated for points L and R and be of known values. Therefore the unknowns remain only x_P, t_P, Y_P and V_P. If Eqs. 95 and 97 are solved simultaneously x_P and t_P become known values. When this solution is substituted in Eqs. 96 and 98 they can be solved simultaneously to produce values of Y_P and V_P. Hence, we have the initial approximation of values of x, t, Y and V at the unknown point P.

The integration can also be approximated by another scheme of finite differences expressed by

$$\int_{x_0}^{x_1} f(x)\,dx = \frac{1}{2}\Big(f(x_0) + f(x_1)\Big)\,(x_1 - x_0). \qquad (99)$$

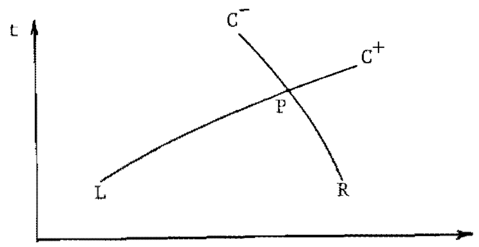

Figure 18. Advancement of the solution in x-t plane.

This scheme will be called second order or trapezoidal approximation and it is represented graphically in Fig. 19.

Expressing Eqs. 90, 91, 92 and 93 by substituting Eq. 99, a new set of equations is obtained

$$(t_P - t_L) + \frac{1}{2}\,(W_{fP} + W_{fL})(x_P - x_L) = 0 \qquad (100)$$

$$(V_P - V_L) + \frac{1}{2}\,\Big(\frac{g}{C_P} + \frac{g}{C_L}\Big)(Y_P - Y_L) + \frac{1}{2}\,(E_P - E_L)(t_P - t_L) = 0 \qquad (101)$$

$$(t_P - t_R) + \frac{1}{2}\,(W_{bP} + W_{bR})(x_p - x_r) = 0 \qquad (102)$$

$$(V_P - V_R) - \frac{1}{2}\,\Big(\frac{g}{C_P} + \frac{g}{C_R}\Big)\,(Y_P - Y_R) + \frac{1}{2}\,(E_P - E_R)(t_P - t_R) = 0 \qquad (103)$$

In the set of Eqs. 100, 101, 102 and 103, W_f, W_b, C and E at Point P are coefficients. They are dependent on x, t, Y and V at the unknown point P and the set of equations is no longer linear and cannot be solved as the set of Eqs. 90, 91, 92 and 93. An iterative method should be used instead. If values of W_{fP}, W_{bP}, C_P and E_P, evaluated from V_P and Y_P which were obtained by solving eqs. 90-93 by the first approximation are substituted into Eqs. 100-103, the second approximation (iteration) of x, t, Y and V at point P is obtained. This procedure of reevaluating the coefficients W_{fP}, W_{bP}, C_P and E_P, substituting them into Eqs. 100, 101, 102 and 103 and solving simultaneously for x_P, t_P, V_P, and Y_P can be repeated until the desired accuracy is obtained.

When a set of points A_1 . . . . . A_i of known initial values are given for time t_1 in the x-t plane (Fig. 20) this method of solution can yield a second set of points B_1 . . . . B_{i-1} of known values which in turn will be used to solve for the third set C_1 . . . . . C_{i-2}.

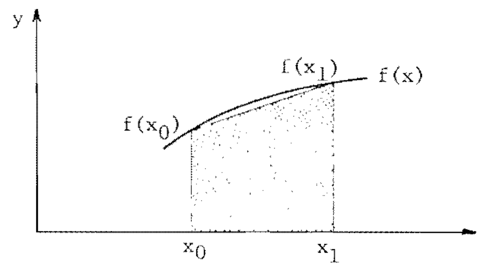

Figure 19. Graphical representation of Eq. 99.

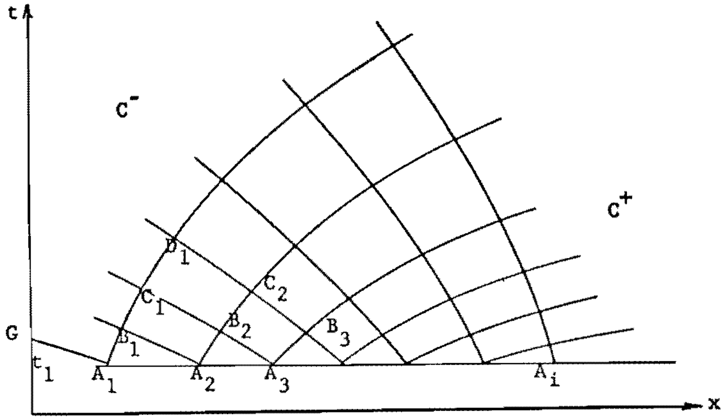

Figure 20. Region of solution for set A_i points.

It should be noted that for each new set there is one point less at which x, t, Y and V can be evaluated. The solution can be found only within the domain of dependence bounded by the initial line t_1 and characteristic line C^+ through A_1 and characteristic line C^- through A_i. In order to expand the region of the solution into zones II and III the backward and forward equations should be combined with given values or functions at the boundary. Backward characteristic line C^- through A_1 (Fig. 20) can be extended until it intersects the boundary at Point G where x, t are known. Now if any other condition can be used at the boundary, a function of Y and V the equations can be solved simultaneously to render a solution. In the upstream boundary, where the inflow discharge is known, such an equation is available. In the downstream boundary such an equation is not always available, and another approach should be used. Discussion of the boundary conditions for the specific layout of the model is presented in the next section.

It should be noted that following the above scheme the characteristic grid becomes uneven in the x-t plane. If the solution is sought for specific locations at specific times, the values from the characteristic grid must be interpolated in two directions. In most situations, a fixed grid in the x-t plane, or a specified time interval is preferred.

Consider a set of points L, M, and R of known initial values on line t in the x-t plane, Fig. 21. The values of Y and V are to be found on line t $+\Delta t$ on a fixed grid. Let P be a typical point on line t + Δt such that x (P) = x (M). The characteristic line C^+ through P intersects LM at point L and the characteristic line C^- intersects MR at point R'. Values of x_P, and t_P are known and Y_P and V_P are to be found. The inte-

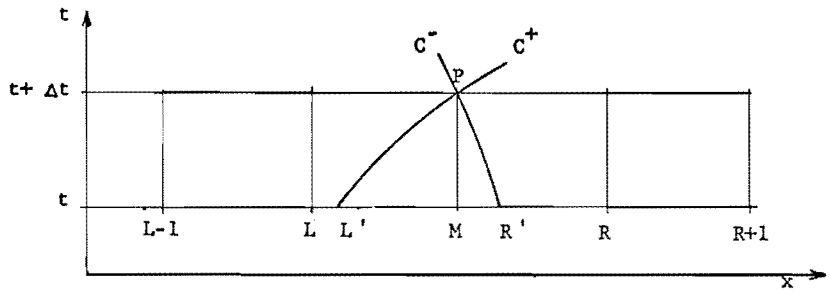

Figure 21. Fixed grid scheme.

gration should be performed along C^+ and C^- from L' and R' respectively. The position of L' and R' is not known and hence the values of $W_{fL'}$, $C_{L'}$, and $E_{L'}$, and $W_{bR'}$, $C_{R'}$ and $E_{R'}$ and not known. Now, let Δt be small enough so that the characteristic lines C^+ between L' and P and the characteristic line C^- between R' and P are very close to a straight line. The slopes of PL' and PR' can be represented by W_{fM} and W_{bM}, respectively, and the coordinates of L' and R' can be calculated by

$$(t_P - t_{L'}) = W_{fM}\,(x_P - x_{L'}), \tag{104}$$

and

$$(t_P - t_{R'}) = W_{bR}\,(x_P - x_{R'}). \tag{105}$$

When the coordinates of L' and R' are known, values of $Y_{L'}$, $V_{L'}$, $T_{R'}$ and $V_{R'}$ can be interpolated from the known values at L, M and R at initial time t. The interpolation can be either linear or quadratic. For the first approximation, a linear interpolation will suffice. The integration will be of the form

$$\int_{x_0}^{x_1} f(x)\,dx = f(x_1)(x_1 - x_0). \tag{105}$$

Eqs. 96 and 98 will become

$$(V_P - V_{L'}) + \frac{g}{C_M}\,(Y_P - Y_{L'}) + E_M\,\Delta t = 0 \tag{107}$$

and

$$(V_P - V_{R'}) - \frac{g}{C_M}\,(Y_P - Y_{R'}) + E_M\,\Delta t = 0 \tag{108}$$

and solved simultaneously to render values of Y_P and V_P as a first approximation.

Using these values, an iteration procedure is used to improve the accuracy by adding the following steps:

1) Recalculation of L' and R' coordinates for iteration (K + 1) by

$$x_{L'}^{(k+1)} = x_p - \Delta t/\frac{1}{2}\left(W_{fP}^{(k)} + W_{fL'}^{(K)}\right) \tag{109}$$

$$x_{R'}^{(k+1)} = x_p - \Delta t/\frac{1}{2}\left(W_{bP}^{(k)} + W_{bR'}^{(k)}\right) \tag{110}$$

2) Interpolate for values of $Y_{L'}$, $V_{L'}$, $Y_{R'}$ and $V_{R'}$ for iteration (k+1). Since improved accuracy is sought quadratic interpolation should be used.

3) Using the (k+1)th values of $Y_{L'}$, $V_{L'}$, $Y_{R'}$, and $V_{R'}$ calculate the (k+1)th values of $W_{fL'}$, $C_{L'}$, $E_{L'}$, $W_{bR'}$, $C_{R'}$ and $E_{R'}$; and

4) Eqs. 101 and 103 in the iterative form will be

$$\left(V_P^{(l+1)} - V_{L'}^{(k+1)}\right) + \frac{1}{2}\left(\frac{g}{C_P^{(k)}} + \frac{g}{C_{L'}^{(k+1)}}\right)\left(Y_P^{(k+1)} - Y_{L'}^{(k+1)}\right) + \frac{1}{2}\left(E_P^{(k)} + E_{L'}^{(k+1)}\right)\Delta t = 0 \tag{111}$$

$$\left(V_P^{(k+1)} - V_{R'}^{(k+1)}\right) - \frac{1}{2}\left(\frac{g}{C_P^{(k)}} + \frac{g}{C_R^{(k+1)}}\right)\left(Y_P^{(k+1)} - Y_{R'}^{(k+1)}\right) + \frac{1}{2}\left(E_P^{(k)} + E_{L'}^{(k+1)}\right)\Delta t = 0 \tag{112}$$

Again, the computation can proceed from one t level to the next. If the grid in x-t plane is given and values of Y and V given at i grid points at level t, then Y and V can be computed for (i-2) grid points at level (t + Δt) using either Eqs. 104, 105, 107 and 108 for the first estimate, and if higher accuracy is desired, using Eqs. 109, 110, 111 and 112 for the iteration procedure. Now using the calculated values at level t + Δt the calculations can proceed to solve for (i-4) grid points at level t + 2Δt, and so on.

1. Center Stations

For convenience the equations will be set in a simpler form.

Let

$$G_{1f} = G_{1b} = g/C_M \tag{113}$$

$$F_{1f} = V_{L'} + G_{1f}\, Y_{L'} - E_M\, \Delta t, \tag{114}$$

and

$$F_{1b} = V_{R'} - G_{1b}\, Y_{R'} - E_M\, \Delta t. \tag{115}$$

Eqs. 112 and 113 become

$$V_P = F_{1f} - G_{1f}\, Y_P, \tag{116}$$

and

$$V_P = F_{1b} + G_{1b}\, Y_P. \tag{117}$$

To avoid confusion note that G and F are expressions of functions, the lower case subscripts 1f, 1b denote first order in forward and backward direction, respectively, and capital subscripts denote the grid point at which the variable is evaluated.

Eqs. 116 and 117 will be called the first order forward routing equation and first order backward routing equation, respectively. For the iteration procedure, second order iteration is used. Let

$$G_{2f} = \frac{1}{2}\left(\frac{g}{C_{L'}} + \frac{g}{C_P}\right), \tag{118}$$

$$G_{2b} = \frac{1}{2}\left(\frac{g}{C_{R'}} + \frac{g}{C_P}\right), \tag{119}$$

$$F_{2f} = V_{L'} + G_{2f}\, Y_{L'} - \frac{1}{2}\left(E_P + E_{L'}\right)\Delta T, \tag{120}$$

and

$$F_{2f} = V_{R'} - G_{2b}\, Y_{R'} - \frac{1}{2}\left(E_P + E_{R'}\right)\Delta t. \tag{121}$$

Eqs. 116 and 117 become

$$V_P = F_{2f} - G_{2f}\, Y_P, \tag{122}$$

and

$$V_P = F_{2f} + G_{2b}\, Y_P. \tag{123}$$

Eqs. 122 and 123 will be called second order forward routing equation and second order backward routing equation, respectively.

In further discussions the subscripts 1 and 2 denoting first approximation and iterated approximation, respectively, will be discontinued. It should be remembered that actually different functions are involved.

A center station is defined as a station that has at least one other station both upstream and downstream within the same reach as shown in

Fig. 21. At a center station two characteristic lines can be obtained and the forward routing equation and the backward routing equation can be solved simultaneously to render a solution for Y_p and V_p.

Eqs. 116 and 117 for first approximation, or Eqs. 122 and 123 for the iteration procedure when solved simultaneously give

$$Y_p = (F_f - F_b) / (G_f + G_b) , \qquad (124)$$

and

$$V_p = (F_f G_b + F_b G_f) / (G_f + G_b), \qquad (125)$$

where F_f, G_f, F_b and G_b are the corresponding functions for the first or the iterated solution.

2. Upstream Boundary Stations

The upstream boundary station is defined as the most upstream station of the reach if or when this station does not affect the flow at the upper reach (Fig. 22).

The forward characteristic line does not exist at this station, therefore a forward routing equation cannot be used. The boundary conditions are known at this station for all t's since the inflow hydrograph is given. Expressing the known discharge by the continuity equation $Q_p = V_p A_p$, where A_p is the cross section area of the channel with defined geometry, the second necessary condition for the solution is obtained. Therefore, for a trapezoidal channel, the two simultaneous equations are

$$V_p = F_b + G_b Y_p, \qquad (126)$$

and

$$Q_p = V_p A_p = V_p (B + ZY_p) Y_p, \qquad (127)$$

where B is the bottom width and Z is the side slope ratio of the channel. By substituting Eq. 126 into Eq. 127 and rearranging a cubic equation of Y_p is obtained.

$$G_b Z Y_p^3 + (F_b Z + G_b B) Y_p^2 + F_b B Y_p - Q_p = 0. \qquad (128)$$

Y_p can be calculated directly from Eq. 128. By substituting the value of Y_p in Eq. 127, V_p is obtained.

As before, F_b and G_b are the corresponding functions for the first or the iterated solution.

3. Downstream Boundary Stations

The downstream boundary station is defined as the most downstream station of the reach where the flow neither affects nor is affected by the flow in the downstream reach as shown in Fig. 23. Only the forward

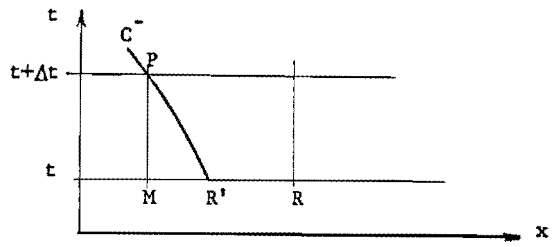

Figure 22. Upstream boundary grid.

routing equation is available here since the boundary condition at any time t is the required solution in this work. If a control such as critical depth exists, a second equation can be used. Another approach is to assume an imaginary channel extending in the downstream direction from point M. If no control section is assumed along this channel the flow will tend to become normal. Values of stations along the imaginary channel can be used to extend the domain of influence to include point P. The disadvantage of this approach is the fact that the number of imaginary stations needed is equal to the number of time steps and will prove to be very expensive in computer time.

When no control section exists along the channel and the flow tends to normal flow, the partial differential equations, Eqs. 73 and 74, can be solved by finite differences. In this case it is assumed that the characteristics of the flow at point P is affected by disturbances from the upstream direction only. Express Eq. 78 as

$$Q_x + TY_t = 0, \qquad (129)$$

and define the finite difference scheme as

$$Q_x = (Q_M - Q_{L'}) / \Delta x'; \quad Y_t = (Y_P - Y_M) / \Delta t \qquad \text{(Fig. 23)}$$

By substituting into Eq. 129, Y_P is the only unknown variable in the equation

$$Y_P = Y_M + \frac{1}{T_M} (Q_{L'} - Q_M) \frac{\Delta t}{\Delta x}. \qquad (130)$$

The values of Y_p can be substituted into Eq. 122 to solve for V_p.

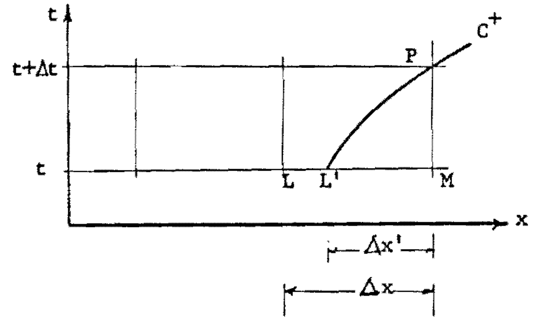

Figure 23. Downstream boundary grid.

4. Junction Stations

Channels with changes in the reach geometry present different boundary conditions. In case of changes, a backwater effect will take place and it will affect the flow characteristics in the upstream direction. At the place where two channels of different geometry meet, a simple two-way junction exists. If a tributary is flowing into the main channel the junction will be a three-way junction. In this particular model, as explained before, a two-way junction was considered at every point where a tributary joins the main channel, taking into consideration the additional discharge from the tributary, but disregarding any backwater effect into the tributary. Fig. 24 shows the plan view and profile of the channel at the junction. The solution scheme at the junction is shown by Fig. 25. Because of the discontinuity in the channel, $Y_U \neq Y_D$ and $V_U \neq V_D$. The forward and backward characteristic equations constitute a set of two equations with four unknowns. Two boundary conditions are added to the forward and backward equations, based on the continuity of the flow and the continuity of the water surface to form a set of four equations. The four simultaneous equations are:

$$V_U = F_f - G_f Y_U \tag{131}$$

$$V_D = F_b + G_b Y_D \tag{132}$$

$$Y_D = Y_U + D \tag{133}$$

$$Q_D = Q_U + Q_T \tag{134}$$

where D is the drop in the channel bottom and Q_T is the tributary flow discharge at time $t = t+\Delta t$. Eq. 134 can be written in terms of flow velocity and depth as

$$V_D (B_{M'} + Z_{M'} Y_D) Y_D = V_U (B_M + Z_M Y_U) Y_U + Q_T \tag{135}$$

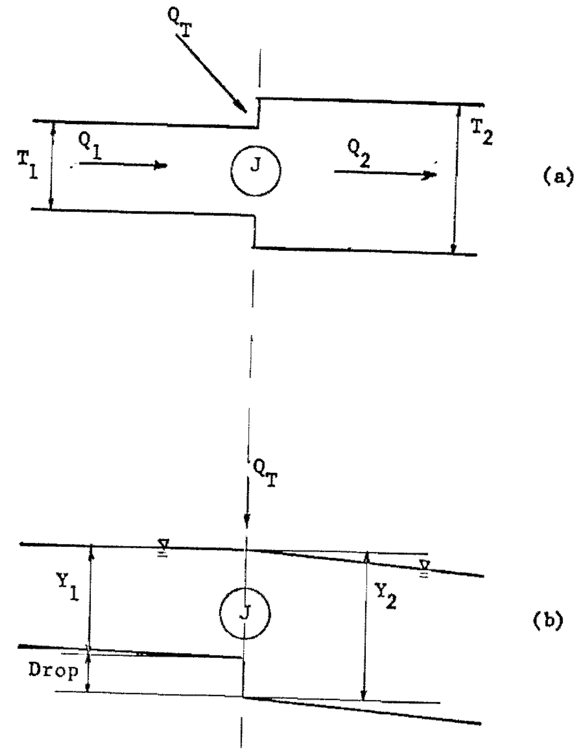

Figure 24. Junction. (a) Channel Plan View. (b) Channel Profile.

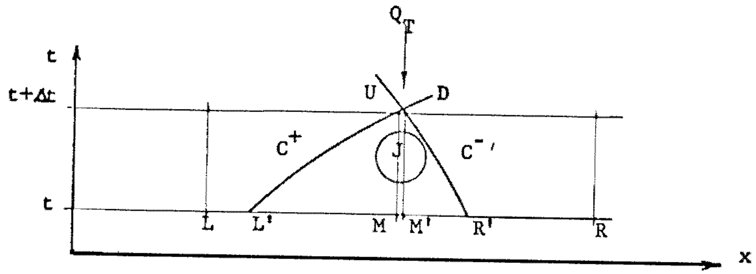

Figure 25. Two Way Junction Grid.

Substituting of Eqs. 131, 132 and 133 into Eq. 135, solving and rearranging in order of Y_U a cubic equation is obtained as

$$a_1 Y_U^3 + a_2 Y_U^2 + a_3 Y_U + a_4 = 0 \tag{136}$$

where

$$a_1 = G_f Z_M + G_b Z_{M'}, \tag{137}$$

$$a_2 = F_b Z_{M'} + G_b B_{M'} + G_f B_M - F_f Z_M + 3DG_b Z_{M'}, \tag{138}$$

$$a_3 = F_b B_{M'} - F_f B_M + 2D (F_b Z_{M'} + G_b B_{M'}) + 3D^2 G_b Z_{M'}, \tag{139}$$

and

$$a_4 = F_b B_{M'} D + D^2 (F_b Z_{M'} + G_b B_{M'}) + D^3 G_b Z_{M'} - Q_T. \tag{140}$$

Y_U can be solved directly from the cubic equation, Eq. 136, and the values substituted into Eqs. 131, 132 and 133. Again, F_f, F_b, G_f and G_b are the corresponding functions for the first or the iterated solution.

D. Application of the Solution

A necessary condition in applying the numberical solution in the case of no lateral flow is that the depth of flow in the channel be greater than zero. Machmeier (29) used a base flow of 4.9 cubic feet per second per square mile (cfsm) equal to one tenth of the mean annual flood, estimated from surface water records of watersheds in southeastern Minnesota. Initial flow of the same value was used in this work.

A rectangular grid is used in the x-t plane. The time interval Δt should be such that the point for which the solution is sought lies within the domain of dependence of the two adjacent points in the previous time step. The time increment is calculated from Eq. 84 by

$$\Delta t = \Delta x / (V+C). \tag{141}$$

Since the velocity varies at each level of t with position along the main channel, it becomes necessary to calculate allowable Δt for each station, and the minimum value of all the stations is used as the time increment for the whole watershed.

The input to the channel system is the outflow hydrograph of the elementary channel given by an array of equal time increments. A linear interpolation is used to obtain the input discharge for the respective watershed time. The solution is then advanced along the main channel (along the x direction in the x-t plane) for time $t = t_i$ from the uppermost station to the watershed outlet using the routing equations for the upstream, center, downstream or junction control according to the respective position of the station in the model. After the flow conditions are solved for all stations for time t_i, the common allowable time

increment is calculated and advanced to $t = t_i + \Delta t$ and the solution advanced again along the main channel.

E. Test Runs

The model watershed and the routing equations were programmed in FORTRAN IV computer language for numerical solution to be performed on the University of Minnesota CDC 6600 digital computer. Test runs were made using the "standard condition" values of the various variables along the main channel of stream order 2 (51 stations).

During the first trial runs it was found that using the time increment Δt as the minimum of all values calculated by Eq. 141 for each station did not insure convergence of the solution. From the beginning, instability was detected and the solution fluctuated. A STOP control statement was used in the event that the depth in the main channel became negative. Other investigators (2), (28) who encountered the same problem suggested using a smaller time interval. The following steps were taken to avoid this problem:

1) the calculated increment Δt was reduced by a linear factor. This factor was increased gradually with every time step as the solutions advanced, to a maximum value of 0.9;

2) the distance between stations, Δx, was set so that the joint effect of the smaller distance and the minimum reduction factor provided a stable solution with the most efficient computer time; and

3) the tributary flow from the elementary channel was set as zero until it reached a value greater than 0.01 percent of the initial flow.

The above steps gave a stable solution with the starting value of the factor 0.7. The number of iterations at every station was set at 2.

As the solution advanced to reach the equilibrium flow in the channel, further inconsistencies were noticed. The discharge at each station along the main channel was greater than the discharge at the adjacent upstream station and exceeded the equilibrium discharge. This was found to be caused by the solution of the junction control. The instability was caused by the backwater effect. The following steps were taken to avoid this problem:

1) backwater effect was ignored as long as the water surface elevation at the downstream station at the junction was not higher than the water surface elevation at the upstream station of the junction. Until then, junction stations were not solved simultaneously but rather as downstream and upstream controls, respectively;

2) the positions of the front of the flood wave moving downstream and the front of the backwater wave moving upstream were checked and quadratic interpolation was used to insure greater accuracy of the values used for the integration along the characteristic lines; and

3) the number of iterations at the junction stations was set as 3 to further insure accuracy of the backwater effect.

All the above mentioned steps were found necessary to achieve consistent results. Some fluctuations could still be detected but they were dampened as the solution advanced.

The solution approached the equilibrium condition very slowly. In the trial runs the program was set to stop the calculations as the flow at the outlet of the watershed reached 99.9 percent of equilibrium. Some fluctuations of the solution were noticed when the solution approached $.999Q_e$. These fluctuations did not cause divergence of the solution but were carried to the adjacent station at the next time step. Increasing the number of iterations at this level controlled these fluctuations but was found to be very costly in computer time.

The overall computer time for the program, with the above mentioned measures, was estimated to be about 12 minutes for one stream order with 51 stations. An exact time could not be calculated since, during the trial runs, continuation decks that were punched at five minute watershed time intervals were used to advance the solution in the next trial. Under these conditions the program was judged to be inefficient and impractical for the study. The following measures were then taken to increase efficiency of the program and tested to their effect on the results:

1) calculations were performed for the stations covered by the flood wave moving downstream and stations covered by backwater wave moving upstream. All stations not covered by the waves were kept at initial values;

2) when the discharge at the upstream station of the reach exceeded 15 percent of equilibrium discharge the iteration process for the stations along the reach was discontinued and the first approximation value was used.

3) when the discharge at the upstream station of the reach exceeded 25 percent of equilibrium discharge the Δx was doubled and the calculations were performed for every second station along the reach. (Dropping of more stations was tried and found to cause fluctuations at a level less than $0.97\ Q_e$);

4) as the discharge of the downstream station of the reach exceeded 85 percent of Q_e the number of iterations was increased to two, and further increased to three when the discharge exceeded $0.96\ Q_e$; and

5) when the discharge at the downstream station of the reach exceeded $0.985\ Q_e$ the routing procedure was discontinued and the solution was advanced by a linear procedure to the pre-calculated equilibrium conditions.

The above measures were found satisfactory and caused a appreciable reduction in computer time. Since the time to virtual equilibrium was of interest it was decided to carry the calculation by the routing procedure, without disturbances, to a level higher than 97 percent of equilibrium. A procedure of dropping out more stations would save more computer time but the stability would have been affected at a lower level than 97 percent of equilibrium.

The program of the model watershed, the numerical routing and the various routines were then extended to the fourth stream order watershed. The program includes the main program, fourteen subroutines and two function subprograms. The program is presented in the Ph.D. Thesis by Golany (University of Minnesota, 1970).

The calculated depth, velocity and discharge of every eighth station in every reach were printed out following each minute of watershed time. Since the test runs were rather long, eight to twelve minutes computer time, they were run in parts. The computation was stopped at a prespecified watershed time and a continuation deck was punched out containing all necessary information. After checking the intermediate results, the calculation proceeded to another specified watershed time, using the data from the continuation deck. At the end of the calculations, the outflow hydrographs of the four stream orders were punched out for every minute of watershed time.

A signal was used in the program to indicate whether to activate the backwater procedure in the junctions. For runs without backwater effect the two stations of each junction were not solved simultaneously, but separately as downstream and upstream controls.

CHAPTER VII

ANALYSIS OF CHANNEL CHARACTERISTICS AND THEIR INTERRELATIONSHIP

The theoretical expression for the time to virtual equilibrium, Eq. 27, provides a potential basis for analyzing the relationship of the time parameter to watershed characteristics. The variables involved have been shown to be the roughness coefficient n, the bed slope of the channel reach S, the length of the reach l, the watershed drainage area A, the cross section wetted perimeter P of each channel reach, and the runoff supply rate q. The wetted perimeter is a variable, dependent on the channel cross section geometry as well as on all other factors that control the flow.

The theoretical expression for T_{ve} was based on some generalized assumptions and has to be tested and verified experimentally. Thus, experiments were designed to study the effect of each independent factor on the time parameter T_{ve}. By doing this, Eqs. 27 and 35 can be tested for the validity of the basic assumptions.

As a first step each of the variables has to be tested for its independency and set in the model in a manner that will permit variations on a watershed basis. Various slope parameters are introduced and S*, which is based on hydraulic considerations, is chosen for the model. The wetted perimeter is then expressed in terms of the independent variables on a watershed basis.

A. The Channel Bed Slope, S

In Eq. 27, the slopes of the individual reaches appear under the summation sign. Since S_i is not constant for all reaches it cannot be "factored out" to be analyzed for its effect on T_{ve}. A slope parameter which will represent the various combinations of the individual slopes in the watershed is therefore needed. The commonly used slope parameters are:

1) mean slope, defined as

$$S_m = \Delta H/L \tag{142}$$

where S_m is the mean slope, ΔH is the difference in elevation along the main channel between the watershed divide and the watershed outlet and L is the total length of the main channel;

2) effective slope, defined as

$$S_{ef} = \Delta H_{.7}/L_{.7} \tag{143}$$

where $L_{.7}$ is the center 70 percent of the main channel length and $\Delta H_{.7}$ is the elevation difference for $L_{.7}$;

3) S*, presented by Taylor and Schwarz (39) and defined as a hypothetical uniform slope for the main channel of the watershed which would give the same travel time for the watershed as reach by reach calculation. In the derivation of the equation for S* an assumption is made that the roughness coefficient and the hydraulic radius are the same for all reaches of the watershed. S* is given by

$$S^* = \left[\frac{L}{\sum (l_i/\sqrt{S_i})} \right]^2 \tag{144}$$

where L is the length of the main channel and l_i and S_i are the length and the slope of the i-th reach, respectively if $l_1 = l_2 = \dots\dots\dots l_i$ the equation becomes

$$S^* = \left[\frac{1}{\sum (1/\sqrt{S_i})} \right]^2$$

4) S_a, shown in Fig. 26. A straight line is drawn from the outlet end of the profile producing areas between it and the bed profile. If the areas above and below the straight line are equal, the slope of the line is by definition S_a.

The total area under the bed profile (A) is equal to the total area of the triangle under the line with the slope S_a. Thus, the area is given by

$$A = \frac{1}{2} h_a L.$$

h_a is then given by

$$h_a = \frac{2A}{L}$$

and

$$S_a = \frac{h_a}{L} = \frac{2A}{L^2} . \tag{145}$$

The slope parameter S* was felt to be the best to represent the overall slope of the main channel, since it is based on hydraulic considerations, despite the fact that the variations of the hydraulic radius were neglected. The mean slope and the effective slope have the disadvantage of not representing the weighted effect of the individual reaches. S_a emphasizes the slope of the lower end but is not defined on a hydraulic basis.

The slopes of the individual reaches for the standard conditions were determined by following Machmeier's (28) relationship for southeast Minnesota,

$$S_R = 0.003155/A_r^{0.20}$$

where A_R is the drainage area at the first station of the reach. The slopes of the various reaches of the watershed at standard condition are presented in Table 2.

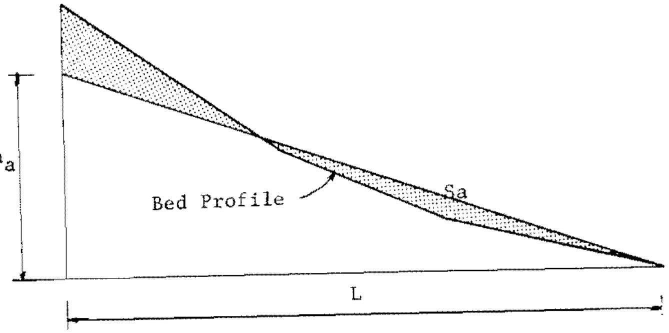

Figure 26. Definition of S_a

Five tests were designed to determine the effect of bed slope on the time parameter T_{ve}. The slope shape (concave) was retained for all runs by adjusting the reach slopes proportionately. For each run the reach slopes were determined by multiplying the "standard" slope of each reach by a slope factor α_s.

The values used for α_s were 2.0, 1.0, 0.75, and 0.5. Table 6 presents a comparison of the resulting slope parameters for the watershed of stream order 4. Table 7 presents the comparison of S* and S_a for the various slopes for stream orders 2, 3, and 4. It should be noted that the various slope values in Table 7 are for the main channel only. The elementary channel, where lateral inflow occurs, was included in the calculation of the slope parameters in Table 6.

α_s	S_m	S_{ef}	S_a	S*
2.0	0.00619	0.00604	0.00546	0.00592
1.5	0.00471	0.00462	0.00414	0.00444
1.0	0.00323	0.00320	0.00283	0.00296
0.75	0.00249	0.00249	0.00218	0.00222
0.5	0.00175	0.00179	0.00152	0.00148

Table 6. Slope parameters S_m, S_{ef}, S_a and S* for stream order 4 and various watershed slopes.

α_s	Stream order 2		Stream order 3		Stream order 4	
	S*	S_a	S*	S_a	S*	S_a
2.0	0.00912	0.00915	0.00730	0.00701	0.00566	0.00531
1.5	0.00684	0.00691	0.00548	0.00530	0.00424	0.00404
1.0	0.00456	0.00467	0.00365	0.00360	0.00283	0.00276
0.75	0.00342	0.00355	0.00274	0.00275	0.00212	0.00212
0.5	0.00228	0.00243	0.00183	0.00190	0.00141	0.00149

Table 7. Slope parameters S* and S_a for stream orders 2, 3, and 4 and various watershed slopes, main channel only

B. The Channel Roughness, n

As discussed in previous chapters, although the roughness coefficient n is known to vary with depth of flow there is lack of agreement as to the nature and magnitude of the variation. At high stages, when overbank flow exists, the roughness coefficient may vary drastically from the values when the flow is confined in the channel bed. In this study the roughness was considered constant with respect to stage and the flow was confined within the channel for all stages.

In Eq. 27 the roughness coefficient appears for each individual reach. The values of n may vary from reach to reach according to the bed roughness, vegetation, etc. However, channel roughness tends to be similar within a given geologic area or a given watershed. Thus, for each experiment with the model watershed, a single value of the roughness coefficient was chosen for all reaches. This makes it possible to "factor out" n in Eq. 27 and to analyze the overall effect of the roughness more conveniently.

The roughness coefficient for the standard condition was taken as n = 0.04. The n- values chosen for the tests were 0.02, 0.03, 0.04, 0.55 and 0.08 to cover the probable range of roughness under natural conditions.

C. The Wetted Perimeter, P.

In Eq. 27, the wetted perimeter of the individual stations appears under the summation sign. The wetted perimeter is not an independent variable but rather is dependent on the discharge, Q, of the channel roughness n, on the bed slope S and on the channel cross section geometry. The wetted perimeter term in Eq. 27 should be expressed in terms of its independent components in order to have Eq. 27 in an analytical form.

The general relationship of P and Q for a given reach was presented in Chapter III. Now the total watershed must be considered. Values of n and sideslope ratio are constant but the bottom width and slope of the main channel vary from reach to reach. Fig. 27 is a log-log plot of the wetted perimeter vs. discharge for reaches 4, 8 and 13. The point of equilibrium discharge for a supply rate of one inch per hour is marked for each reach. By connecting the points of equilibrium discharge of each reach a straight line (dashed in Fg. 27) is obtained, yielding the relationship

$$P_i = K\, Q_i^{0.412} \qquad (146)$$

where P_i is the wetted perimeter of the reach, Q_i is the equilibrium discharge of the reach and K is the coefficient.

Eq. 146 relates the wetted perimeter of any reach of the model watershed for a steady uniform flow at normal conditions to the equilibrium discharge of the reach. The equation will apply only to the given channel geometry and the given equilibrium discharge.

The equilibrium discharge is given by $Q_i = 646\ q\ A_i$. The excess rainfall supply rate, q, is taken as 1.0 in/hr., constant for all runs in this study. It can be seen from Fig. 27 that if the supply rate changes, the line connecting the equilibrium discharges for the various reaches will shift. It will be a straight line, but with a slightly different slope. Thus, the exponent in Eq. 146, relating the wetted perimeter to the equilibrium discharge, is a dependent variable rather than a constant. It is a function of the channel cross section as well as the supply rate.

The relationship of P and Q is established now on a <u>watershed basis</u>. The wetted perimeter of any reach is given as a function of the <u>equilibrium discharge</u> as it varies <u>between reaches</u> of the model watershed.

In order to analyze the effect of the roughness coefficient n and the bed slope S on the wetted perimeter, values of P_i were calculated for normal flow by Manning's equation for values of Q_i, varying the roughness and the slope as chosen for the tests. Tables 8 and 9 present the equilibrium discharge Q_i for each reach with the calculated values of P_i for the series of n and the series of S*, respectively. The results are shown graphically in Figs. 28 and 29 respectively.

It can be seen in Figs. 28 and 29 that the slope of the lines is a constant and the variations in n and S affect the coefficient. Regression analyses of the data of Figs. 28 and 29 yield the relationship between P and Q as given by Eq. 146. The values of the coefficient K for the various roughness values are presented in Table 10. The results plot as a straight line on log-log scale as shown in Fig. 30. A regression analysis of the data yields the equation

$$K = 6.671\ n^{0.363} \qquad (147)$$

Table 11 presents the values of the coefficient K for the various values of slope parameter S* for each stream order. Fig. 31 presents the graphical results.

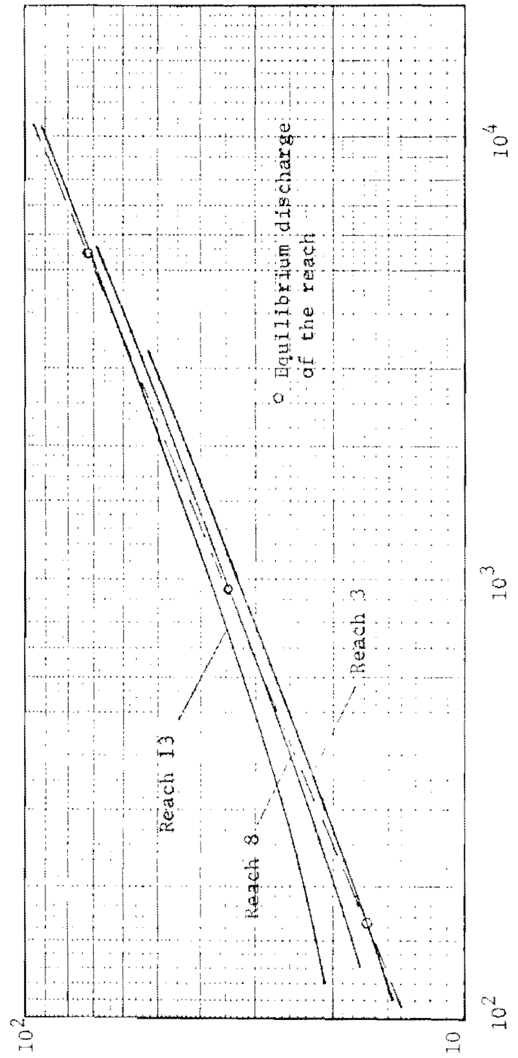

Figure 27. Wetted perimeter as a function of discharge for individual reaches and channel as a whole.

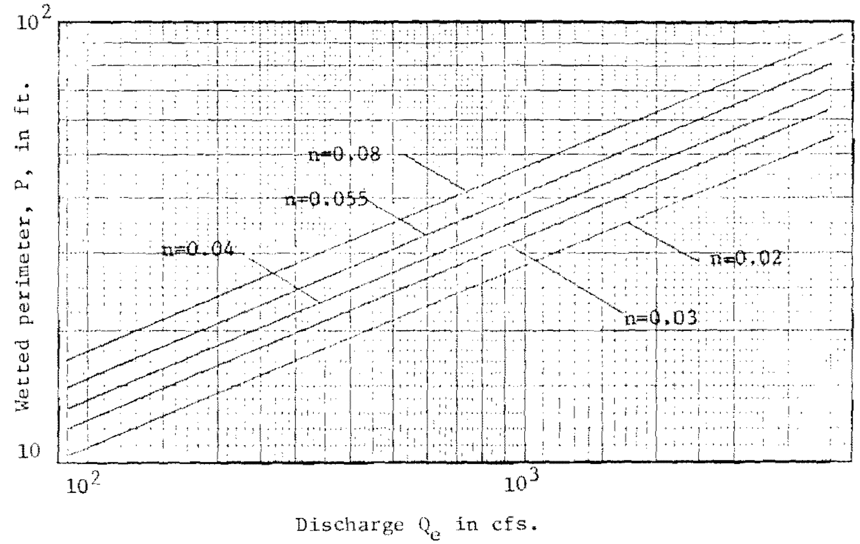

Figure 28. Wetted perimeter, P_i vs. equilibrium discharge Q_i as it varies between reaches of the model watershed for various n values.

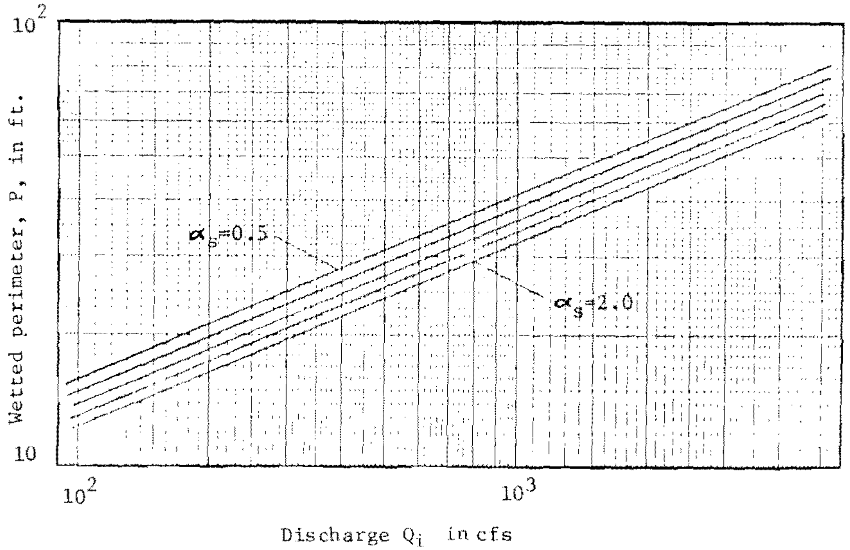

Figure 29. Wetted perimeter P_i vs. equilibrium discharge Q_i as it varies between reaches of the model watershed for various S values.

Reach No.	Q_i cfs.	P in feet for				
		n=0.02	n=0.03	n=0.04	n=0.055	n=0.08
2	97.26	10.75	12.36	13.63	15.38	17.68
3	163.27	13.13	15.15	16.81	18.92	21.78
4	163.27	13.13	15.15	16.81	18.92	21.78
5	489.80	20.62	23.92	26.63	30.03	34.64
6	555.11	21.65	25.08	27.91	31.46	36.28
7	881.64	25.71	29.82	33.20	37.44	43.18
8	946.95	26.85	31.17	34.72	39.17	45.19
9	946.95	26.85	31.17	34.72	39.17	45.19
10	2,840.85		49.07	54.72	61.79	71.36
11	3,167.39		51.11	56.99	64.36	74.31
12	5,061.29		52.52	69.75	78.99	91.00
13	5,387.82		63.99	71.39	80.63	93.12

Table 8. Variations of wetted perimeter with roughness for uniform equilibrium flow in various reaches (q = 1.0 in./hr.)

Since the slope parameter S* varies for the different stream orders, the regression analyses yield three lines in the form

$$K = c_j \, S^{*-0.185} \tag{148}$$

where c_j is a coefficient for a given n that varies with the stream order.

By substituting Eqs. 147 and 148 in Eq. 146 the wetted perimeter, P_i, for any reach is now given by

$$P_i = C_j \, S^{*-0.185} \, n^{0.363} \, Q_i^{0.412} \tag{149}$$

where Q_i is the equilibrium discharge for the reach in cubic feet per second and C_j is a new coefficient. The values of C_j for Eq. 148 and C_j for Eq. 149 for the various stream orders are given in Table 12.

Eq. 149 gives the wetted perimeter of any reach as a function of several watershed characteristics, assumed to have independent effects. The procedure is laborious but is necessary to eliminate the dependent

Reach No.	Q_i cfs.	P in feet =2.0	=1.5	=1.0	=0.75	=0.5
2	97.96	12.10	12.73	13.69	14.42	15.54
3	163.27	14.83	15.62	16.81	17.73	19.12
4	163.27	14.83	15.62	16.81	17.73	19.12
5	489.80	24.41	24.69	26.63	28.11	30.35
6	555.11	24.55	25.88	27.91	29.46	31.80
7	881.64	29.18	30.78	33.20	35.04	37.84
8	946.95	30.50	32.17	34.72	36.66	39.59
9	946.95	30.50	32.17	37.72	36.66	39.59
10	2,840.85	47.99	50.67	54.72	57.80	62.46
11	3,167.39	49.93	52.78	56.99	60.20	65.05
12	5,061.29	61.14	64.57	69.75	73.69	79.65
13	5,387.82	62.58	66.08	71.39	75.42	81.51

Table 9. Variations of wetted perimeter with slope for uniform equilibrium flow in various reaches (q = 1.0 in./hr.)

n	K
0.02	1.1622
0.03	1.857
0.04	2.057
0.055	2.325
0.08	2.675

Table 10. Coefficient K in Eq. 146 as a function of the roughness

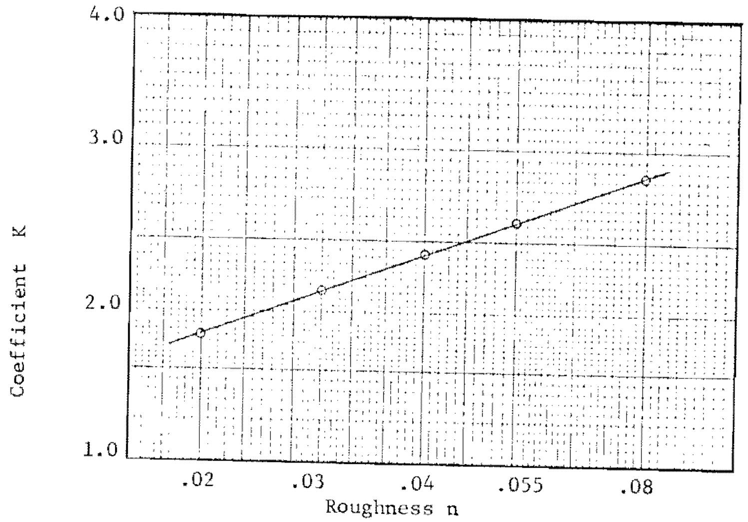

Figure 30. Coefficient K (Eq. 147) as a function of the roughness n(α_s=1.0)

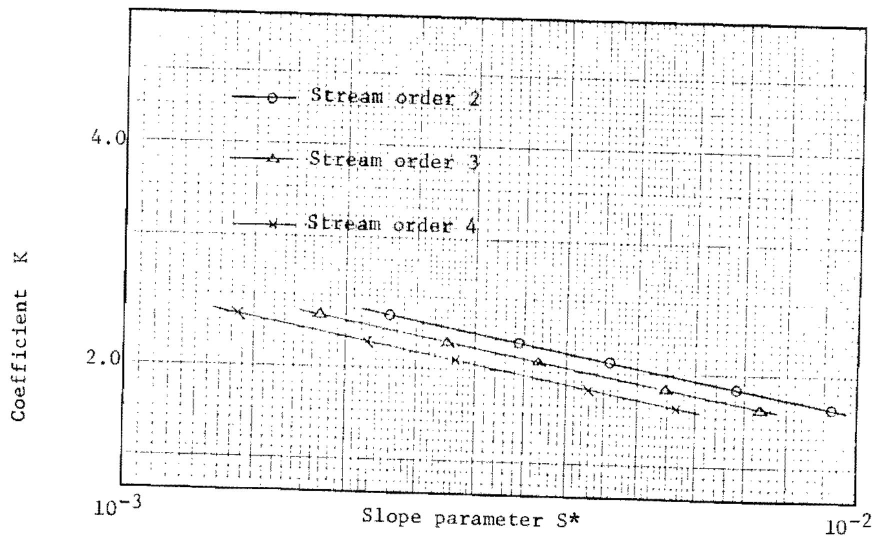

Figure 31. Coefficient K (Eq. 147) as a function of S* (n=0.04)

Coefficient K	Slope parameter S* Stream Or. 2	Stream Or. 3	Stream Or. 4
1.817	0.00912	0.00730	0.00566
1.916	0.00684	0.00548	0.00424
2.057	0.00456	0.00365	0.00283
2.178	0.00342	0.00274	0.00212
2.350	0.00228	0.00183	0.00141

Table 11. Coefficient K in Eq. 146 as a function of the slope parameter S* (n = 0.04)

Stream Order	c_j (Eq. 148)	c_j (Eq. 149)
2	0.760	2.252
3	0.728	2.204
4	0.697	2.156

Table 12. Values of the Coefficients for Eqs. 148 and 149.

term P_i from Eq. 27. However, it is based on uniform flow calculations which can be made for any main channel system.

The channel bottom width for each reach in the model watershed was determined using Machmeier's (28) general relationship of channel geometry in southeastern Minnesota. The sideslope ratio was set as 1:1. The bottom width and the sideslope ratio of each reach are input variables in the model watershed's program.

D. Drainage Area and Main Channel Length

The watershed model was designed to fit best Gray's (11) relationship of channel length to drainage area (Eq. 39.) Thus, the drainage area A and the main channel length L are given as one dependent on the other. The outlet of the model is at the end of the fourth stream order where the elementary channel is designated as stream order one. Thus, the outlets of stream orders 2, 3 and 4 can be used to analyze the combined effect of A and L on the time to virtual equilibrium.

E. Runoff Supply Rates

The effect of the runoff supply rate on the time to virtual equilibrium was thoroughly investigated by Machmeier (28) using a similar watershed model. He found the relationship

$$T_{ve} = 2.097\ q^{-0.232}$$

for a watershed area of 21.35 square miles, indicating a mild non-linear relationship. Considering this and the limitations of time and computer cost, the effects of supply rate, q, were not included in this study.

CHAPTER VIII

EXPERIMENTAL RESULTS

The data obtained from the numerical routing procedure on the watershed model are presented in tabular form in Appendix A. Selected hydrographs are presented in this chapter to illustrate the effects of the various factors tested on the time to virtual equilibrium. Results of the runs with and without backwater effect are compared in this chapter. The results of the other tests are presented here and analyzed and discussed in Chapter IX.

A. Results of Runs With and Without Backwater

It was recognized from the beginning of this work that backwater could have a significant effect on the time to virtual equilibrium and a great deal of effort was devoted to incorporating the backwater effect into the model. As described in Chapter IV, Section C, backwater was considered in the main channels only.

In order to study the backwater effect, two tests were made with the model for the standard conditions, one with and one without backwater. The results of this comparison are presented in Table 13. These results indicate the importance of the backwater in the model watershed. As can be expected, the time to virtual equilibrium with backwater effect is greater than the time to virtual equilibrium without backwater effect, since part of the flow has to fill up additional storage in the channel system. It can also be noted that the discrepance increases with the increase of watershed area, perhaps due to the decrease in the slope of the main channel. Also, the elementary channel, which had no backwater, becomes of lesser relative importance as the watershed size is increased.

Stream Order	T_{ve} in min. with backwater	T_{ve} in min. w/out backwater	Difference in min.	Difference %
2	32.41	30.75	1.66	5.1
3	52.53	46.22	6.31	12.0
4	83.25	70.55	12.70	15.3

Table 13. Time to virtual equilibrium of the model watershed with and without backwater effect.

Figs. 32 and 33 show the water surface profile for a typical single reach, Reach 9, in stream order 4, for various watershed times from zero to time of equilibrium for the two cases without and with backwater effect, respectively. Stations 185 to 217 (reach 9) comprise a reach where no lateral inflow occurs. The stations are spaced 107.7 feet apart with a total length of 3517 feet. The slope of the channel bed is 0.003 feet per foot and is shown on the figures. The water surface profile shows the nonsteady flow characteristics.

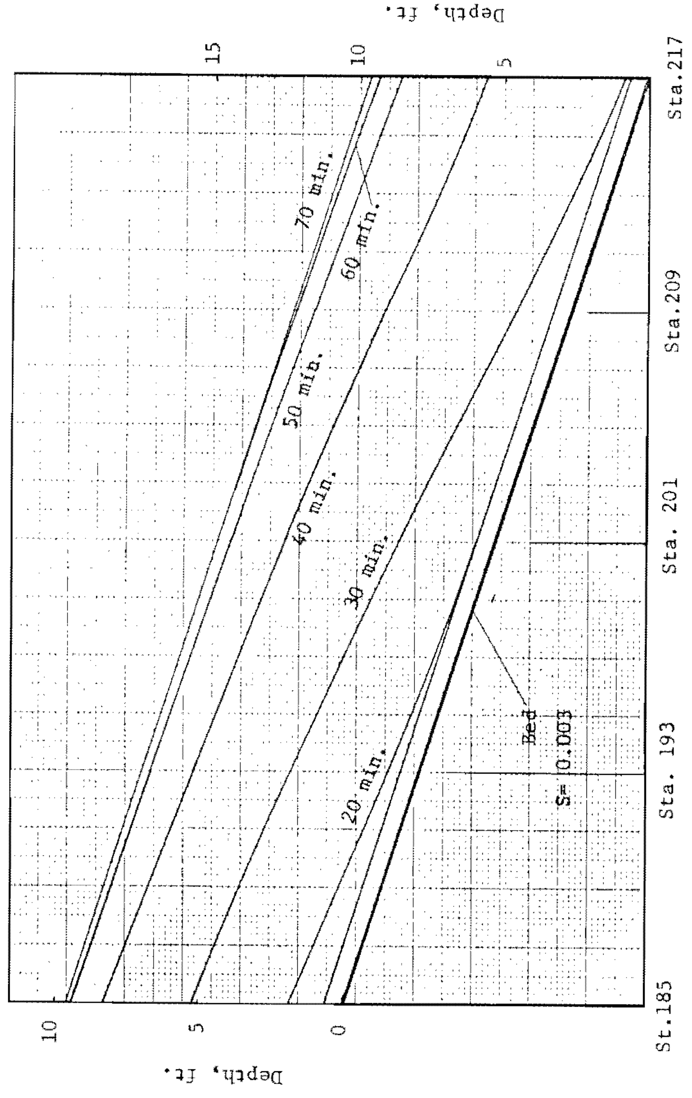

Figure 32. Water surface profiles for Reach 9. No backwater.

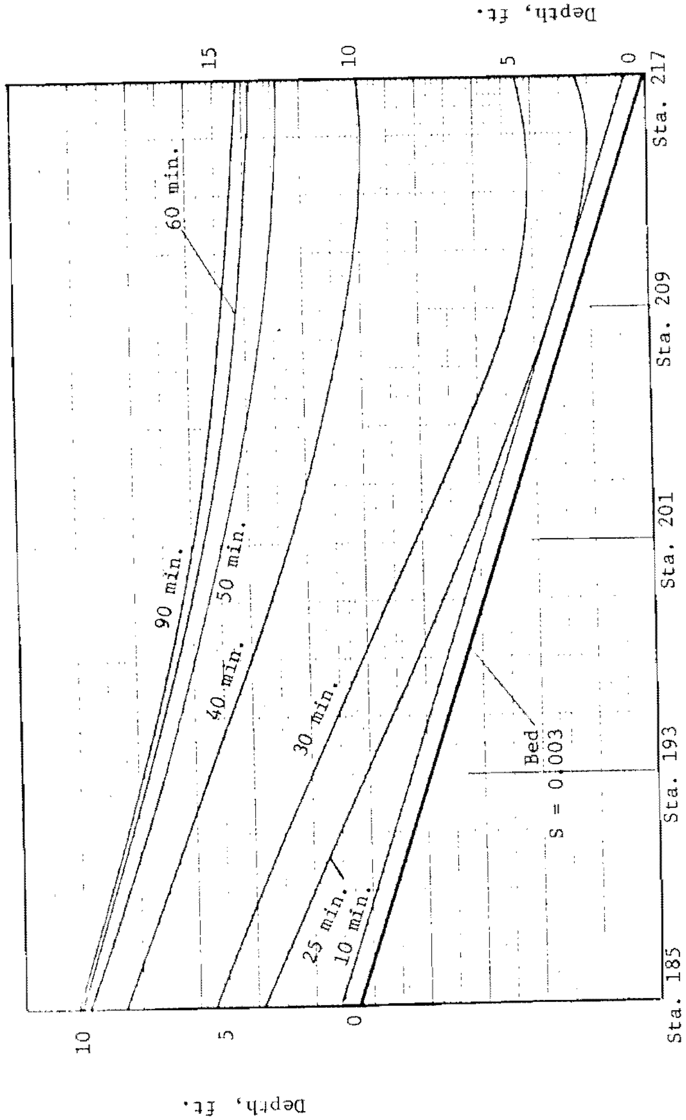

Figure 33. Water surface profiles for Reach 9. With backwater.

The flood wave movement in the downstream direction is clearly seen in Figs. 32 and 33 for both cases. The backwater front moving upstream is noticeable in Fig. 33. It begins as a reverse flow at the lower end of the reach. As the system approaches equilibrium, the change in the flow depth is rather slow, as can be observed for both cases. In both cases the equilibrium flow depth and velocity occur at the uppermost station first, and move slowly downstream. For the case with backwater effect, the flow at the upper portion of the reach can be very close to equilibrium while the backwater effect continues to build up the depth, and all stations of the reach approach the equilibrium conditions simultaneously.

Fig. 34 shows the comparison between the two cases for station 217. The discharge hydrograph (Fig. 34a) for the case with backwater effect shows a negative discharge at the beginning of the flow when the backwater wave moves upstream before the flood wave reaches the station. Corresponding to the negative discharge is a negative velocity (Fig. 34b) indicating flow in the upstream direction for a brief period. The flow depth is much higher with backwater effect and the corresponding velocity is lower.

Fig. 35 presents the comparison of the two cases for station 84 in the upper part of the watershed. The effect of the backwater on the velocity and flow depth are similar to those shown in Fig. 34. Note that the backwater effect on the discharge becomes larger and more significant in the lower part of the watershed.

It can be observed in Figs. 32 and 33 that in each case, at the base flow, normal flow exists as the initial condition. As the flow rate increases, a nonsteady flow condition occurs. As the flow approaches equilibrium, the case with no backwater effect approaches normal flow while the case with backwater effect approaches a steady nonuniform flow condition. At station 217, during the nonsteady flow phase, the energy slope is steeper than the bed slope for the case without backwater effect and flatter than the bed slope (part of the time even reversed) for the case with backwater effect. Thus, for the case without backwater the velocity is greater than normal velocity and smaller than normal with backwater effect. It follows that the time to equilibrium, compared to travel time as predicted on the basis of uniform flow, can be expected to be smaller for the case without backwater and larger for the case with backwater.

With subcritical flow conditions the backwater is affected or produced by the flow condition in the next reach downstream. Thus, when backwater occurs, for a given reach to be at equilibrium, its downstream control must be at equilibrium. In other words, each reach is affected by the flow conditions of the next reach and the whole channel system will approach the equilibrium condition simultaneously.

At this point the reader should be reminded of the instability that appeared in the routing solution as the system approached equilibrium. The need for the large number of iterations to insure stability is explained by the fact that, since the whole system approaches equilibrium simultaneously, any inaccuracy at any point will affect the whole system.

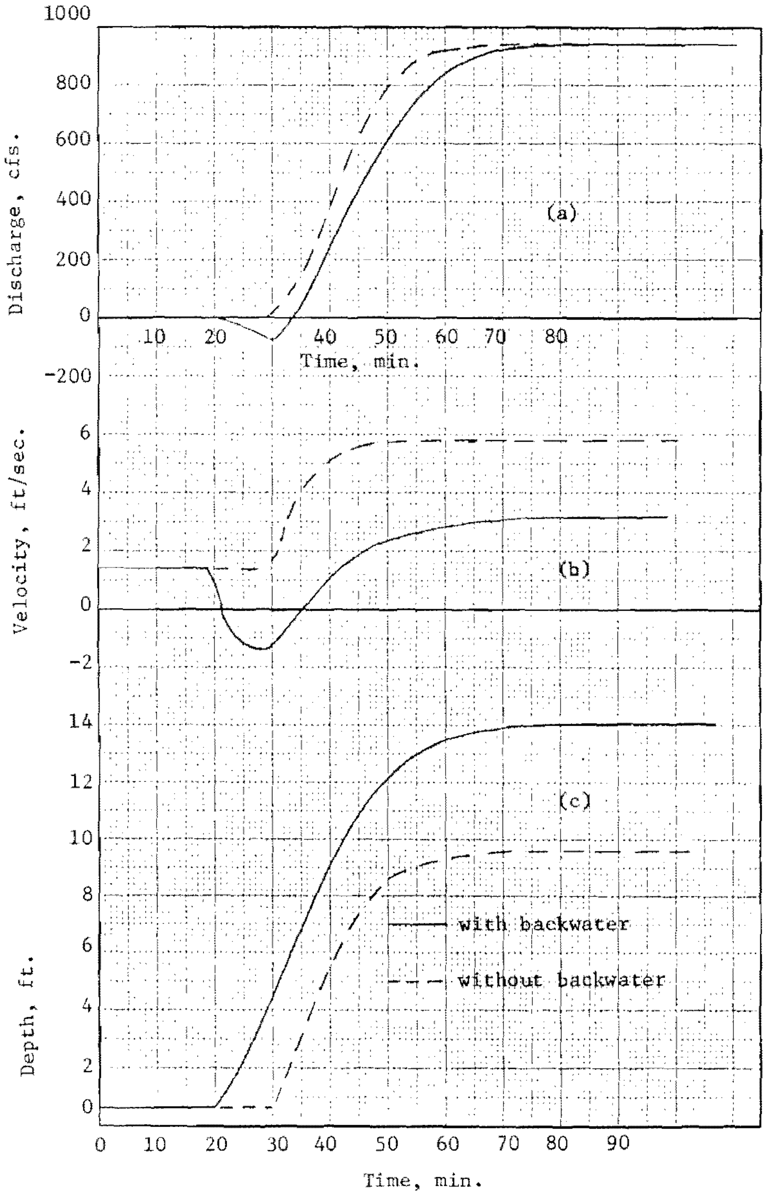

Figure 34. Comparison between backwater effect and no backwater for station 217. (a) Discharge, (b) Velocity, (c) Depth

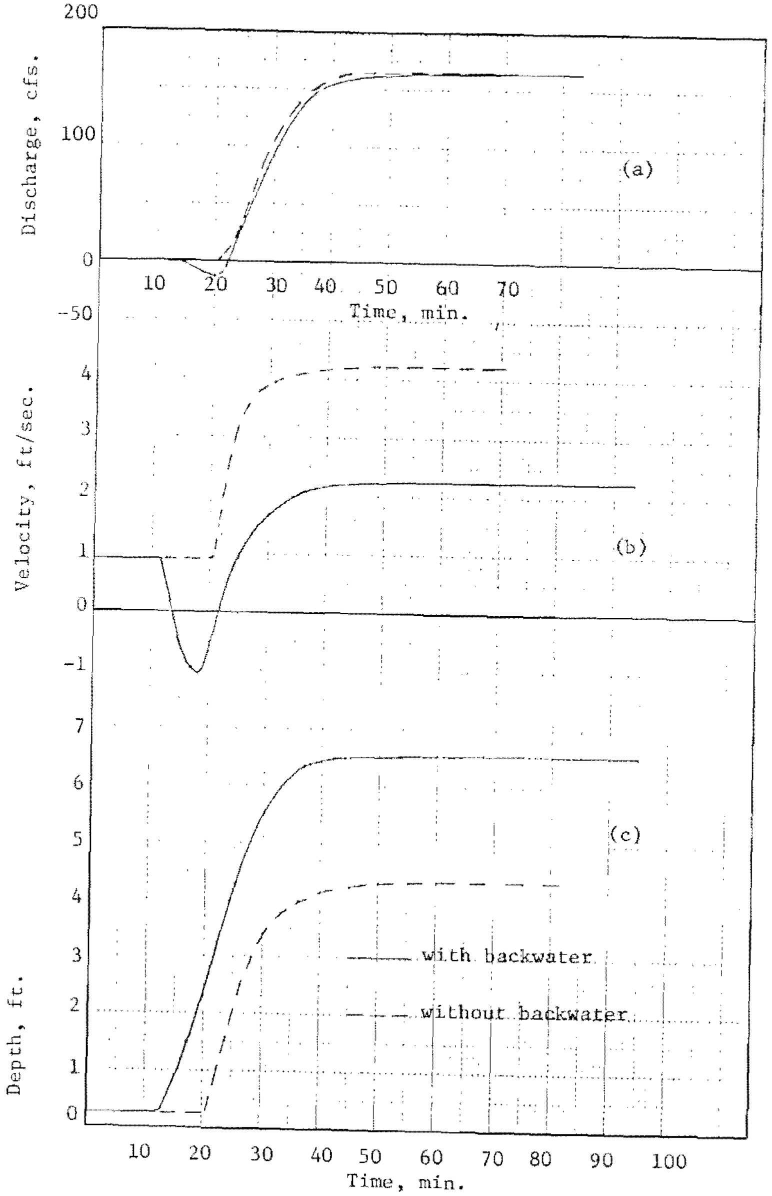

Figure 35. Comparison between backwater effect and no backwater for station 84. (a) discharge. (b) velocity. (c) depth.

In deriving Eq. 27, an assumption was made that the time to equilibrium is equal to the summation of the travel time for the individual reaches. This implies that, to an observer who follows the first drop of excess rainfall from the watershed divide along the main channel, the flow appears to be uniform at equilibrium condition at all watershed times, since equilibrium occurs almost immediately at the divide and progresses downstream. Evaluating this assumption in view of the above discussion, it can be seen that this assumption may hold for the case of no backwater effect, where the flood wave moves in a downstream direction and the equilibrium condition follows the crest of the flood wave. In the case with backwater effect the flow has nonsteady characteristics until the time of equilibrium when the whole system reaches the steady nonuniform flow condition simultaneously.

As shown above, for the case with backwater effect, the system reaches a steady nonuniform flow condition at equilibrium. For nonuniform flow the slope to be considered is the friction slope rather than the bed slope. Since the friction slope varies spatially, a single value, to be used in Eq. 27, cannot readily be evaluated. The term of the wetted perimeter in Eq. 27 should also be represented by a single value for the reach, a condition that does not exist for non-uniform flow. Thus, Eq. 27 should be considered applicable to the case of steady uniform flow only, i.e., to the case of a channel system without backwater effect.

When lateral inflow exists the flow is at a nonuniform state. In this model the lateral inflow was considered for the overland flow phase as well as for the elementary channel. Thus, Eq. 27 should be reevaluated for the case of flood routing through a channel system where backwater effect exists. This analysis is presented in the next chapter.

B. Results of Runs With Various Roughness Coefficients

In order to study the effect of the roughness coefficient on the time to virtual equilibrium, five test runs were conducted with the model with a different n- value for each run. Backwater effect was considered in all test runs. The value of n was varied from 0.02 to 0.08. The hydrographs from zero watershed time to the time of equilibrium for watersheds 2, 3 and 4 for the various n-values are presented in Tables 30-34 of Appendix A.

Fig. 36 presents the rising hydrographs to equilibrium for stream order 4, for the various n-values. As one would expect, an increase in n reduces the rate of rise and increases time to equilibrium. The time to virtual equilibrium for stream orders 2, 3 and 4 with each value of n are presented in Table 14. The same results are shown graphically in Fig. 37 on a log-log scale. It can be seen that the time to virtual equilibrium cannot be represented by a simple power function of n. In general, the time to virtual equilibrium increases with the increase of the roughness coefficient. The rate of increase varies from one stream order to the other. It should be noted that a single value of n was applied to all reaches of the watershed. Further discussion is presented in the following chapter.

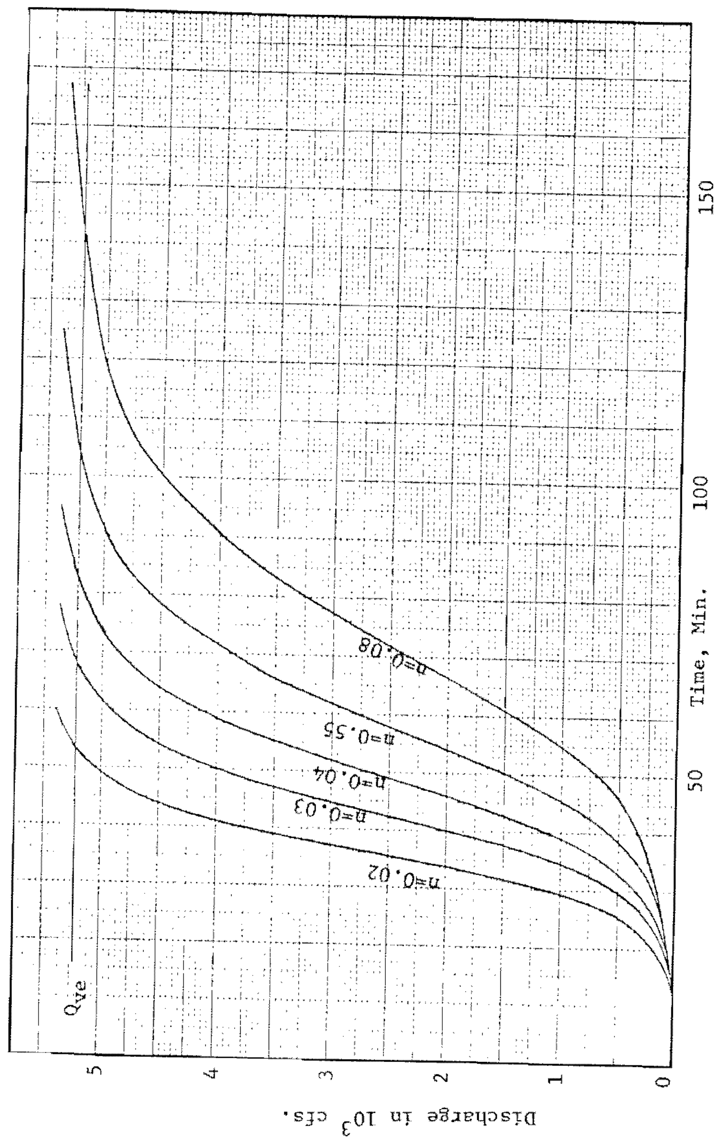

Figure 36. Rising hydrographs for stream order 4 for various n. (q=1.0 in/hr., S*=0.00283)

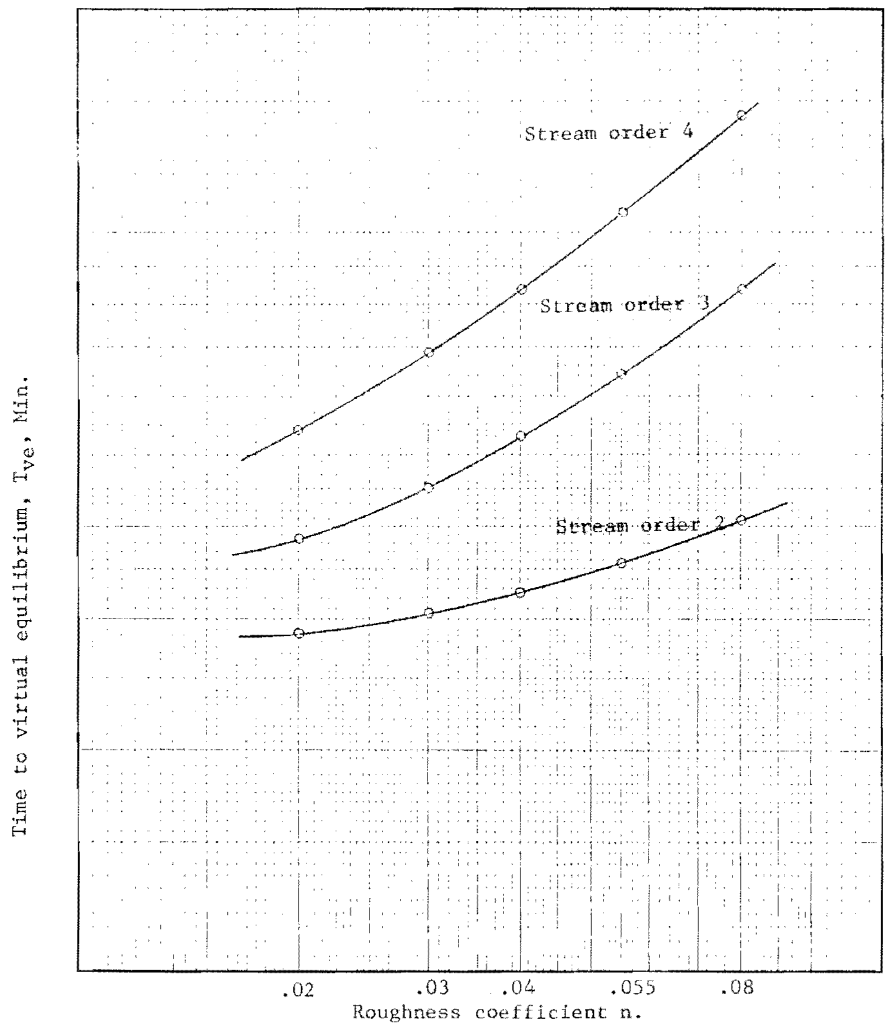

Figure 37. Time to virtual equilibrium as a function of the roughness. (q = 1.0 in/hr., α_s = 1.0)

n	T_{ve} in Min. Stream Order 2	Stream Order 3	Stream Order 4
0.02	28.69	38.36	53.93
0.03	30.47	45.27	68.56
0.04	32.41	52.53	83.25
0.055	35.40	63.75	105.31
0.08	40.57	83.83	142.68

Table 14. Time to virtual equilibrium for stream orders 2, 3 and 4, n series (q = 1.0 in/hr., α_s = 1.0).

C. Results of Runs with Various Slope Parameters

In order to study the effect of the channel slope on the time parameter, time to virtual equilibrium, five test runs were conducted with the model. In all five tests, all variables except the slope were kept constant at the standard conditions. The backwater effect was considered in all test runs.

Tables 34-38 in Appendix A present the hydrographs from zero watershed time to equilibrium for watershed orders 2, 3 and 4 for the various values of slope studied. Figure 38 presents the rising hydrographs to equilibrium for stream order 4.

The results of the five tests are presented in Table 15. The various slope factors (α_s) used are listed together with the slope parameter, S*, and the reusulting time to virtual equilibrium for stream orders 2, 3 and 4. The same results are also shown graphically in Fig. 39 on a log-log scale.

In this case again, the time to virtual equilibrium does not plot as a straight line for the various S* values. In general, the time to virtual equilibrium increases as the slope decreases, as expected.

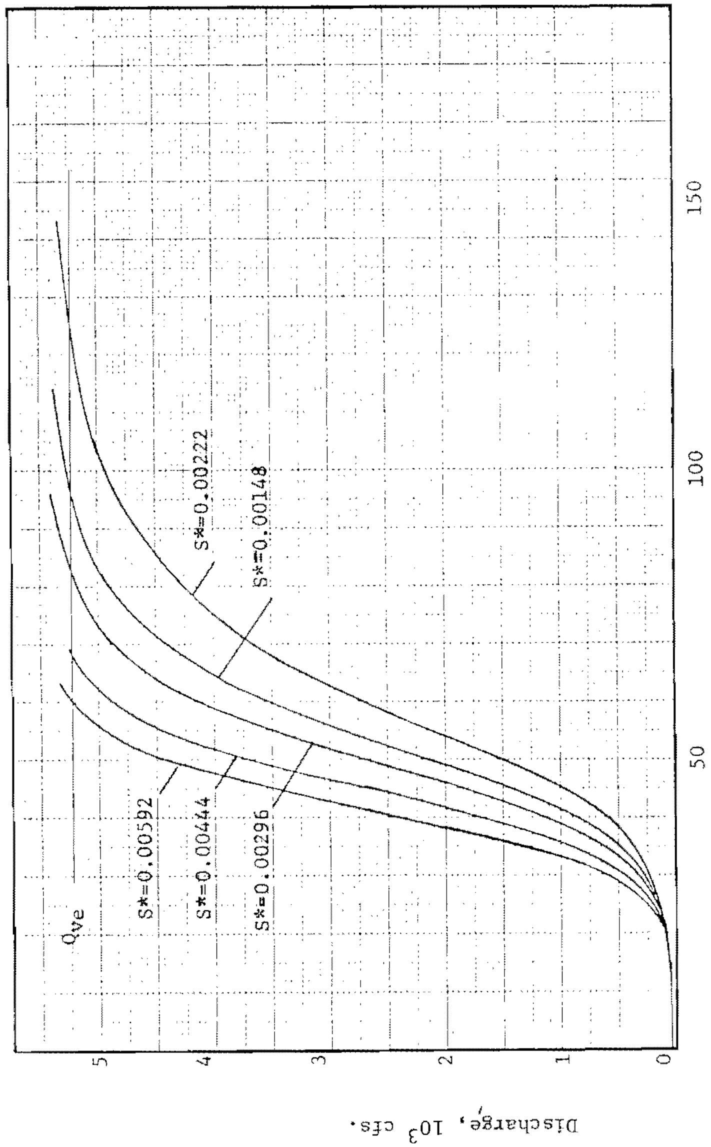

Figure 38. Rising hydrographs for stream order 4 for various S* (q=1.0 in/hr., n=0.04)

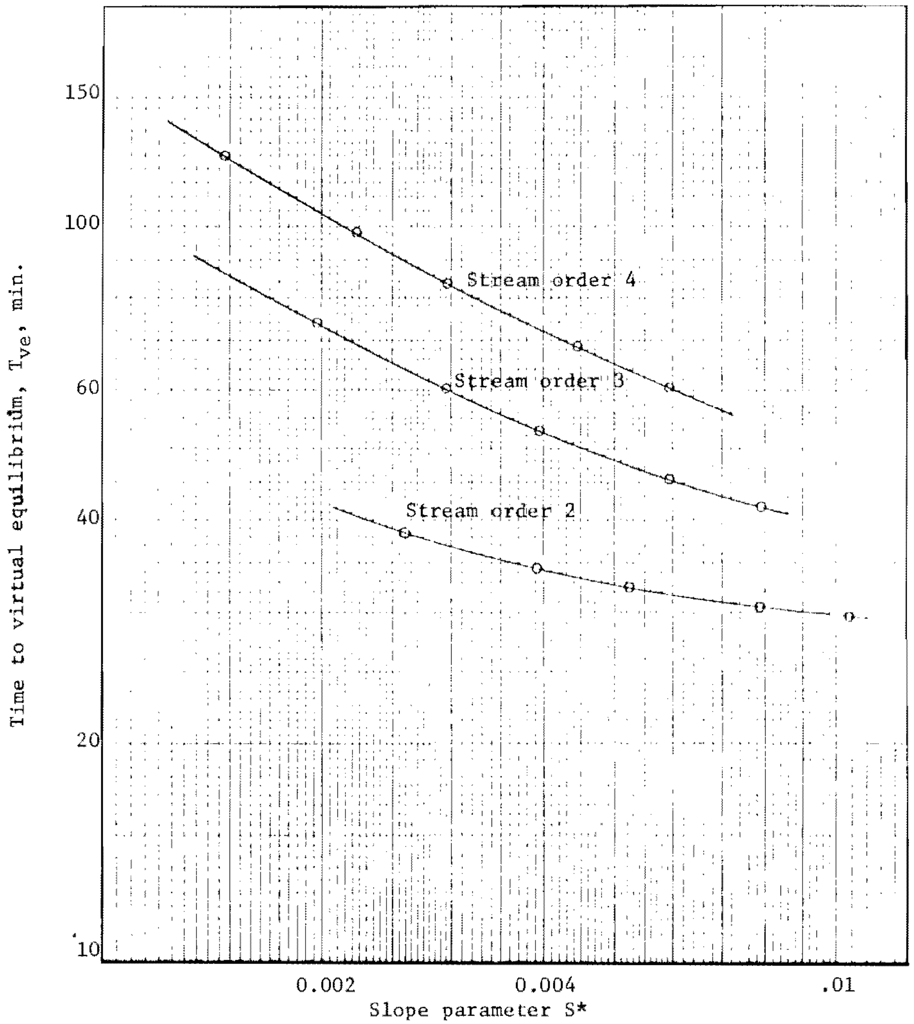

Figure 39. Time to virtual equilibrium as a function of the slope parameter S* (q = 1.0 in/hr., n = 0.04).

Slope Factor	Stream Order 2		Stream Order 3		Stream Order 4	
α_s	S*	T_{ve} Min.	S*	T_{ve} Min.	S*	T_{ve} Min.
2.0	0.01043	29.16	0.00787	41.75	0.00592	60.62
1.5	0.00783	30.54	0.00590	45.35	0.00444	68.43
1.0	0.00522	32.41	0.00394	52.53	0.00296	83.25
0.75	0.00391	34.38	0.00295	59.67	0.00222	97.64
0.5	0.00261	38.46	0.00197	73.98	0.00148	124.39

(T_{ve} in Min.)

Table 15. Time to virtual equilibrium for stream orders 2, 3 and 4, S-series (q = 1.0in/hr., n = 0.04).

CHAPTER IX

ANALYSIS AND DISCUSSION

The results, as presented in Chapter VIII, show the variations of the time to virtual equilibrium for the various test-runs. It is evident that interaction occurs and the data should be further analyzed to provide a general solution. An expression of the travel time on a watershed basis without backwater effect as a function of the independent factors is suggested. The, travel time T_t is shown to be a suitable flow parameter that can be used in predicting the hydrograph parameter channel rise time, T_{ch}. Following this, the results for T_{ch} with backwater effect are related to S and n, and further related to T_t to render a graphical solution for predicting T_{ch} for the model watershed.

A. Travel Time and T_{ve} for the Model Watershed Without Backwater Effect.

As shown in the previous chapters, the flow in the channel system at equilibrium is a steady nonuniform flow. The wetted perimeter of each reach varies from station to station, due mainly to the backwater effect. Table 16 presents the flow conditions at equilibrium for the standard roughness and slope. The equilibrium discharge is listed for each reach together with the resulting flow depth and wetted perimeter for the upper and lower stations of each reach. For comparison, the normal flow conditions without backwater effect are given for each reach. It can be seen that the backwater effect, in most cases, covers the entire reach and the flow depth of the uppermost station is slightly higher than the normal flow depth. For a nonuniform flow the friction slope also varies from station to station along the reach. Since bed slopes and normal wetted perimeter are used in Eq. 27, it applies only to the case of normal flow without backwater effect.

For normal flow the travel time can be calculated for each reach for a given equilibrium discharge, slope, roughness coefficient and cross section geometry and summed up for the watershed. Since the effect of the individual factors on the time to virtual equilibrium of the watershed is desired, a more general equation, on a watershed basis, is needed.

The results of the analysis in Chapter VII, Section C for the model watershed will be incorporated into the general equation for the T_{ve}, Eq. 27. Subsequent equations will apply specifically to the model watershed. Eq. 27 is considered now as an equation of the watershed travel time without backwater effect, designated as T_t, and is repeated here for convenience, using K instead of 0.087.

$$T_t = K\, q^{-2/5} \sum_{i=2}^{m} \frac{l_i\, n_i^{3/5}\, P_i^{2/5}}{S_i^{3/10}\, A_i^{2/5}} \qquad (27)$$

By substituting Eq. 152 in Eq. 27 the travel time becomes

Reach	Bottom width ft.	Q_i cfs.	End of Reach	Flow depth Ft.	P Ft.	Normal depth Ft.
2	4.0	97.96	upper	3.428	13.70	3.426
			lower	4.111	15.61	
3	4.50	163.27	upper	4.354	16.81	4.354
			lower	4.354	16.81	
4	4.50	163.27	upper	4.356	16.82	4.354
			lower	6.539	23.00	
5	6.0	489.80	upper	7.329	26.65	7.294
			lower	7.522	27.30	
6	6.50	555.11	upper	7.577	27.95	7.570
			lower	8.772	31.32	
7	7.5	881.64	upper	9.170	33.45	9.086
			lower	9.461	34.30	
8	7.5	946.95	upper	9.623	34.70	9.623
			lower	9.623	34.70	
9	7.5	946.95	upper	9.629	35.00	9.623
			lower	14.083	47.30	
10	10.5	2840.85	upper	15.739	55.00	15.634
			lower	16.313	56.60	
11	11.0	3167.39	upper	16.473	57.60	16.262
			lower	19.184	64.93	
12	12.5	5061.29	upper	20.326	70.11	20.241
			lower	20.556	70.64	
13	13.0	5387.83	upper	20.643	71.38	20.643
			lower	20.643	71.38	

Table 16. Equilibrium flow conditions

$$T_t = \frac{\bar{K}}{q^{0.4}} \sum \frac{l_i n_i^{0.6} \left(C_j S^{*-0.185} n_i^{0.365} Q_i^{0.412} \right)^{0.4}}{S_i^{0.3} A_i^{0.4}} \qquad (150)$$

The roughness coefficient n has a single value for all reaches. Thus, by substituting Eq. 25 ($Q_i = 646 q A_i$) and "factoring out" the common terms the equation becomes

$$T_t = \bar{K} C_j^{0.4} \frac{n^{0.745}}{q^{0.235} S^{*0.074}} \sum_{i=2}^{m} \frac{l_i}{A_i^{0.235} S_i^{0.3}} \qquad (151)$$

Now, let the relative slope be defined as $k_i = S_i/S^*$ and substitute $S_i = k_i S^*$ in Eq. 151. The travel time becomes

$$T_t = \bar{K} C_j^{0.4} \frac{n^{0.745}}{q^{0.235} S^{*0.374}} \sum_{i=2}^{m} \frac{l_i}{A_i^{0.235} k_i^{0.3}} \qquad (152)$$

Values of the relative slope, k_i, for the various reaches are given in Table 17 for stream orders 2, 3 and 4. For each stream order the values of k_i are constant for the given reach regardless of the slope parameter S^* of the particular test. The coefficient $\bar{K}$ depends on the units used in the equation. For T_t in minutes, q in inches per hour, l in miles and A in square miles,

$$\bar{K} = \frac{5280}{1.486^{0.6}\, 646^{0.235}\, 60} = 15.166 \qquad (153)$$

Eq. 152 relates the travel time of the channel system for normal flow condition at equilibrium, to the independent measureable watershed characteristics.

The exponent of the supply rate q in Eq. 152 agrees very well with the value of 0.232 obtained experimentally by Machmeier (28). The only parameter in the equation that is not part of the watershed characteristics is q. As shown by Machmeier, the exponent indicates the non-linearity of the runoff. The time to virtual equilibrium decreases for higher supply rates. The exponent was derived from Eqs. 27 and 146 as

$$q^{-0.4}\, q^{0.4x} = q^{-0.4+0.4x} = q^{-0.235} \qquad (154)$$

where x is a function of the channel geometry and the supply rate. The exponents of n, S^* and A were derived in the same manner. The question is "How does the supply rate affect the exponent?" In order to study this effect, the exponent of Q in Eq. 146 was calculated for the model watershed channel system for various supply rates. The exponent of q in Eq. 151 was calculated accordingly. The various supply rates and the calculated exponents are given in Table 18. It can be seen that the exponent of Q increases with an increase in the supply rate and that the wetted perimeter will increase accordingly. The exponent of q in Eq. 151 decreases with the decrease of the supply rate but, since the decrease is small compared with the decrease of the supply rate, the effect on the travel time is not significant. If an exponent of -0.235 corresponding to a supply rate of 1.0 inch per hour were used for all supply rates the error in the calculated travel time would range from +5% for q = 0.1 to about -1% for q = 2.0. It should be noted that this is a 20 to 1 variation in g. Thus, the relative effect of the supply rate is small and the exponent x = 0.412 in Eq. 146 should be considered primarily a function of the cross section geometry.

Reach	k_i Stream Order 2	Stream Order 3	Stream Order 4
2	1.031	1.288	1.661
3	0.943	1.178	1.519
4		1.178	1.519
5		0.904	1.166
6		0.904	1.166
7		0.904	1.166
8		0.822	1.060
9			1.060
10			0.848
11			0.848
12			0.742
13			0.742
$\sum \frac{l_i}{A_i^{0.235} k_i^{0.3}}$	: 0.482	1.921	3.761

Table 17. Values of the relative slope k_i for the model watershed for various stream orders.

Supply rate in/hr.	Exponent of Q in Eq. 146	Exponent of q in Eq. 151
0.1	0.383	-0.255
0.25	0.400	-0.240
1.0	0.412	-0.235
2.0	0.524	-0.230

Table 18. Exponent of Q (Eq. 146) and q (Eq. 151) for various supply rates.

Tables 19 and 20 present the calculated travel time for the various n-values and S-values utilized, respectively. The watershed travel time was calculated by applying Manning's equation to each reach for the equilibrium discharge and summing the travel times of the individual reaches ($T_t = \sum \frac{l_i}{v_i}$).

n	T_t in Min. Stream Order 2	Stream Order 3	Stream Order 4
0.02	4.30	18.25	38.50
0.03	5.81	24.67	52.10
0.04	7.19	30.59	64.63
0.055	9.12	38.83	82.09
0.08	12.08	51.45	108.83

Table 19. Calculated travel times for selected n-values for stream orders 2, 3 and 4 ($q = 1.0$ in/hr, $\alpha_s = 1.0$)

Slope Factor	T_t in Min.					
	Stream Order 2		Stream Order 3		Stream Order 4	
α_s	S*	T_t	S*	T_t	S*	T_t
2.0	0.00912	5.56	0.00730	23.61	0.00566	49.86
1.5	0.00684	6.19	0.00548	26.29	0.00424	55.52
1.0	0.00456	7.19	0.00365	30.59	0.00283	64.63
0.75	0.00342	8.01	0.00274	24.07	0.00212	72.00
0.5	0.00228	9.32	0.00183	39.66	0.00141	83.85

Table 20. Calculated travel times for selected S*-values for stream orders 2, 3 and 4 ($q = 1.0$ in/hr., $n = 0.04$)

	n			S*		
	S.O. # 2	S.O. # 3	S.O. # 4	S.O.#2	S.O.#3	S.O. #4
Coeff. a	79.180	333.787	722.28	0.996	3.736	7.190
Coeff. y	0.745	0.747	0.749	-0.373	-0.373	-0.374
Cor. coeff.	.9999	.9999	.9999	-0.9999	-.9999	-1.000

Table 21. Coefficient a, and exponent y in Eq. 155 expressing travel time as function of n and S* for the model watershed.

The results are presented graphically on a log-log scale in Figs. 40 and 41 for the n-series and S-series, respectively. The regression analyses yield equations in the form of

$$T_t = a\,B^y \qquad (155)$$

where a is the coefficient, B is the variable (n or S) and y is an exponent. The values of a and y and the correlation coefficient (of the log-values) are given in Table 21 for stream orders 2, 3 and 4.

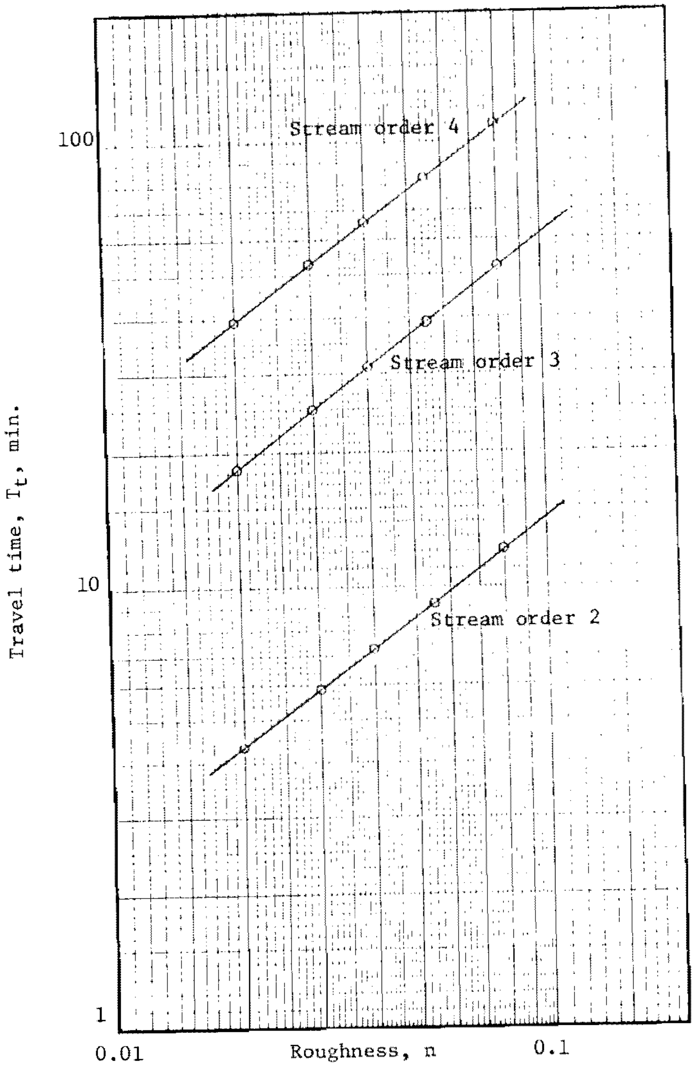

Figure 40. Travel time as function of the roughness coefficient n (q = 1.0 in/hr., α_s = 1.0).

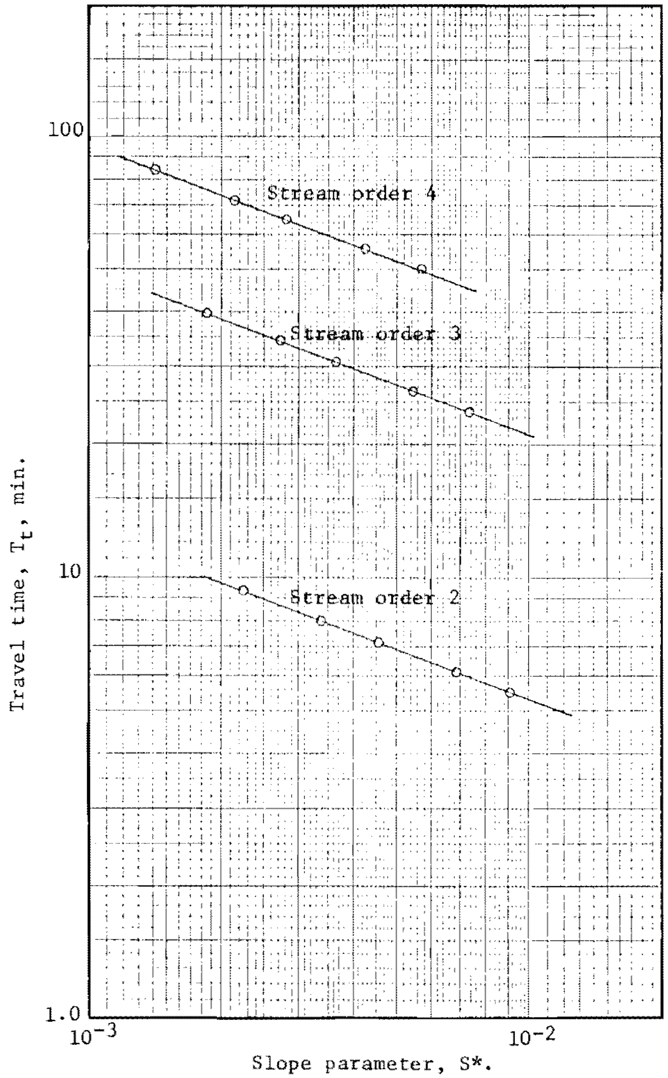

Figure 41. Travel time as function of the slope parameter S* (q = 1.0 in/hr., n = 0.04).

As should be expected, the travel time is directly related to the changes in the roughness coefficient n and inversely related to the changes in the slope parameter S*. The exponents are consistent and agree very well with those suggested by the theoretical consideration (Eq. 152).

The travel time is a "flow type" time parameter. By definition is in the time for a water particle to travel from the outlet of the elementary watershed to the watershed outlet by a steady uniform flow at equilibrium. Therefore, it is the main channel travel time for a case with no backwater effect. The travel time can be calculated for normal flow at equilibrium by

$$T_t = \sum (l_i/v_i).$$

Evaluating T_t for other watershed by direct application Eq. 152 is not possible since the exponents in the equation and the constant C_i depend on the channel geometry, and thus apply only to the model watershed. However, Eq. 152 has significance as an analytical form and serves as a model which may not vary greatly.

As mentioned before, only one case without backwater effect was tested. The data are therefore limited to one value of S and n (at standard condition) for stream orders 2, 3 and 4. Table 22 presents a comparison of the travel time, calculated by Eq. 20, and the time to virtual equilibrium routed by the model without backwater effect for the standard condition.

Stream Order	T_{ve}(min.)	T_t (Min)
2	30.75	7.19
3	46.22	30.59
4	70.55	64.63

Table 22. Comparison of travel time T_t and time to virtual equilibrium without backwater effect, T_{ve-} (q = 1.0 in/hr., n = 0.04, α_s = 1.0).

The data plot as a straight line in Fig. 42 and the relationship is given by

$$T_{ve-} = 25.5 + 0.695\ T_t \qquad (156)$$

where T_{ve} is the time to virtual equilibrium without backwater effect in minutes. The value of the Y-intercept, 25.5 minutes, is the same as the time to virtual equilibrium observed from the hydrograph for the elementary watershed for the run with standard condition. If the time to virtual equilibrium is subtracted from both sides of Eq. 156 the left side becomes, by definition, the channel rise time without backwater effect, T_{ch-}. Note that if T_{ch-} vs. T_t is plotted on log-log scale it will yield a straight line with the exponent equal to 1.0 and a coefficient of 0.695.

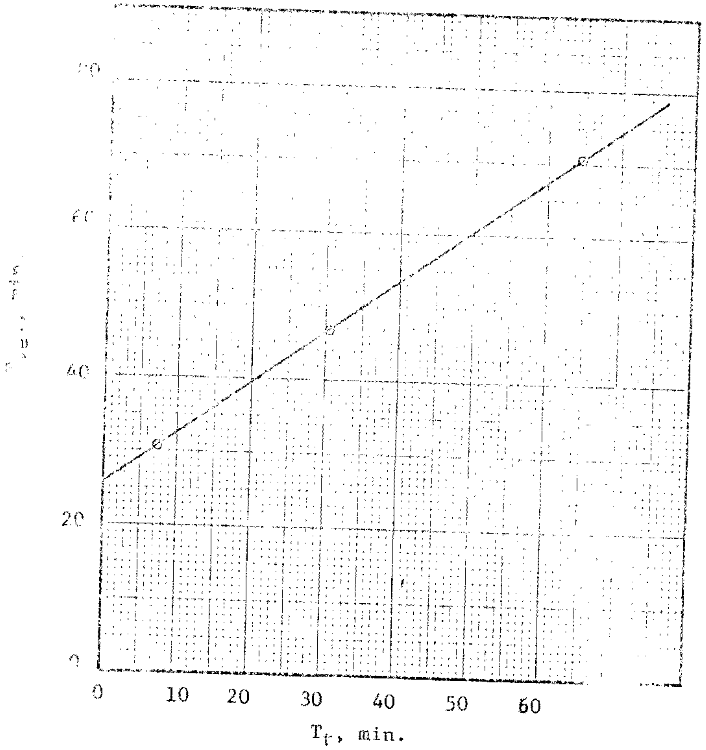

Figure 42. Time to virtual equilibrium without backwater effect T_{ve-} vs. travel time (q = 1.0 in/hr., n = 0.04, α_s = 1.0)

Based on the limited data, Eq. 156 suggests that the channel rise time without backwater effect is some percentage of the travel time, a calculated quantity.

F. Channel Rise Time T_{ch} for Various Slopes and Roughnesses.

An expression for the travel time in the main channel of the model watershed has been developed (Eq. 152), but this applies only to the special case of uniform flow at equilibrium, i.e., for the case without backwater effect. The need, of course, is for a method of determining T_{ve} for the watershed, including backwater effect.

Comparison of Figs. 37 and 39 to Figs. 40 and 41 indicates that the roughness coefficient n and the watershed slope parameter S* have the same general effects on the time to virtual equilibrium as their effects on the travel time. The travel time was considered for the part of the channel system where the flow is uniform and without lateral inflow.

Therefore, it was decided to study the effects of n and S* on the part on the time to virtual equilibrium that is caused by the nonsteady flow in the same part of the channel system. At the time when the flow at the outlet station of the watershed reaches 97% of the supply rate most of the watershed is already at equilibrium. Therefore, the time to equilibrium of the elementary watershed was subtracted from the time to virtual equilibrium as calculated by the routing procedure for the watershed. The residual, designated the channel rise time T_{ch}, is the additional time in minutes needed for the channel system to reach virtual equilibrium after the elementary channel is at equilibrium, including backwater effect.

The time to equilibrium of the elementary watershed can be calculated or estimated by available methods such as Izzard's (20), Morgali's (30) or kinematic wave routing (10), without use of a complete watershed model. Thus,

$$T_{ve} = T_{el} + T_{ch} \tag{157}$$

where T_{el} is the time to equilibrium of the elementary watershed. Note that T_{ve}, T_{el} and T_{ch} are hydrograph time parameters. As indicated earlier, the channel rise time without backwater effect, T_{ch-}, which is a hydrograph type time parameter, can be related to the travel time, a "flow type" time parameter. If the channel rise time with backwater effect, T_{ch}, can also be related to T_t, the time to virtual equilibrium will then be obtained by Eq. 157. As the first step, the effect of the slope and the roughness is analyzed in this section.

Table 23 presents the time to equilibrium of the elementary watershed, the time to virtual equilibrium for each stream order, and the channel rise time for the various tests. Values for T_{ve} are from the watershed model results (Tables 14 and 15). Values for T_{el} are from elementary watershed routing results (Tables 28 and 29 of Appendix A) and values of T_{ch} were obtained by subtraction using Eq. 157. It can be seen that T_{ch} increases with stream order, with roughness and with a decrease in channel slope, since all these changes reduce the flow velocity.

Values of T_{ch} from Table 23 were plotted against roughness for each stream order in Fig. 43. The data plot as straight lines on log-log scales, despite the fact that T_{ch} is defined as time difference and that it includes backwater effects.

The general equation is given by

$$T_{ch} = c\, n^{x}. \tag{158}$$

The values of c and x by regression analysis are given in Table 24, as well as the correlation coefficient of the log-values.

It can be seen that each stream order yields a different relation of channel rise time, T_{ch}, to the roughness coefficient n. The difference in the exponents, although small, appears significant. In general, the tendency shown by these lines is the same as shown by the plot of T_t vs. n (Fig. 40) but the exponents have larger values. It should be remembered

Test	T_{el}	S.O.# 2 T_{ve}	S.O.# 2 T_{ch}	S.O. # 3 T_{ve}	S.O. # 3 T_{ch}	S.O. # 4 T_{ve}	S.O. # 4 T_{ch}
n=0.02	26.04	28.69	2.65	38.36	12.32	53.93	27.88
0.03	26.18	30.47	4.29	45.27	19.09	68.56	42.38
0.04	26.30	32.41	6.11	52.53	26.23	83.25	56.95
0.055	26.44	35.40	8.96	63.75	37.31	105.31	78.87
0.08	26.63	40.57	13.94	83.83	57.20	142.68	116.05
α_s=2.0	26.32	29.16	3.33	41.75	15.43	60.62	34.30
1.5	26.22	30.54	4.32	45.35	19.13	68.43	42.21
1.0	26.30	32.41	6.11	52.53	26.23	83.25	56.95
0.75	26.52	34.38	7.86	59.67	33.14	97.64	71.12
0.5	26.46	38.46	12.01	73.98	47.52	124.39	97.83

Table 23. Time to equilibrium of elementary watershed, time to virtual equilibrium and channel rise time for Stream Orders 2, 3 and 4 for the various values of α_s (with n =.04) and various values of n (with α_s = 1.0).

	Stream Order 2	Stream Order 3	Stream Order 4
Coefficient c	290.08	930.12	1557.22
Exponent x	1.2004	1.1071	1.0281
Corr. Coeff. r	.9999	.9999	.9999

Table 24. Regression analysis results for channel time rise vs. the roughness (Eq. 158).

	Stream Order 2	Stream Order 3	Stream Order 4
Coefficient b	0.0450	0.2830	0.6852
Exponent z	-0.9139	-0.8098	-0.7547
Corr. Coeff. r	.9991	.9993	.9998

Table 25. Regression analyses results of channel rise time vs. slope parameter (Eq. 159).

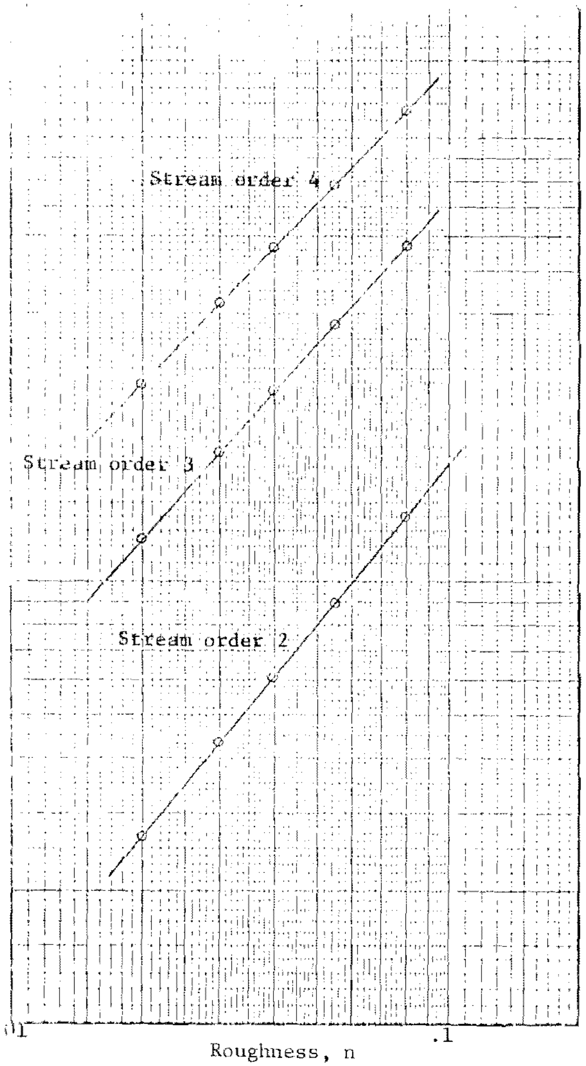

...nnel rise time, T_{ch} vs. roughness, n, for various stream ...ders (q = 1.0 in/hr., α_s = 1.0).

that for each stream order the slope parameter S*, the length of the main channel and the watershed area were kept constant but they vary from one stream order to the other.

Fig. 44 is a plot of channel rise time vs. the slope parameter, for stream orders 2, 3 and 4. Again, straight lines are obtained by using a log-log scale. The regression yields an equation of the type

$$T_{ch} = b\ S^{*z} \qquad (159)$$

and values of the coefficient b and the exponent z are given in Table [illegible]

It can be seen that each stream order yields a different relation of T_{ch} to the slope parameter S*. In this case the roughness coefficient was kept at standard condition (0.04) for all stream orders for all r... the main channel length and the watershed drainage area are constant ... each stream order but vary from one to another. In general, T_{ch} is inversely related to the slope parameter S* as was also shown for the ... of T_t vs. S* (Fig. 41).

C. Channel Rise Time (T_{ch}) as a Function of Travel Time (T_t).

As shown before, the travel time as well as the channel rise time can be given as power functions of the roughness and the slope parameter. Thus, the plots of T_{ch} vs. T_t for the various n and S*-values on log scales produce straight lines. The exponents and the coefficients of these lines are shown to be functions of the watershed characteristics S*, n and watershed size.

Fig. 45 is a plot of T_{ch} vs. T_t for the model n-values and the standard slope log-log scale. The data for the travel time are given in ... 19 and for the channel rise time in Table 23. The dashed lines connect points of equal n-values. Each point along a dashed line has a different slope parameter, a different channel length and a different drainage area. The solid lines connect points of equal slope parameter, equal channel length and equal drainage area, but each point has a different n-value. Thus, the slopes and the coefficients of the solid lines are independent of n and the changes in the exponents and the coefficients of the solid lines are functions of the drainage area, the length and the slope parameter.

Fig. 46 presents the plot of T_{ch} vs. T_t for the model S*-values ... a log-log scale. The data for the channel rise time T_{ch} are from Table 23 and for T_t from Table 20. All points on the graph have the same roughness coefficient, n = 0.04, but each has a different slope parameter, S*, the values of which are given in Table 20. Each dashed line has a fixed slope factor, α_s. The solid lines connect points that have the same main channel length and the same drainage area.

Fig. 46 can be modified so that the points along the dashed lines will have the same S*-values. For each stream order the equations are available from previous analyses as a function of the independent variable S*, while all other variables are [illegible] for travel [illegible]

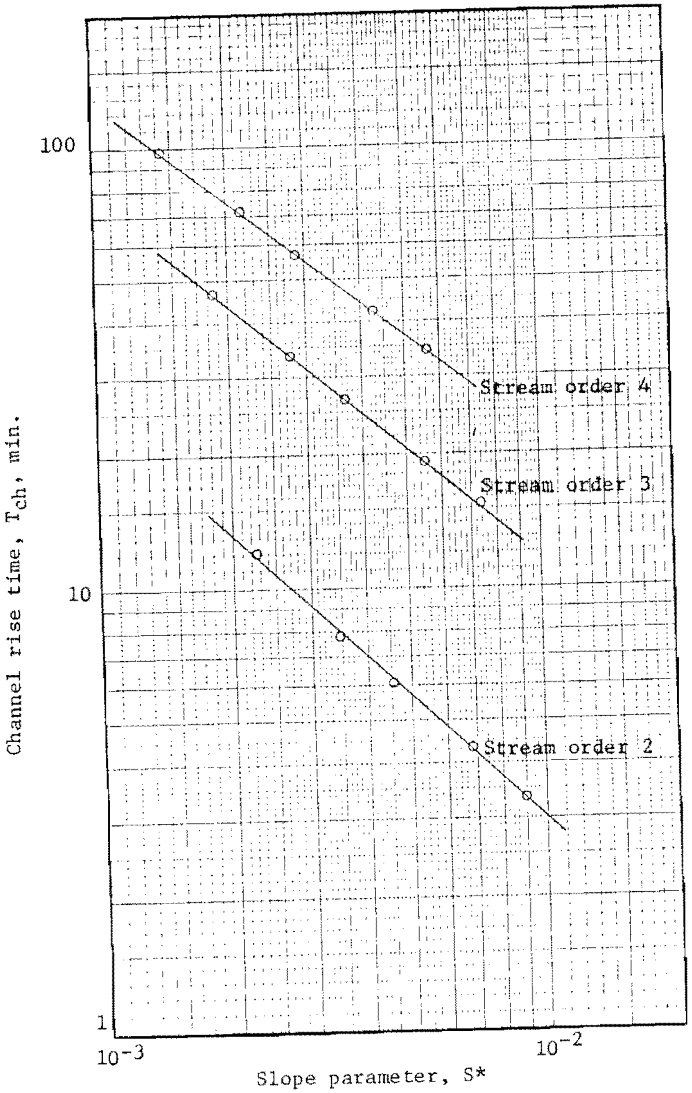

Figure 44. Channel rise time, T_{ch}, vs. the slope parameter, S*, for various stream orders (q = 1.0 in/hr, n = 0.04).

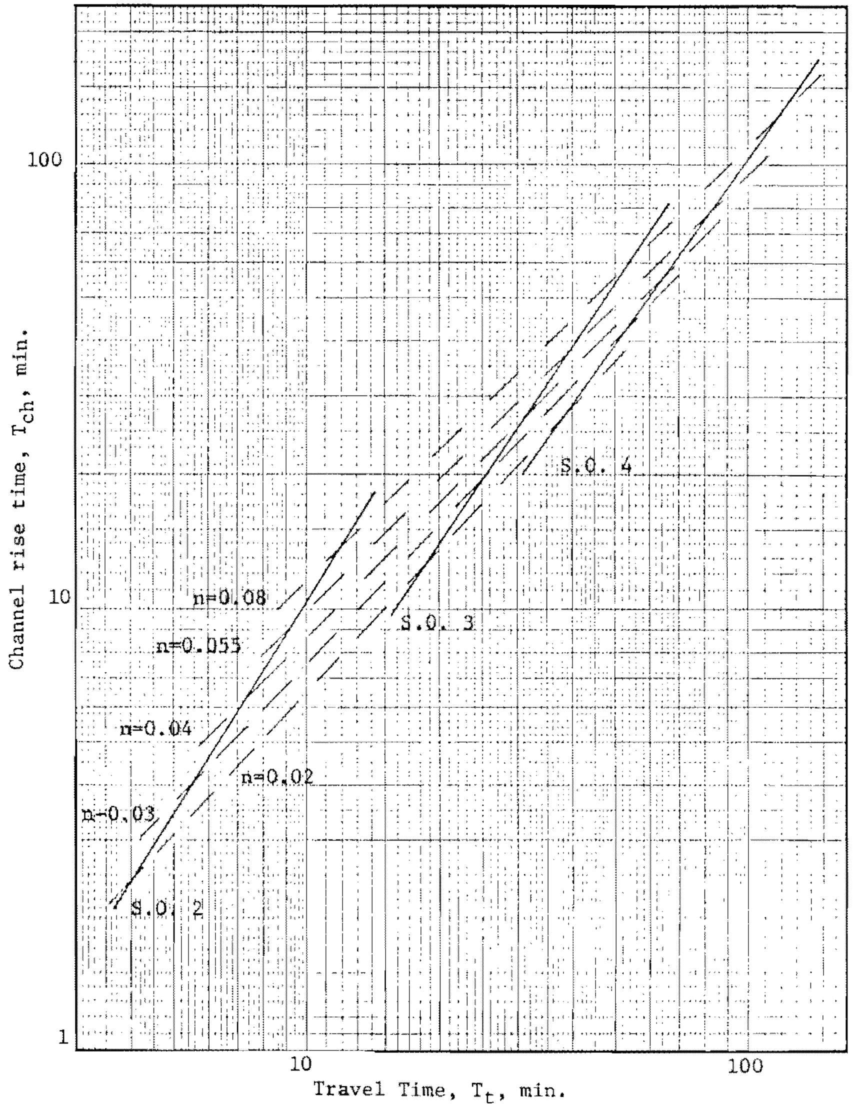

Figure 45. Relationship of channel rise time to channel travel time for the model n-values and stream orders (q=1.0 in/hr., α_s=1.0).

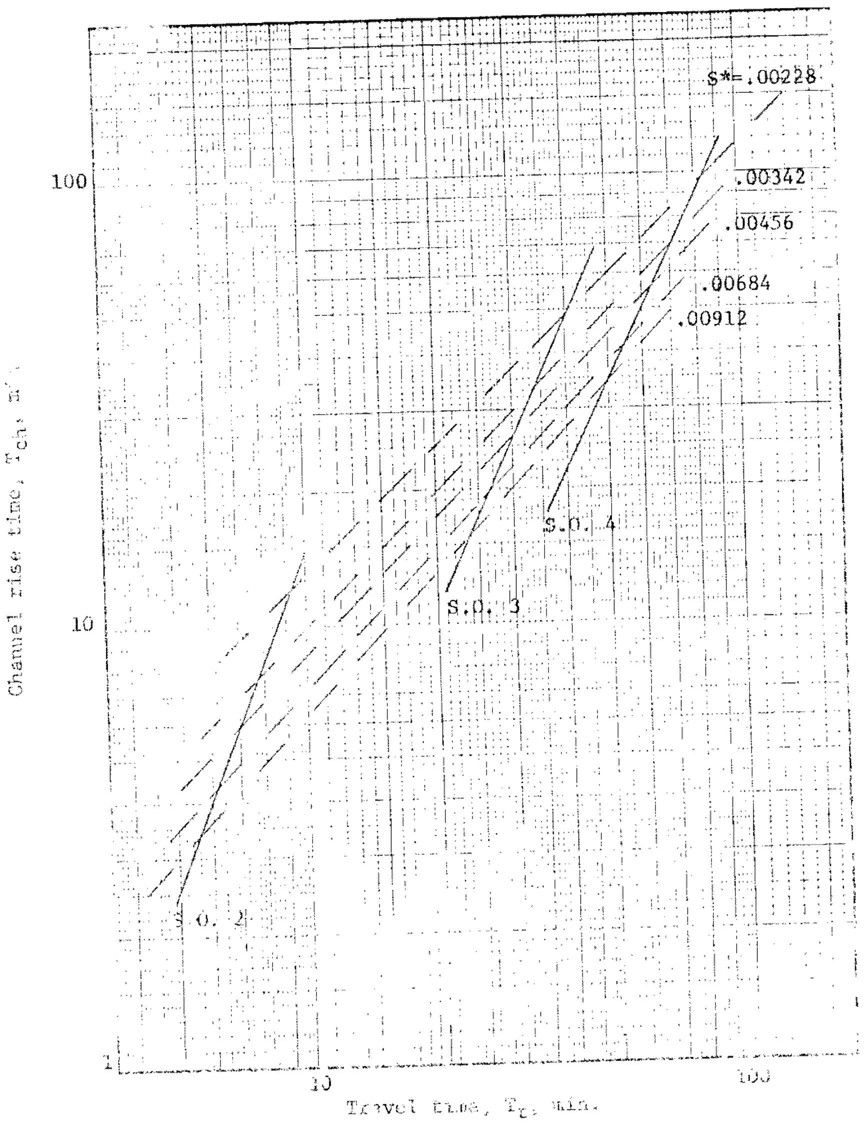

Figure 46. Relationship of channel rise time to channel travel time for the model S* values and stream orders (q_e = [illegible] in/hr., n = 0.04)

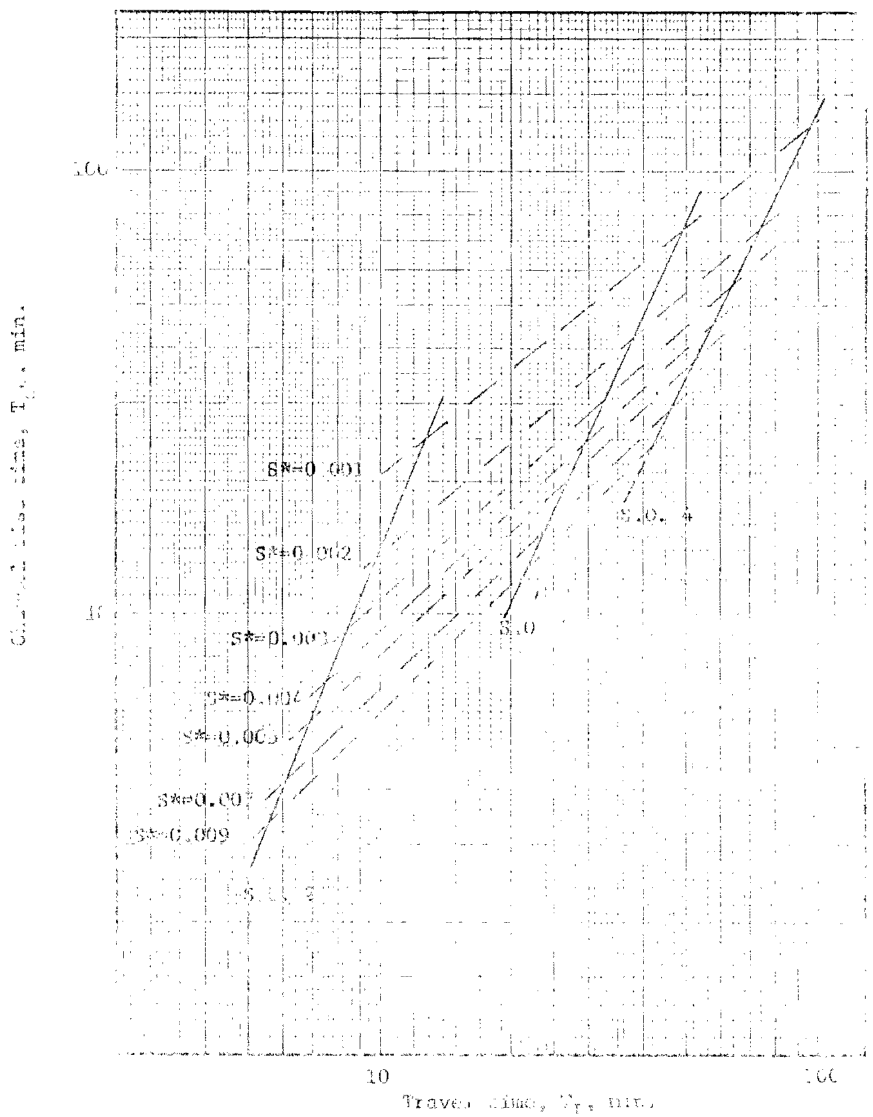

Figure 47. Relationship of channel rise time to channel travel time for selected S*-values calculated by Eqs. [illegible] and [illegible] (q_e = [illegible] in/hr., n= 0.04).

presented in Figs. 41 and 44, respectively. The equations, repeated here for convenience, are

$$T_t = a\ S^{*y} \tag{155}$$

and

$$T_{ch} = b\ S^{*z} \tag{159}$$

where a and b are the coefficients and y and z are the exponents given in Tables 21 and 25, respectively, for the various stream orders. By using these equations with the corresponding values for each stream order for various S*, a new set of data is obtained. Table 26 gives values of T_t and T_{ch} calculated by Eqs. 155 and 159 for various S*, equal for the three stream orders.

These data are presented graphically on log log scale in Fig. 47. The solid lines connect points on the same stream order which have the same main channel length and the same watershed drainage area. All points have the same roughness coefficient n. The dashed lines connect points of equal slope parameter S* for the three stream orders. The small change in the slope of the solid lines in Fig. 47 is a function of the main channel length and the watershed area, independent of the slope parameter S*. The change in the slope of the dashed lines in Fig. 47 is a function of the slope parameter S* for n = 0.04 independent of the main channel length and the watershed drainage area.

Regression analysis of data for each slope, Figs. 45, 46 and 47, yields equations of the form

$$T_{ch} = p\ T_t^{\ m} \tag{160}$$

where p is the coefficient and m is the exponent for each slope. Table 27 presents the coefficients p, the exponents m, obtained by regression analyses of the dashed lines in Fig. 47.

The coefficients p and the exponents m when plotted against the various values of S* on a log log scale yield straight lines. The regression equations of these lines are

$$p = 0.0217\ S^{*-0.713}$$

for the coefficient and

$$m = 1.452\ S^{*0.0845}$$

for the exponent. Similar plots and regression equations can be obtained for the solid lines and the dashed lines in Figs. 44, 45 and 46. In the case shown above, p and m are given as power function of a combination of two or three variables. This implies that

$$T_{ch}\ (n,S^*,L,A) = p_i(n,S^*,L,A)\ T_t(n,S^*,L,A)^{\ m_i(,S^*,L,A,)} \tag{161}$$

S*	Stream Order 2 T_t	Stream Order 2 T_{ch}	Stream Order 3 T_t	Stream Order 3 T_{ch}	Stream Order 4 T_t	Stream Order 4 T_{ch}
0.001	12.70	24.88	49.69	76.09	95.36	125.96
0.002	9.80	13.21	38.33	43.41	73.57	74.64
0.003	8.42	9.10	32.94	31.24	63.21	54.95
0.004	7.56	7.00	29.58	24.74	56.76	44.24
0.005	6.95	5.71	27.21	20.16	52.21	37.38
0.007	6.13	4.20	23.99	15.72	46.04	29.00
0.009	5.58	3.34	21.83	12.84	41.91	23.98

Table 26. Travel time, T_t, and channel rise time, T_{ch}, calculated by Eqs. 155 and 159.

S*	p	m
0.01	3.217	0.807
0.02	1.858	0.861
0.04	1.102	0.916
0.05	0.936	0.934
0.07	0.738	0.960
0.09	0.621	0.980

Table 27. Values of p and m in Eq. 160 for various S*.

and in each case the variables n, S*, L and A have different exponents. An analytical expression in the form of Eq. 161, even if it could be developed from the data, would be of limited practical value since the various coefficients involved cannot be evaluated from physical characteristics of actual watersheds.

Instead, a graphical solution was developed for the relation of channel rise time to travel time. The dashed lines in Fig. 47 represent T_{ch} as a function of the T_t for a channel system with a roughness coefficient n = 0.04 for various slope parameters S*. These lines are independent of the main channel length and the watershed drainage area. If the travel time is calculated for a channel system of given length, watershed drainage area, and main channel slopes, for an assumed roughness value of n = 0.04, the channel rise can be obtained by using the dashed lines of Fig. 47. This value of T_{ch} must be converted to the channel rise time value for the true estimated roughness coefficient n for the channel system. Table 27 provides the necessary data for a conversion graph. For the tests of the n-series, each stream order has a different slope parameter, S*, and T_{ch} is given for all n values tested.

Fig. 48 combines Fig. 47 and a conversion graph to provide a graphical solution. One enters Fig. 48 at the proper value of T_t (at the top), moves down to the line representing the slope parameter S* for the given watershed, moves across to the appropriate value of n, and then down to obtain T_{ch} in minutes.

D. Evaluation of the Method

Evaluation of the time to virtual equilibrium of the watershed model was the sole objective of this study. It was shown that the time to virtual equilibrium of a watershed is composed of two parameters. One is the time to virtual equilibrium of the elementary watershed and the second is the channel rise time.

The time to virtual equilibrium of the elementary watershed can be calculated or estimated from the physical characteristics by one of the available methods such as the kinematic wave routing or Morgali's equation.

The channel rise time, T_{ch}, is a hydrograph time parameter and includes the backwater effect as well as the non-steady flow conditions during the rise phase. It has been shown that T_{ch} can be related to the travel time of a channel system, which is a flow type time parameter and has no relation to hydrograph times. The relation is a power function of the type

$$T_{ch} = p\,T_t^{\,m}$$

where p, m, and T_t are, in turn, power functions of watershed factors. For the case without backwater effect the exponent m is shown to equal one. Note that very limited data were used and the results are by no means conclusive.

The exponents in the equation relating T_{ch} and T_t to S* and n were shown to depend on the channel cross section geometry. Thus, all results presented apply directly to the model watershed only. The graphical solution shows interactions of n, S*, [illegible] can be used to general[illegible]. Additional data for the model [illegible] are necessary [illegible] records.

E. Evaluation of the Model

A mathematical model was used in this study to represent the physical [illegible] represent the actual [illegible]

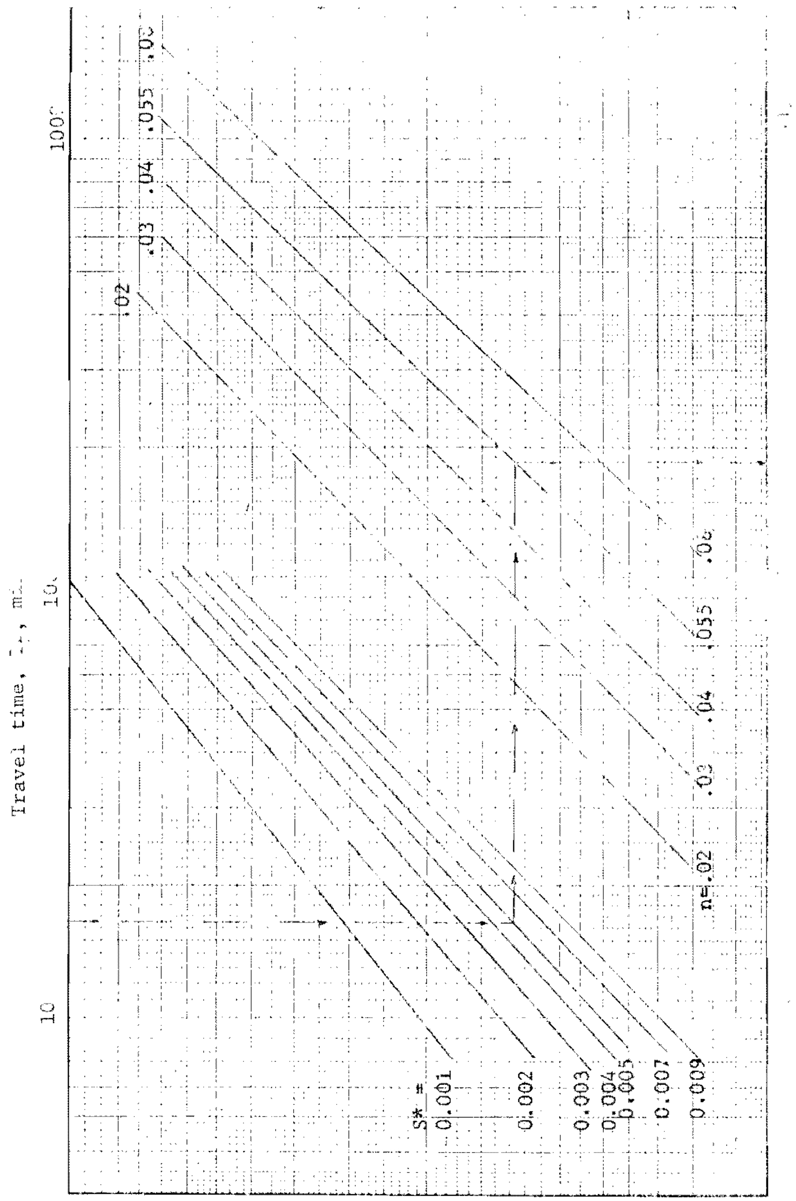

Figure 48. Graphical solution for converting travel time, T_t, to channel rise time, T_{ch}

verification was possible. The model was designed as an investigation tool and not to simulate any given prototype. The use of identical tributaries in a symmetrical order along a straight channel provides an idealized model that proved to be flexible enough and efficient within practical limits for this type of study.

In evaluating the model the reader should be aware of the following facts and limitations:

1) although the model does not represent a particular watershed prototype, the variations of hydraulic characteristics from station to station of the model watershed were based on the Leopold-Maddock studies. The absolute, or initial values were based on data from southeastern Minnesota, making the model representative of watersheds in the region;

2) the routing along the channel is performed by solving the dynamic equations of unsteady flow by the method of characteristics. Assumptions such as flow linearity were not used in any part of the system. Other investigators have used the dynamic routing technique in simulating actual unsteady flows and comparison with flow data has indicated good accuracy;

3) the backwater effect was considered in this model. The technique of solving the flow conditions at junction points was also used by other investigators with satisfactory results and verified by comparison with laboratory data. A possible source of discrepancy between the model and an actual watershed can be the fact that two-way junctions were considered in the model and the backwater effect was simulated in the main channel, at stream orders 2 to 4, only;

4) the overbank flow that occurs in many natural watersheds for large floods was not simulated in the model. In the model, a cross section was assumed to extend as high as needed to contain the flow within the main channel. Overbank flow causes a marked discontinuity in the hydraulic characteristics of the flow and would probably affect the results;

5) lateral inflow was assumed to occur in the elementary watershed only, i.e., from overland flow. Beyond this point, it seems reasonable to assume that lateral inflow along the main channel is small and that it has a negligible effect on the main channel flow; and

6) the watershed model was used in this study for the sole purpose of determining the time to virtual equilibrium and how various watershed factors affect T_{ve}. This requires by definition a constant input (excess rainfall) of long duration. By its nature, therefore, T_{ve} is a parameter which cannot be determined directly from observed data.

Bearing in mind the above facts, the writers believes that the model can be considered as a satisfactory tool for investigating theories of runoff on watershed basis. It is believed that the results represent

the actual runoff process. However, because of the limitations stated above, emphasis should be given to the general relationship between the factors involved rather than to the absolute values.

CHAPTER X

SUMMARY AND CONCLUSIONS

A. Summary

In this study a mathematical model of a watershed was developed to route the runoff as unsteady flow. The model watershed includes the overland flow plane, the elementary channel and the channel system. It is 5.2 square miles in area and is of the fourth stream order. The [illegible] geometrical and morphological relationships and the physical characteristics of small watersheds in southeastern Minnesota were used in developing the model. Excess rainfall was used as input to the system and was routed by numerical solution of the kinematic wave equation through the overland flow plane and the elementary channel. The outflow hydrographs of the elementary channel were used as input to the channel system where the flow was routed by successive numerical solutions of the [illegible] wave equations of the unsteady flow to obtain the runoff hydrograph of the watershed. Backwater effect was considered above the major junctions in the main channels of all stream orders except order one.

The model was used to study the effects of the watershed characteristics length, slope and roughness of the main channel and watershed area on the time parameter, time to virtual equilibrium, which has been found useful in predicting peak discharges. The effect of each factor was studied by varying it independently while keeping the others constant. The roughness and the slope were varied, with five values of each, within their normal range. The length and area were taken at three points, the outlet stations of stream orders 2, 3 and 4.

B. Conclusions

The study indicates that in practice, the time to virtual equilibrium of a watershed is best determined as a sum of two parameters. One is the time to virtual equilibrium of the elementary watershed, including the overland flow. The second is the channel rise time, defined as the time elapsed from T_{ve} of the elementary watershed to T_{ve} of the watershed at the outlet. For a given region, the variation in the time to virtual equilibrium of elementary watersheds should be relatively small. On the other hand, the channel rise time increases with the size of the watershed. Thus, the relative effect of the overland flow on the time to virtual equilibrium of the watershed decreases as the watershed size increases, and vice versa.

The channel rise time, T_{ch}, is not equal to the travel time for uniform flow, due primarily to the backwater effect. However, the travel time can be used to determine the channel rise time since both time parameters are functions of the same physical characteristics of the watershed, namely, the drainage area, the channel length, roughness, slope and cross section geometry.

In addition to the watershed characteristics, the time to virtual equilibrium is also affected by the runoff supply rate. The time to virtual equilibrium decreases as the supply rate increases. Thus, the non-linearity of the runoff process is shown clearly by Eq. 152.

The travel time T_t can be calculated for uniform flow reach by reach. An empirical expression of T_t on a watershed basis is given by Eq. 152 for the model watershed. T_t is directly related to the 0.745 power of the roughness coefficient and inversely related to the 0.235 power of the runoff supply rate and to the 0.374 power of the slope parameter S*. The exponent of the supply rate agrees with the value suggested by Machmeier (29). The exponents have been shown to vary slightly with the channel cross section geometry.

The channel rise time, T_{ch}, has been shown to relate to the travel time, T_t, as a power function. The exponent is dependent on the roughness coefficient, n, and the slope parameter S*. A graphical solution for T_{ch} is suggested as follows:

1) calculate the travel time T_t for the channel system reach by reach using the equilibrium discharge, the cross section geometry and the bed slope. Use the roughness coefficient value n = 0.04 as the base value;

2) convert the travel time of the channel system to T_{ch} by using a conversion graph of the type shown in Fig. 48, using the appropriate values of S* and n for the watershed.

To obtain the time to virtual equilibrium for the watershed, the T_{ve} of the elementary watershed should be added to the T_{ch}. The time to virtual equilibrium of the elementary watershed can be determined by routing the excess rainfall by the kinematic wave solution or estimated by any of the methods of overland flow time such as Morgali's equation.

C. Need for Further Studies

Although this study has resulted in some definite relationships between the watershed and channel physical characteristics and the time parameter T_{ve}, they are considered, at this stage, applicable to the model watershed only and not to watersheds in general. Additional studies should be conducted with the model to make the results more complete and to advance the general understanding of the factors involved in the runoff process.

Further studies are needed for evaluation of the effect of the channel cross section geometry. The bottom width and the side slope ratio should be varied independently and analyzed for their effect on the travel time and the time to virtual equilibrium.

The watershed slope parameter, S*, was used in this study. Its adequacy for representing the effects of channel slope should be studied further. A concave profile shape was used in the model. Other profile shapes (convex, constant, variable) should be studied for their effect on the travel time and the time to virtual equilibrium.

The roughness coefficient n was assumed constant for all reaches in this study. In nature the roughness coefficient can vary between reaches and with flow depth. The model watershed can be used to derive a watershed roughness parameter by testing various combinations of roughness along the main channel and their effects on the time parameters.

The watershed model could also be used with various supply rates as input, in order to study the effect on the time to virtual equilibrium when backwater is considered.

The studies reported here are, of course, subject to the inherent limitations of the model as indicated in the previous chapter. For future tests, some modifications in the model might improve the results. Backwater effect was limited to the main channel only and was shown to have a significant effect. However, further testing, considering the backwater in the tributaries as well as the main channel, are necessary to study the exact effect of backwater. Simulation of overbank flow for discharges with backwater effect is a necessary future improvement.

The routing was performed by solving for the flow conditions at each time step successively for all stations along the main channel. Changing the procedure so that the outflow hydrograph of a given stream order is routed through the additional reaches of the next stream order would permit the expanding of the model to higher stream orders, larger areas and a longer main channel. This modification might prove to add to the flexibility and to the computer efficiency of the model.

REFERENCES

1. Amorocho, J. "Measures of the Linearity of Hydrologic Systems", Jour. of Geophys. Res., Vol. 68, No. 8, April, 1963.

2. Baltzer, R.A. and Chintu, L. "Computer Simulation of Unsteady Flow in Waterways", Jour. of Hydr. Div., Proc. of ASCE, Vol. 94, No. HY 4, July 1968.

3. Bell, F.C. "Estimating Design Floods from Extreme Rainfall", Hydrology Papers, Colorado State Univ., Fort Collins, Colo., July 1968.

4. Bell, F.C. and On Kar, Songthan. "Characteristic Response Times in Design Flood Estimation", Four. of Hydrology, Vol. 8, No. 2, June 1969.

5. Brakensiek, D.L. "Kinematic Flood Routing", Trans. of ASAE, Vol. 10, No. 3, 1967.

6. Chow, V.T. "Handbook of Applied Hydrology", McGraw-Hill, New York, 1964.

7. Chow, V.T. "Open Channel Hydraulics", McGraw-Hill, New York, 1959.

8. Crawford, N.H., and Linsley, R.K. "The Synthesis of Continuous Streamflow Hydrographs on a Digital Computer", Stanford Univ. Dept. of C.E. Tech. Rep. No. 12, July 1962.

9. Diskin, M.J. "A Basic Study of the Linearity of the Rainfall Runoff Process in Watersheds", Ph.D. Thesis, Univ. of Illinois, Urbana, Ill., 1964.

10. Foster, G.R., Huggins, L.F. and Meyer, L.D. "Simulation of Overland Flow on Short Field Plots", Water Resources Res., Vol. 4, No. 6, 1968.

11. Gray, D.M. "Derivation of Hydrographs for Small Watersheds from Measurable Physical Characteristics", Iowa State Univ., Res. Bulletin 506, Ames, Iowa, June 1962.

12. Harbaugh, T.E. "Time Distribution of Runoff from Watersheds", Ph.D. Thesis, Univ. of Illinois, Urbana, Ill., 1966.

13. Harbaugh, T.E. and Chow, V.T. "A Study of the Roughness of Conceptual River System or Watershed", 12th Congress of International Ass. of Hydraulic Res., Fort Collins, Colo., September 1967.

14. Henderson, F.M. "Open Channel Flow", McMillan Co., New York, 1966.

15. Hickok, R.B., Keppel, R.V. and Rafferty, B.R. "Hydrograph Synthesis for Small Arid Land Watershed", Jour. of ASAE, October 1959.

16. Hill, J.K. "Runoff Hydrograph as a Function of Rainfall Excess", Water Resources Res., Vol. 5, No. 1, February 1969.

17. Horner, W.W. and Flynt, E.L. "Relation Between Rainfall and Runoff from Small Urban Areas", Tran. of ASCE, Vol. 101, 1935.

18. Horner, W.W., and Jens, S.W. "Surface Runoff Determination with Using Coefficients", Tran. ASAE, Vol. 107, 1942.

19. Isaacson, E., Stoker, J.J. and Troesch, A. "Numerical Solution of Flood Prediction and River Regulation Problems", Report II, IMM - NYU 205, New York Univ., January 1954.

20. Izzard, C.F. "Hydraulics of Runoff from Developed Surfaces" Highway Res. Board Proc., Vol. 26, 1946.

21. Kirpich, Z.P. "Time of Concentration of Small Agricultural Watersheds", Civil Engineering, Vol. 10, No. 6, June 1940.

22. Larson, C.L. "A Two Phase Approach to the Prediction of Peak Rates and Frequency of Runoff from Small Watersheds", Tech. Paper No. 53, Stanford Univ., Dept. of C.E., June 1965.

23. Larson, C.L. and Machmeier, R.E. "Peak Flow and Critical Duration for Small Watersheds", Trans. of ASAE, 1968.

24. Laurenson, E.M. "A Catchment Storage Model for Runoff Routing", Jour. of Hydrology, Vol. 2, 1964.

25. Leopold, L.B. and Maddock, T. "The Hydraulic Geometry of Stream Channel and Some Physiographic Implications", USGS Prof. Paper 252, 1953.

26. Linsley, R.K., Kohler, M.A. and Paulhus, "Applied Hydrology", McGraw-Hill, New York, 1949.

27. Linsley, R.K., Kohler, M.A. and Paulhus, J.L.H.,"Hydrology for Engineers", McGraw-Hill, New York, 1958.

28. Lister, M. "The Numerical Solution of Hyperbolic Partial Differential Equations by the Method of Characteristics", Chap. 15 of "Mathematical Methods for Digital Computer", Eds. Ralson, A., Wilf, H.S., John Wiley, New York, 1960.

29. Machmeier, R.E. "The Effect of Runoff Supply Rates and Duration on Runoff Time Parameters and Peak Outflow Rates", Ph.D. Thesis, Univ. of Minn. 1966.

30. Machmeier, A.E. and Larson, C.L. "Runoff Hydrographs for Mathematical Watershed Model", Jour. of Hyd. Div., November, 1968.

31. Minnesota Highway Dept. "Drainage Manual", Minn. Highway Dept., Sec. 5, 294.223, July, 1963.

32. Morgali, J.R. "Hydraulic Behavior of Small Drainage Basin" Tech. Rep. 30, Stanford Univ. Dept. of C.E., October 1963.

33. Mozayeny, B., and Song, C.S. "Propagation of Flood Wave in Open Channels", ASCE Jour. of Hydr. Div., Vol. 95, No. HY 3, May, 1969.

34. Parsons, D.H. "Depth of Overland Flow", U.S. Soil Conservation Service, SCS - TP - 82, 1949.

35. Pilgrim, D.H. "Measurement of Time of Concentration and Hydrograph Characteristics of Small Rural Catchments Using Radioactive Tracers", Water Res. Foundation of Australia, 7th Annual Report, June 1962.

36. Ramser, C.E. "Runoff from Small Agricultural Areas", Jour. of Agric. Res., Vol.34, No. 9, May 1927.

37. Schaake, J.C. "Synthesis of the Inlet Hydrograph", Rept. No. 3, Dept. of Sanitary Eng. and Water Resources, John Hopkins Univ., Baltimore, Maryland, June 1965.

38. Snyder, F.F. "Synthetic Unit Graphs", Tran. Am. Geophys. Union, Vol. 19, 1938.

39. Stall, J.B., and Fok, Y.S. "Hydraulics and Stream Geometry", Paper No. 67-739, Winter Meeting ASAE, Detroit, Mich., December 1967.

40. Stoker, J.J. "Numerical Solution of Flood Prediction and River Regulation Problems", Rept. I, IMM-NYU 200, New York Univ., 1953.

41. Taylor, A.B., and Schwarz, H.E. "Unit Hydrograph Lag and Peak Flow Relation to Basin Characteristics", Trans. Am. Geophys. Union, Vol. 33, April, 1952.

42. U.S. Soil Conservation Service. "Hydrology", Engineering Handbook Sec. 4, U.S. Dept. of Agric. SCS.

43. U.S. Soil Conservation Service. "Method for Estimating Volume and Rates of Runoff in Small Watersheds", U.S. Dept. of Agric. SCS - TP 149, January 1968.

44. U.S. Weather Bureau. "Rainfall Frequency Atlas of the United States", Tech. Paper No. 40, U.S. Dept. of Commerce, May 1961.

45. Wei, T.C. "Effect of Time and Areal Distribution of Rainfall on Runoff Hydrographs", Ph.D. Thesis, Univ. of Minnesota August 1970.

46. Wooding, R.A. "A Hydraulic Model for the Catchment-Stream Problem", Jour. of Hydrology, Vol. 3, 1965.

47. Woolhiser, D.A., and Liggett, F.A. "Unsteady, One-Dimensional Flow Over a Plane - the Rising Hydrograph", Water Resources Res., Vol. 3, No. 3, 1967.

APPENDIX A OUTFLOW HYDROGRAPHS

Time	Discharge, cfs. n = 0.02	n = 0.03	n = 0.04	n = 0.055	n = 0.08
0	0.000	0.000	0.000	0.000	0.000
2	0.000	0.000	0.000	0.000	0.000
4	0.035	0.024	0.018	0.013	0.009
6	0.634	0.422	0.317	0.230	0.158
8	3.689	3.266	2.450	1.782	1.225
10	5.898	5.754	5.633	5.473	5.234
12	8.338	8.217	8.114	7.984	7.804
14	11.045	10.929	10.834	10.718	10.560
16	13.988	13.893	13.795	13.694	13.546
18	17.144	17.100	17.019	16.907	16.771
20	20.615	20.546	20.461	20.371	20.226
22	24.377	24.260	24.152	24.057	23.914
24	28.395	28.218	28.105	27.986	27.832
26	32.379	32.178	32.142	32.059	31.871
28	32.407	32.407	32.407	32.407	32.407

Table 28. Outflow hydrographs of elementary watershed for various n-values (q = 1.0 in/hr, α_s = 1.0).

Time	Discharge, cfs. α_s = 2.0	α_s = 1.5	α_s = 0.75	α_s = 0.5
0	0.000	0.000	0.000	0.000
2	0.000	0.000	0.000	0.000
4	0.025	0.022	0.015	0.013
6	0.448	0.388	0.274	0.224
8	3.465	3.000	2.122	1.732
10	5.777	5.720	5.564	5.457
12	8.235	8.187	8.057	7.971
14	10.945	10.898	10.783	10.708
16	13.910	13.858	13.755	13.680
18	17.101	17.084	16.959	16.891
20	20.538	20.543	20.426	20.362
22	24.248	24.247	24.119	24.053
24	28.248	28.095	27.993	27.979
26	32.130	32.234	32.086	32.028
28	32.407	32.407	32.407	32.407

Table 29. Outflow hydrograph of elementary watershed for S* series (q = 1.0 in/hr, n = 0.04).

Time Min.	Discharge cfs.		
	Stream Order 2	Stream Order 3	Stream Order 4
0	1.23	7.14	40.60
5	1.23	7.14	40.60
10	7.31	9.74	40.96
15	41.91	31.16	74.74
20	82.29	138.06	166.24
25	128.96	375.69	429.37
30	162.32	685.09	1160.72
35	163.27	870.15	2382.43
40		932.19	3737.10
45		946.95	4635.15
50			5074.76
55			5259.47
60			5387.82

Table 30. Outflow hydrographs for test-run n = 0.02 for stream orders 2, 3 and 4 (q = 1.0 in/hr, α_s = 1.0).

Time, Min.	Discharge, cfs.		
	Stream Order 2	Stream Order 3	Stream Order 4
0	1.2	7.1	40.6
5	1.2	7.1	40.6
10	2.9	7.7	40.6
15	27.6	19.7	53.6
20	72.9	75.8	118.2
25	118.9	212.3	233.9
30	157.3	461.0	507.2
35	163.3	711.0	1030.5
40		858.7	1987.8
45		917.8	3052.2
50		943.7	3976.0
55		946.9	4578.0
60			4948.3
65			5147.8
70			52.56.9
75			5341.0
80			5387.8

Table 31. Outflow hydrographs for test-run n = 0.03 for stream orders 2, 3, and 4 (q = 1.0 in/hr, α_s = 1.0).

Time Min.	Discharge, cfs.		
	Stream Order 2	Stream Order 3	Stream Order 4
0	1.2	7.1	40.6
10	1.3	7.2	40.6
15	13.0	12.6	42.6
20	48.3	28.6	63.9
25	97.6	82.2	124.6
30	140.1	193.7	219.3
35	158.0	351.3	360.3
40	162.8	537.6	574.4
45	163.3	696.1	961.5
50		802.7	1486.4
55		868.9	2107.0
60		904.4	2765.7
65		922.8	3389.3
70		934.9	3903.6
75		946.9	4302.2
80			4599.7
85			4816.2
90			4979.2
95			5091.1
100			5171.5
105			5225.8
110			5268.9
115			5315.1
120			5355.6
125			5387.8

Table 32. Outflow hydrographs for test-run n = 0.055 for stream orders 2, 3 and 4 (q = 1.0 in/hr, α_s = 1.0).

Time Min.	Discharge, cfs. Stream Order 2	Stream Order 3	Stream Order 4
0	1.2	7.1	40.6
10	1.2	7.2	40.6
20	30.4	19.9	49.4
30	124.6	106.1	145.7
40	158.0	327.1	330.5
50	163.3	595.6	671.6
60		784.4	1405.5
70		870.8	2326.3
80		911.2	3245.6
90		928.3	3968.4
100		941.9	4483.3
110		946.9	4792.9
120			4999.7
130			5131.6
140			5212.9
150			5266.4
160			5317.2
170			5367.1
180			5387.8

Table 33. Outflow hydrographs for test-run n = 0.08 for stream orders 2, 3 and 4 (q = 1.0 in/hr, α_s = 1.0).

Time Min.	Discharge, cfs. Stream Order 2	Stream Order 3	Stream Order 4
0	1.2	7.1	40.6
5	1.2	7.1	40.6
10	1.5	7.4	40.6
15	17.7	16.5	47.2
20	63.2	43.9	87.9
25	109.6	140.6	172.7
30	150.9	305.5	323.8
35	162.2	540.3	596.7
40	163.3	731.6	1118.2
45		849.0	1838.9
50		905.0	2682.6
55		928.9	3486.8
60		946.4	41.24.9
65		946.9	4566.1
70			4871.6
75			5061.6
80			5179.1
85			5251.7
90			5319.2
95			5379.6
100			5387.8

Table 34. Outflow hydrographs for standard conditions for stream orders 2, 3 and 4 (q = 1.0 in/hr, n = 0.04, α_s = 1.0).

Time Min.	Discharge, cfs. Stream Order 2	Stream Order 3	Stream Order 4
0	1.2	7.1	40.6
5	1.2	7.1	40.6
10	4.7	7.8	40.6
15	31.6	20.2	53.2
20	77.9	83.4	132.2
25	123.4	235.8	244.8
30	159.8	518.6	583.2
35	163.3	780.8	1280.6
40		902.3	2302.7
45		941.2	3463.9
50		946.9	4407.2
55			4963.5
60			5215.6
65			5359.5
70			5387.8

Table 35. Outflow hydrographs for test-run α_s = 2.0 for stream orders 2, 3 and 4 (q = 1.0 in/hr, n = 0.04).

Time Min.	Discharge, cfs. Stream Order 2	Stream Order 3	Stream Order 4
0	1.2	7.1	40.6
5	1.2	7.1	40.6
10	1.9	7.4	40.6
15	23.9	18.6	50.4
20	71.8	61.4	111.1
25	117.4	193.0	212.3
30	157.0	413.1	436.5
35	163.3	677.3	894.8
40		846.0	1680.0
45		916.9	3674.1
50		944.5	3674.1
55		946.9	4424.0
60			4889.1
65			5139.5
70			5263.4
75			5365.5
80			5387.8

Table 36. Outflow hydrographs for test-run α_s = 1.5 for stream orders 2, 3 and 4 (q = 1.0 in/hr, n = 0.04).

Time, Min.	Discharge, cfs. Stream Order 2	Stream Order 3	Stream Order 4
0	1.2	7.1	40.6
5	1.2	7.1	40.6
10	1.4	7.3	40.6
15	15.6	14.8	45.4
20	57.0	36.8	77.1
25	104.0	112.4	148.6
30	145.6	251.4	271.2
35	159.3	453.5	473.8
40	163.3	645.6	843.8
45		778.3	1427.4
50		856.3	2116.4
55		898.8	2859.6
60		920.3	3514.3
65		933.7	4024.6
70		946.5	4412.3
75		946.9	4688.0
80			4892.4
85			5035.2
90			5132.2
95			5201.4
100			5250.5
105			5234.5
110			5341.9
115			5384.9
120			5387.8

Table 37. Outflow hydrographs for test-run α_s = 0.75 for stream orders 2, 3 and 4 (q = 1.0 in/hr, n = 0.04).

Time Min.	Discharge, cfs. Stream Order 2	Stream Order 3	Stream Order 4
1	1.2	7.1	40.6
10	1.3	7.3	40.6
20	48.8	29.8	66.5
30	137.2	191.9	216.6
40	153.6	529.1	585.5
50	163.3	763.0	1511.7
60		867.1	2706.4
70		918.0	3657.9
80		929.3	4279.5
90		944.9	4676.6
100		946.9	4939.7
110			5198.0
120			5262.2
140			5324.8
150			5382.3
160			5387.8

Table 38. Outflow hydrographs for test-run $\alpha_s = 0.5$ for stream orders 2, 3 and 4 (q = 1.0 in/hr, n = 0.04).